(2)

# NAVAL POSTGRADUATE SCHOOL
## Monterey, California



# THESIS

A COMPARISON OF HIGH-LATITUDE IONOSPHERE PROPOGATION PREDICTIONS FROM AMBCOM WITH MEASURED DATA

by

David J. Wilson

March 1991

Thesis Advisor: Richard W. Adler

Unclassified

security classification of this page

## REPORT DOCUMENTATION PAGE

| | | | |
|---|---|---|---|
| 1a Report Security Classification Unclassified | | | 1b Restrictive Markings |
| 2a Security Classification Authority | | | 3 Distribution Availability of Report |
| 2b Declassification Downgrading Schedule | | | Approved for public release; distribution is unlimited. |
| 4 Performing Organization Report Number(s) | | | 5 Monitoring Organization Report Number(s) |
| 6a Name of Performing Organization<br>Naval Postgraduate School | 6b Office Symbol<br>*(if applicable)* EC/AB | | 7a Name of Monitoring Organization<br>Naval Postgraduate School |
| 6c Address *(city, state, and ZIP code)*<br>Monterey, CA 93943-5000 | | | 7b Address *(city, state, and ZIP code)*<br>Monterey, CA 93943-5000 |
| 8a Name of Funding Sponsoring Organization | 8b Office Symbol<br>*(if applicable)* | | 9 Procurement Instrument Identification Number |
| 8c Address *(city, state, and ZIP code)* | | | 10 Source of Funding Numbers |
| | | Program Element No | Project No / Task No / Work Unit Accession No |

11 Title *(include security classification)* A COMPARISON OF HIGH-LATITUDE IONOSPHERE PROPAGATION PREDICTIONS FROM AMBCOM WITH MEASURED DATA

12 Personal Author(s) David J. Wilson

| 13a Type of Report | 13b Time Covered | 14 Date of Report *(year, month, day)* | 15 Page Count |
|---|---|---|---|
| Master's Thesis | From To | March 1991 | 115 |

16 Supplementary Notation The views expressed in this thesis are those of the author and do not reflect the official policy or position of the Department of Defense or the U.S. Government.

| 17 Cosati Codes | | | 18 Subject Terms *(continue on reverse if necessary and identify by block number)* |
|---|---|---|---|
| Field | Group | Subgroup | high latitude, ionosphere, AMBCOM, propagation modeling |
| | | | |
| | | | |

19 Abstract *(continue on reverse if necessary and identify by block number)*

This thesis examines the performance of SRI's Ambient Communications (AMBCOM) model for high-latitude propagation prediction. It is one in a series of studies, conducted at the Naval Postgraduate School, to establish the relative merits of several computer-based propagation prediction models using a standard set of measured data.

AMBCOM modeled the propagation path between a transmitter located in the polar cap region and several midlatitude receiver sites. Model predictions were matched to measured data obtained during two high-latitude communication experiments (campaigns). The absolute difference between model signal-to-noise ratio (SNR) and measured SNR was considered as error. Error statistics were accumulated to show the distribution of the error by campaign and frequency. The percentage, by frequency, of matched AMBCOM predictions in reference to total predictions for a given frequency was considered a measure of AMBCOM performance.

AMBCOM exhibited small absolute values of average error, i.e., 7-11 dB, and high percentages of matched records. The average error was typically distributed between -20 and +20 dB. Unfortunately, these are only relative measures of model performance. The site antenna and environmental data used to model high latitude campaigns were estimated not measured, and some variation in AMBCOM results may be attributable to poor estimates. The measured data were not designed specifically for model validation, and further comparisons are needed with new measured data.

| 20 Distribution Availability of Abstract | 21 Abstract Security Classification | |
|---|---|---|
| ☒ unclassified unlimited ☐ same as report ☐ DTIC users | Unclassified | |
| 22a Name of Responsible Individual<br>Richard W. Adler | 22b Telephone *(include Area code)*<br>(408) 646-2352 | 22c Office Symbol<br>EC/AB |

DD FORM 1473,84 MAR 83 APR edition may be used until exhausted
All other editions are obsolete

security classification of this page

Unclassified

Approved for public release; distribution is unlimited.

# A COMPARISON OF HIGH-LATITUDE IONOSPHERE PROPAGATION PREDICTIONS FROM AMBCOM WITH MEASURED DATA

by

David J. Wilson
Major, United States Marine Corps
B.S., Oregon State University, 1975

Submitted in partial fulfillment of the
requirements for the degree of

MASTER OF SCIENCE IN ELECTRICAL ENGINEERING

from the

NAVAL POSTGRADUATE SCHOOL
March 1991

Author: 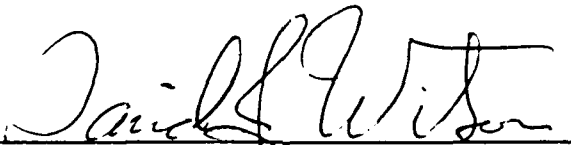

David J. Wilson

Approved by: 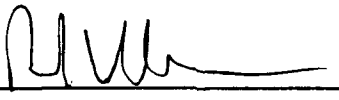

Richard W. Adler, Thesis Advisor

Wilbur R. Vincent, Second Reader

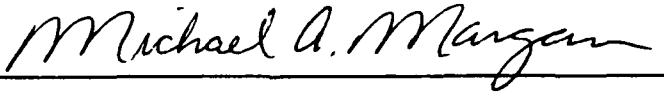

Michael A. Morgan, Chairman,
Department of Electrical and Computer Engineering

## ABSTRACT

This thesis examines the performance of SRI's Ambient Communications (AMBCOM) model for high-latitude propagation prediction. It is one in a series of studies, conducted at the Naval Postgraduate School, to establish the relative merits of several computer-based propagation prediction models using a standard set of measured data.

AMBCOM modeled the propagation path between a transmitter located in the polar cap region and several midlatitude receiver sites. Model predictions were matched to measured data obtained during two high-latitude communication experiments (campaigns). The absolute difference between model signal-to-noise ratio (SNR) and measured SNR was considered as error. Error statistics were accumulated to show the distribution of the error by campaign and frequency. The percentage, by frequency, of matched AMBCOM predictions in reference to total predictions for a given frequency was considered a measure of AMBCOM performance.

AMBCOM exhibited small absolute values of average error, i.e., 7-11 dB, and high percentages of matched records. The average error was typically distributed between -20 and +20 dB. Unfortunately, these are only relative measures of model performance. The site antenna and environmental data used to model high latitude campaigns were estimated not measured, and some variation in AMBCOM results may be attributable to poor estimates. The measured data were not designed specifically for model validation, and further comparisons are needed with new measured data.

## TABLE OF CONTENTS

## LIST OF TABLES

## LIST OF FIGURES

## ACKNOWLEDGEMENTS

The author wishes to express his appreciation to Dr. Richard W. Adler and Mr. W. R. Vincent for their unfailing aid and encouragement throughout the course of this work. Their patience and guidance have been invaluable.

The author also wishes to thank Dr. Robert Hunsucker, Dr. Tudor Jones, Dr. Mike Warrington, Ms. Jane Perry, Mr. Bob R. Rose and Ms. V. Elaine Hatfield for their technical assistance.

Finally, the author wishes to thank his wife and children for their encouragement and assistance throughout his graduate studies.

# I. INTRODUCTION

## A. GENERAL

During the summer of 1986 URSI sponsored a Workshop on the Practical Aspects of Ionospheric Modeling. The conference was attended by thirty-three scientists from five countries. The goal of the conference was to bring together ionospheric scientists and practioners to discuss ionospheric modeling. One of the recommendations which resulted from this conference was the following:

> There is a need to have a standardized set of data that can be used to verify ionospheric models. These data should be independent of the models that are being verified. The data need to be representative of the entire range of season, solar, and geomagnetic activity variations that is observed in practice. [Ref. 1: p. 7-13]

The purpose of this thesis is to examine the accuracy of propagation predictions from the Ambient Communications (AMBCOM) computer-based model. This is done by comparing the signal-to-noise ratio (SNR) data generated by AMBCOM with the SNR data recorded during Project NONCENTRIC. The Project NONCENTRIC data are the signal and noise strengths of transmissions which were broadcast from one site via an omni-directional antenna to several receiver sites during three high latitude communication experiments (campaigns) [Ref 2].

This thesis is divided into five chapters. The first chapter is a brief overview of the morphology of the high latitude ionosphere as it applies to AMBCOM. Chapter one also describes previous computer-based model evaluation work. The second chapter will describe the AMBCOM algorithms. Chapter three will characterize the Project NONCENTRIC data and describe how the data were assembled. The fourth chapter will compare the AMBCOM data with the Project NONCENTRIC data. The thesis then concludes with recommendations in chapter five.

## B. THE POLAR IONOSPHERE

### 1. The Earth's Magnetic Field

The earth's magnetic field may be approximated by an earth-centered dipole field which is tilted slightly out of the axis of the earth's rotation. At the present time the northern pole of the dipole is located approximately at 78.8° N, 70.9°W using the geographic coordinate system [Ref. 3: p. 83]. As illustrated in Figure 1 on page 2 the earth's magnetic field is distorted from the expected dipole shape by the effect of the

solar wind. Traveling at speeds near the earth of 200 to 700 km/s, the solar wind bends the earth's magnetic field into a teardrop shape with the tail of the field located opposite of the earth's sunward side [Ref. 1: pp. 2-14;2-21]. The tail of the field can extend outward several earth radii depending upon the force of the solar wind [Ref. 1: p. 2-17].

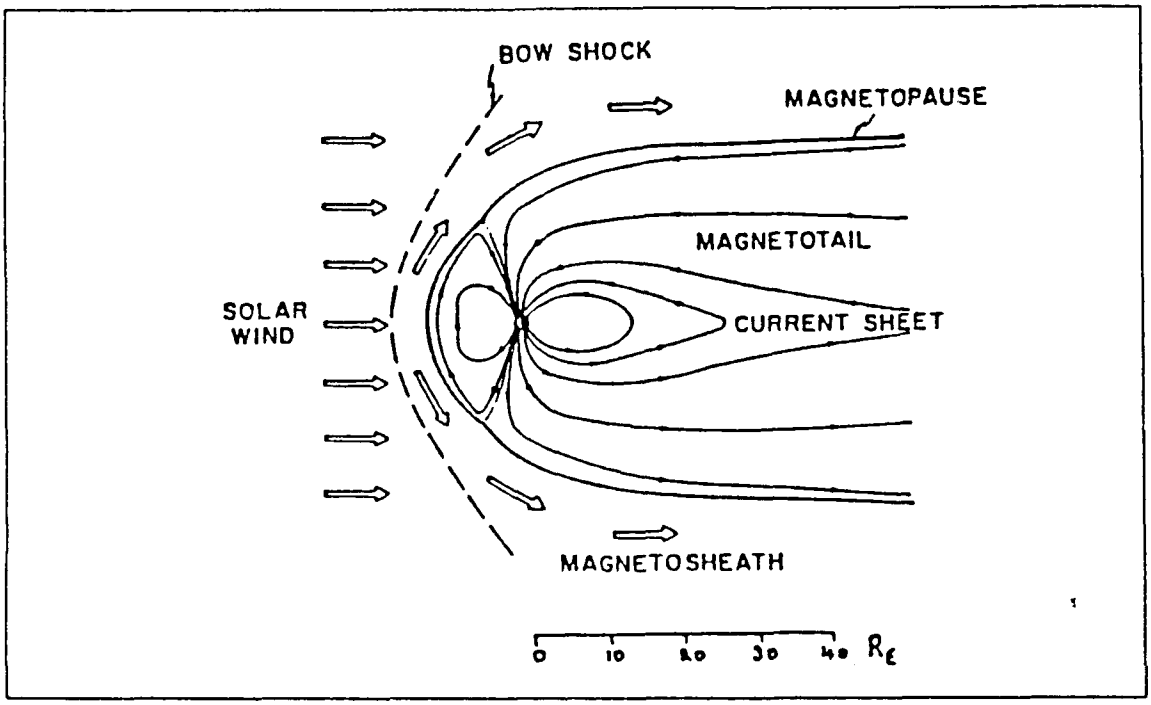


**Figure 1. The earth's magnetic field showing the effects of the solar wind.** [From Ref. 6: p. 2-25]

AMBCOM uses the three-hour $K_p$ index of worldwide magnetic disturbance to specify the current state of the earth's magnetic field. This index is based upon local K indices which are semi-logarithmic values prepared at twelve selected observatories located between 48° and 63° geomagnetic latitude, north and south. The local K indices are values assigned by a local observatory to describe the condition of the planetary magnetic field at the measuring site. These local K values are then corrected and used to calculate the planetary $K_p$ index. [Ref. 4: pp. 49-51]

The $K_p$ index is calculated at three hour intervals for a total of eight periods per day. The $K_p$ index ranges in value from zero, the least disturbed state, to nine which represents the most disturbed magnetic field. Typically the $K_p$ indices are calculated monthly and published in tabular form. The $K_p$ indices used for this thesis were prepared by the Geophysikalisches Institut, University of Gottingen and tabulated in the

Journal of Geophysical Research [Ref. 5]. These $K_p$ indices were as low as zero and as high as seven which means that the geomagnetic field varied from a nondisturbed to a considerably disturbed state.

When studying or modeling the ionosphere, the geomagnetic coordinate system is commonly used to map the ionosphere to an earth-bound coordinate system. This is understandable in light of the fact that the earth's magnetic field plays a prominent part in the formation and variability of the ionosphere. The geomagnetic coordinate system is based upon the geographic location of the earth's magnetic poles. The geomagnetic equator is displaced 90° from the geomagnetic poles. The longitudinal origin for this geomagnetic system is the meridian line which passes through the north and south geomagnetic poles and through the geographic south pole [Ref. 3: p. 84]. Davies [Ref. 4: p. 40] relates the two systems with the equations

$$\sin \Phi = \sin \phi \sin \phi_0 + \cos \phi \cos \phi_0 \cos(\lambda - \lambda_0) \tag{1}$$

and

$$\sin \Lambda = \frac{(\cos \phi \sin(\lambda - \lambda_0))}{\cos \Phi}, \tag{2}$$

where

$\phi_0$ = geographical latitude for the northern geomagnetic pole,

$\lambda_0$ = geographical longitude for the northern geomagnetic pole,

$\phi$ = geographical latitude,

$\lambda$ = geographical longitude,

$\Phi$ = geomagnetic latitude and

$\Lambda$ = geomagnetic longitude.

Although AMBCOM makes the geographic-to-geomagnetic coordinate conversion for the user, an understanding of the geomagnetic coordinate system is useful with regard to understanding the AMBCOM model.

## 2. Particle Precipitation

As the solar wind passes the earth, electrons, protons and other particles are captured by the earth's magnetic field. A captured particle does not fall directly to the earth but follows a spiral path along the magnetic field lines with velocity components parallel and perpendicular to the magnetic field. As a particle moves to higher latitudes the magnitudes of the components of its velocity vector change, but the total particle

energy remains constant. This is due to the bending of the magnetic field lines relative to a particle's velocity as the earth's magnetic field returns to the ground at the magnetic poles. Increasingly the particle's velocity becomes perpendicular to the magnetic field. The forward motion of the particle towards the pole stops and then reverses. The particle then begins follow a spiral path towards the opposite geomagnetic pole, and, again, the components of the particle's velocity vector change as the magnetic field lines bend earthward. Forward motion again stops and reverses. This point of reflection is called the mirror point.

Depending upon the location of the mirror point, the particle can be trapped in the earth's magnetic field indefinitely. If the particle's mirror point, which is dependent upon its pitch angle when it entered the earth's geomagnetic field, is above the atmosphere then the particle will continue to reflect between the north and south mirror points. If the mirror point is within the atmosphere then the particle may collide with other particles in the upper atmosphere, lose energy and precipitate into the polar ionosphere. This particle precipitation leads to increased radio signal absorption, i.e. auroral absorption and polar cap absorption (PCA), as well as visual displays of aurora borealis. Energetic electrons are the major cause of auroral absorption and the visible aurora. These particles have an energy level of about 10-100 KeV. PCA is attributed to the heavier but more energetic 10 MeV protons. [Ref. 6: pp. 2-18;2-20]

### 3. The Auroral Oval

The auroral oval, see Figure 2 on page 6, is the region where the visible aurora is most often observed (between 64° and 70° north geomagnetic latitude) [Ref. 4: p. 51]. The visible aurora is the result of the precipitation into the upper atmosphere of electrons which have been carried to the polar regions by the earth's magnetic field. Since the amount of precipitation depends upon the number of particles available, any occurrence which increases the number of particles captured by the earth's magnetic field will increase particle precipitation in the auroral zone. During a solar event, such as a solar flare, large numbers of high energy particles are ejected from the sun. These particles speed towards the earth and cause a disturbance in the earth's geomagnetic field which leads to particle precipitation in the polar regions. Jones [Ref. 2] makes the metaphorical comparison of particles traveling along the magnetic field lines as being in tubes something like a tube of toothpaste. When a disturbance occurs in the earth's magnetic field the particles (which are moving between the mirror points) are "squeezed out" into the high latitude upper atmosphere. This results in higher propagating frequencies and auroral absorption.

The size and location of the auroral oval at any given time is variable because of its dependence upon particle precipitation which varies with solar activity . The oval is usually thicker and extends equatorward on its midnight side and migrates poleward on the noon side [Ref. 7: p. 348]. The midnight side of the oval is where substorm activity begins before it follows the electrical potential gradient toward the oval's noon side [Ref. 8: pp. 431-437]. In addition to the visible aurora these particles also produce ionization which results in auroral absorption, sporadic E, and other high latitude phenomena which do not always coincide with the location of the auroral oval [Ref. 4: pp. 332-336].

Equatorward of the auroral oval is a region of low ionization density called the midlatitude trough. The midlatitude trough is caused by ionospheric currents resulting from the large electrical potential difference between the day and night side of the polar region. Hargreaves [Ref. 1: p.7-7] describes the trough as a nighttime occurrence between 60° and 65° geomagnetic latitude during all seasons. During the summer months the midlatitude trough occurs closer to midnight. At night and during magnetic storms the trough moves equatorward. The midlatitude trough is of interest to the communicator because it effects propagation paths. Critical frequencies within the trough can be as low as 1 MHz. Higher frequency transmissions along paths with reflection points in the midlatitude trough are not reflected downward and pass into space.

**4. High Latitude Propagation Anomalies**

The higher latitude ionosphere is not as dependent upon direct solar x-ray and ultraviolet radiation for the creation of ionization layers such as the D, E, sporadic E or F layers. The layering of the polar ionosphere is produced by a combination of solar radiation and particle precipitation. The contribution of particle precipitation is observable as increased ionization density in the E layer and a reduction in $F_1$ ionization density during periods when the solar zenith angle ($\chi$) is greater than 90° [Ref. 9: p. 28]. As can be seen in Figure 3 on page 7, auroral absorption exhibits two maximums, one at midnight and one at noon. Hargreaves [Ref. 10: p. 1358] states that there is a definite correlation between the amount of magnetospheric disturbance and increased auroral absorption. An increase in the $K_p$ index would presage an increase in auroral absorption due to particle precipitation into the auroral oval. Hargreaves [Ref. 10 : p. 1358] states that increases in the density and speed of the solar wind correlate with changes in $K_p$. An increase in solar activity results in an increase in the number of particles captured by the earth's geomagnetic field. One result of this process is more auroral absorption.

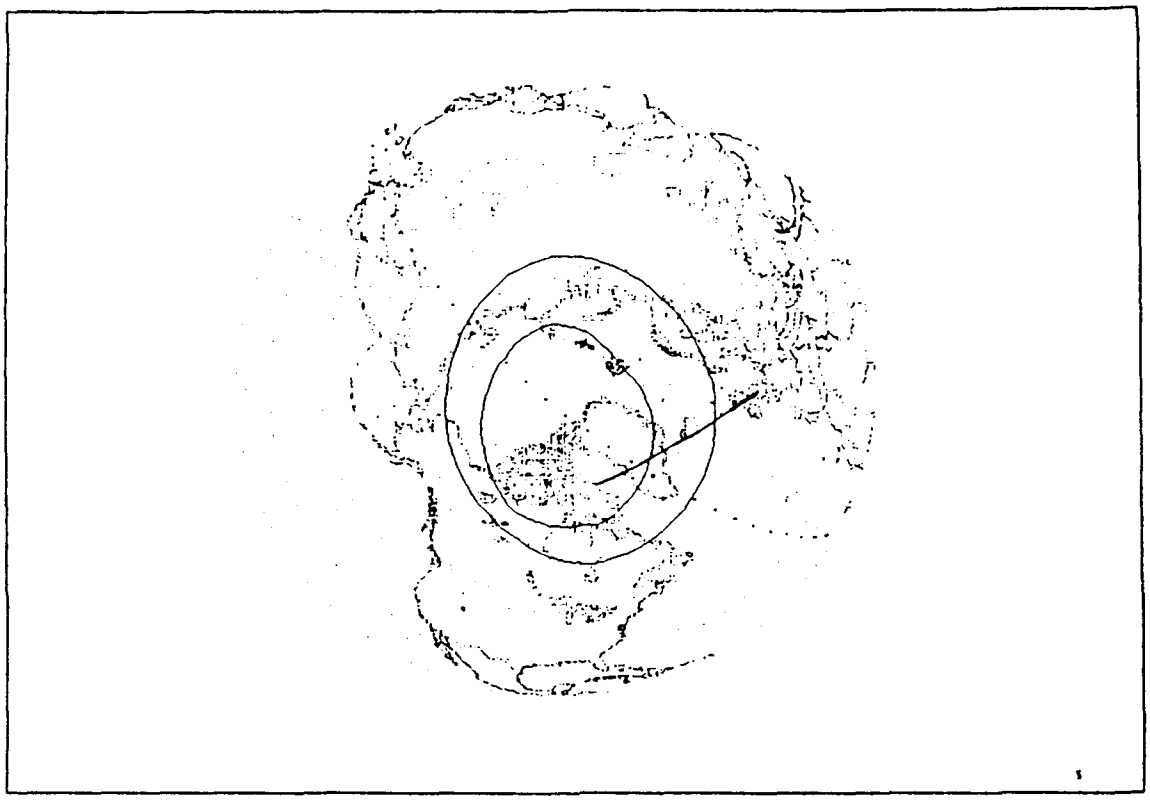

**Figure 2. The auroral oval and the propagation path from Clyde River to site O.**

In addition to the auroral absorption, communication signals at high latitudes may follow non-great-circle (NGC) propagation paths. At lower latitudes HF signals generally follow a great circle path from transmitter to receiver. High latitude signals can be reflected in a direction that is perpendicular to the great circle propagation path. Hunsucker [Ref. 7: pp. 348-351] states that NGC propagation may be attributable to sidescattering due to irregularities in the ionosphere. The incidence of NGC modes have been found to vary with the amount of magnetic activity. The final result for the communications engineer and the AMBCOM user is that signal strengths predicted by a model may not match measured signal strengths because the effects of NGC are not included in the model. During times when magnetic activity is high, the inability of the computer-based model to accurately predict signal strengths at given frequencies may be attributable in part to non-great-circle paths.

The occurrence of sporadic E ($E_s$) at higher latitudes is important to communication in the HF band. $E_s$ provides additional paths for propagation at HF frequencies

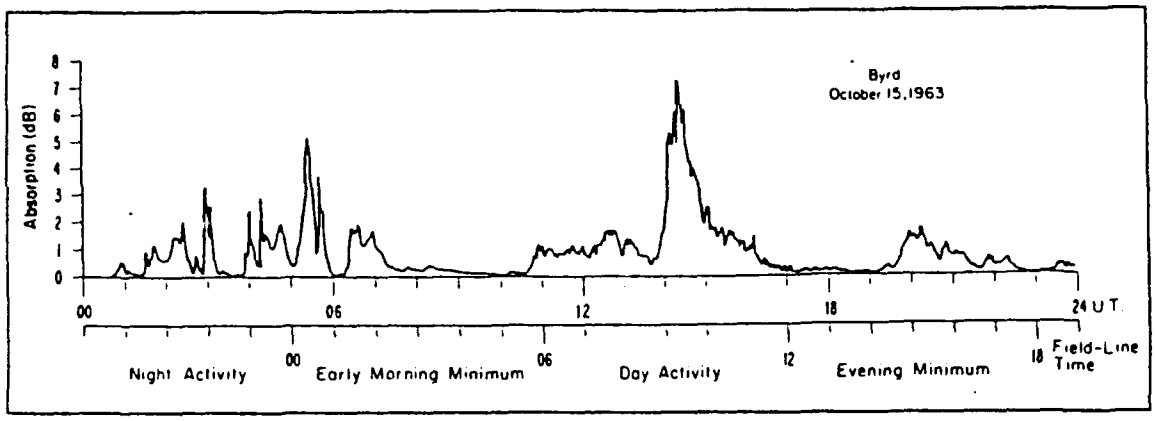


**Figure 3. A typical day in auroral absorption. [From Ref. 10: p. 1361]**

as well as some attenuation of signals propagated by other modes. Hunsucker [Ref. 7: p. 353] described the effect of $E_s$ resulting from measurements taken for propagation paths between Thule (Greenland) and College (Alaska) as well as for a path from Andoya (Norway) and College as follows:

> In particular, for winter-night sunspot minimum conditions on the Thule-College and Andoya (Norway)-College path, $E_s$ modes had an average occurrence over 50%. $E_s$ MOF's as high as 46 MHz with typical values of 18 MHz were observed.

As can be seen in Figure 4 on page 8 the percentage of sporadic E varies with time and latitude. In the auroral oval the average percentage of $E_s$ is at a maximum during the evening hours and at its lowest at noon. Hunsucker [Ref. 7: p. 351] states that $E_s$ is more prevalent and with higher maximum observable frequencies (MOF's) during the winter months compared to summer months. $E_s$ was included in some path calculations made by AMBCOM. In addition some effort was made to adapt the percentage of $E_s$ to the time of day and year. The results from $E_s$ calculations were then compared to data from AMBCOM which included no $E_s$ calculations. [Ref. 7: p. 351]

The polar ionosphere does include F layers similar to those found at the midlatitudes. The distinction between the polar F2 layer and the F1 layer may not be as dramatic as at lower latitudes. F1 mode propagation is frequently observed during the summer, especially in the morning. This is because the F2 layer critical frequency decreases with increasing latitude at a faster rate than the F1 critical frequency. [Ref. 7: p. 335]. The F1 mode is the dominant means of long-range propagation during periods of low sunspot activity, particularly during the low end of the eleven year sunspot cycle.

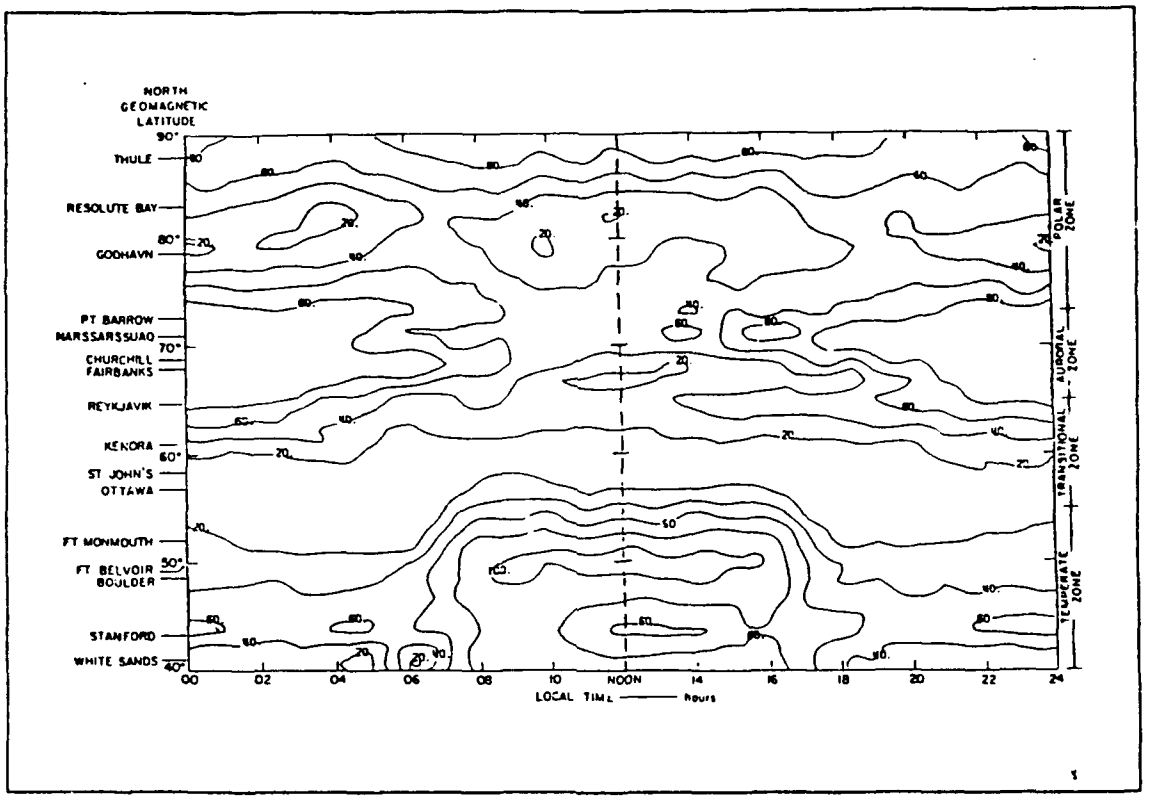


**Figure 4. The average percentage of sporadic E by geographic latitude and time of day. [From Ref. 7: p. 352]**

Vondrak [Ref. 9: p. 38] noted that the ionization density profiles recorded by the Chatanika radar showed a valley between the E layer and the F2 layer when the layer was not sunlit. This valley disappeared during the day and during periods of high particle precipitation.

## C. PREVIOUS PROPAGATION MODEL STUDIES

How accurately can high latitude propagation be predicted using the computer models that are presently available? Presently there is not a complete answer to this question. Although individual studies have been carried out comparing the output from computer models to the data recorded from transpolar and polar communication paths, these studies were not intended to be comprehensive comparisons of the accuracy of numerous models relative to one another using one set of recorded transmissions.

### 1. The Rockwell International Study

During fiscal year (FY) 1987, Rockwell International completed a transauroral high-frequency (HF) radio transmission experiment (TAHFE). The experiment consisted of recording, at Cedar Rapids, IA, transmissions from Barrow, AK. The transmissions were made by stepping through a selected set of frequencies at specific times. Figure 5 on page 10 is a block diagram of the equipment used for this experiment.

In addition to the transmissions, data were recorded which described the ionosphere, solar activity and HF channel parameters at any given time. Solar geophysical data were collected from the U.S. NOAA Space Environment Services Center (SESC) [Ref. 11: p. 2]. The HF channel parameters where measured by Rockwell International engineers using the advanced link quality analyzer (ALQA). These data were recorded on computer disk for later analysis. Using SESC data and with the aid of solar event alerts from the Geophysical Institute at Fairbanks, AK, the experiments were able to match measured channel parameters to solar activity. [Ref. 11: pp. 1-3]

Three computer models, i.e., IONCAP, MINIMUF and AMBCOM, were used to generate predicted maximum useable frequencies (MUF) using the recorded solar-geophysical data as a primary input for the prediction models. All models produced good approximations of MUF values that were actually recorded during the experiment. AMBCOM was able to predict the effects of solar events upon the transpolar path such as the a communications blackout on 12 November 1986. [Ref. 11]

### 2. High-Latitude HF Predictions From RADAR C and AMBCOM

Nikhil Dave of the Naval Ocean Systems Center (NOSC), San Diego, California, conducted a comparison of the data produced by two models (RADAR C and AMBCOM) and polar sounder data recorded for the Winipeg-Resolute Bay path during 1959 and data recorded during 1964 over the two paths (Andoya-Ft. Monmouth and Andoya-College during 1964). The former data were recorded during a period of high sunspot activity and the latter data during a period of low activity. The intent of the study was to produce a predicted MUF and to compare it with recorded data. AMBCOM was found to be more accurate than RADAR C because AMBCOM includes adjustments for auroral absorption and other polar anomalies. [Ref. 12 ]

### 3. The Naval Postgraduate School Studies

The work at the Naval Postgraduate School was intended to compare the performance of as many models as possible to the same measured data, antenna gain, and control parameters. NPS students examined the relative performance of IONCAP, PROPHET, and AMBCOM. In the future, a new high-latitude propagation model,

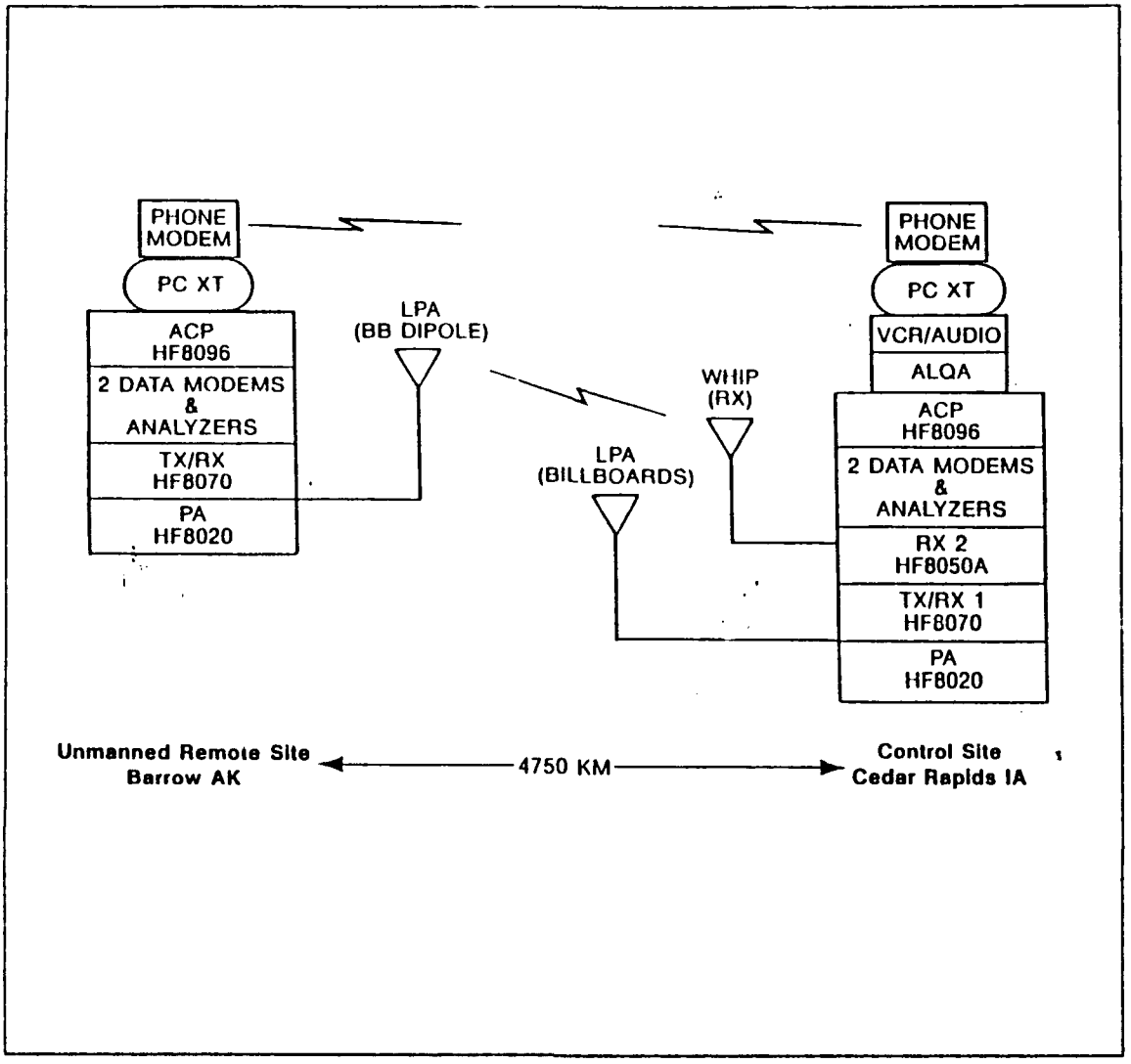


**Figure 5. TAHFE equipment suite that was used for the Rockwell experiments.** [From Ref. 11]

ICEPAC, will be studied. The comparison of data generated by IONCAP and PROPHET were completed and published [Ref. 13 and 14 ], and may be compared to this AMBCOM analysis (see Appendix D). It is hoped that the results of these studies will guide the future creation of a standard model validation data base and the establishment of guidelines for computer-based propagation prediction model evaluation.

# II. THE AMBIENT COMMUNICATIONS MODEL (AMBCOM)

## A. INTRODUCTION

This chapter provides a brief description of applicable portions of AMBCOM. Details of the internal functioning of AMBCOM are contained in the user's guides published by SRI International [Ref. 15 , 16 and 17].

AMBCOM is designed for batch processing using card images as input. Separate programs support each of the function areas modelled, i.e., the ionosphere model is generated by a program which passes its data to another program for raytracing calculations. The system flow is first explained followed by the programs and inputs which generate the high latitude data.

## B. SYSTEM FLOW

The AMBCOM system is a multiprogram batch system written in FORTRAN and was run on a VAX 3100 workstation at NPS. Programs NATGEN, RAYTRA, and COMEFF were used to generate the high-latitude data, as shown in Figure 6 on page 12. Data are passed between these programs by means of saved data files. [Ref. 15 : pp. 107-155]

Since AMBCOM programs pass data through standard files, the user must be careful with regard to the timing of program execution. Several campaigns were modeled in this study. If two campaign decks were executed simultaneously and the programs did not terminate due to file access collisions, then the accuracy of the contents of a passed file could not be guaranteed. The user has the option of either changing the names of the passed files so that these file names differ from one campaign input stream to another or to simply run one campaign input stream at a time. The latter method was chosen so that each execution of AMBCOM would not share the assets of the VAX 3100.

The execution input streams were constructed for all 25 days of a particular campaign in only one computer run. Separate AMBCOM input streams were created for each site during the campaign. This entails the construction of an input stream for NATGEN, RAYTRA, and COMEFF, representing each $K_p$ three-hour interval and eight intervals per day for 25 days. Each campaign input stream was approximately 13,300 lines in length, and required two and half hours of execution time.

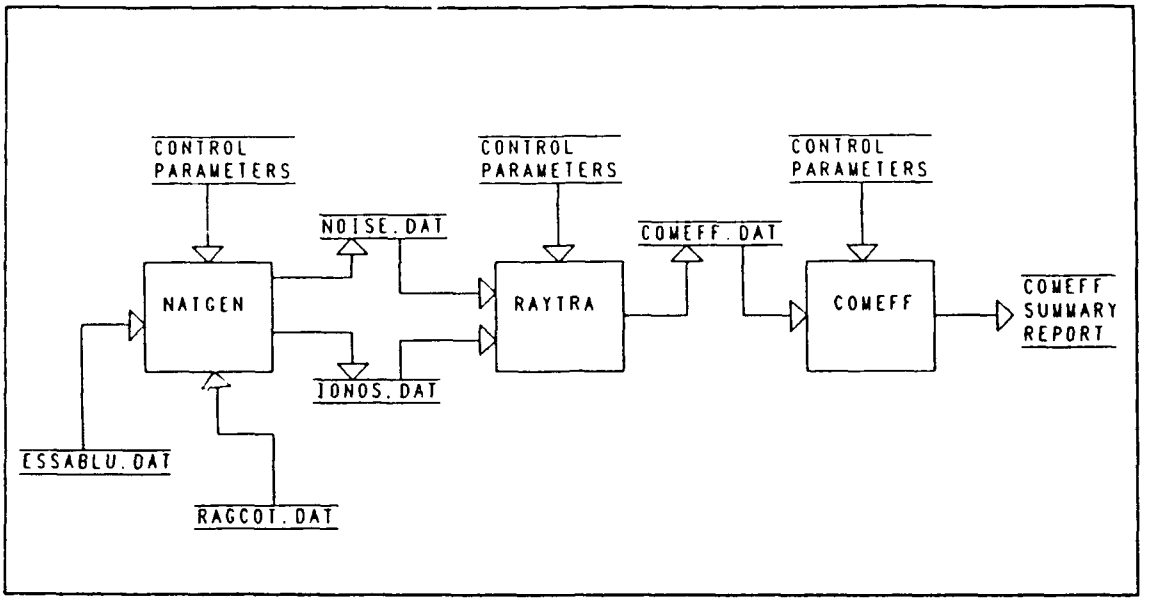


**Figure 6. AMBCOM system flow showing the passage of data between programs.**

The data produced by AMBCOM for each of the three hour intervals was accumulated in files for later processing. This is not a problem because the VAX 3100 workstation allows the use of multiple generation data sets. These data sets were easily concatenated at the end of the campaign's execution stream into one large file representing all the data for one campaign.

## C. NATGEN

### 1. Overview

The purpose of NATGEN is to model the ionosphere along the communication path between two points. NATGEN builds a model of the F2, F1, and E layers at control points along the path. The control points are evenly spaced at 100 km increments with a maximum of 41 control points for paths longer than 4000 km. The control points are not necessarily located at the signal reflection points since raytracing is performed in RAYTRA. [Ref. 15: pp.23-24]

NATGEN begins by reading ionospheric coefficients provided by the Institute for Telecommunications Sciences (ITS) in Boulder, Colorado, based upon the month, day, and the current sunspot number. AMBCOM uses the ITS Blue Deck[1] as the

[1] A reference to earlier coefficient files that were issued on color trimmed computer cards.

starting point for the modeling of the $F_2$, $F_1$ , and E layer at each control point. Additional parameters describing atmospheric noise, ground conductivity, and ground permitivity along the path are read and passed to RAYTRA. [Ref. 15 : p.23]

The semithicknesses, heights of maximum ionization, and the critical frequencies for the $F_2$, $F_1$ and E layers at each of the control points are passed as outputs from NATGEN. ITS upper, median and lower decile values for sporadic E critical frequencies are passed to RAYTRA which performs all $E_s$ calculations. NATGEN also passes on the location of the transmitter and receiver sites, the time of year, time of day, the current $K_p$ index, the sunspot number, distance between control points, the number of control points, and the path length. [Ref. 16: pp.123-124]

**2. Layer modeling**

The ITS provides the vertical incident critical frequency ( $f_o$ ) for the E layer, the $F_2$ layer, and sporadic E. The E layer critical frequency ($f_oE$) is always set to the median decile values. For the sporadic E and the $F_2$ layer, the upper, median, and lower decile values represent the critical frequencies 90%, 50%, and 10%, respectively, of the days for a given time and month [Ref. 18: p.89]. NATGEN allows the user to choose which of the $F_2$ layer values will be used as the $F_2$ critical frequency ($f_oF2$) for all ionospheric calculations. The default $f_oF2$ value is the median decile number. Two additional parameters for the $F_2$ layer are the ratio of the semithickness of the layer ($y_m$) to the height of maximum density ($h_m$) and the maximum usable frequency for a 3000 km path (M3000). [Ref. 15: p.25]

Using these coefficients, AMBCOM models the ionosphere at the control points. The $F_2$, $F_1$ and E layers are represented as three parabolic layers with the values for the $F_1$ layer derived from the $F_2$ and E layer models. The height and semithickness of the E layer are set at 115 km and 25 km respectively. The $F_2$layer height is calculated using the ITS coefficients in a two step process. First the peak height of the $F_2$ layer ( $HP_{F2}$) is calculated using the Shimazaki equation [Ref. 15: p. 26]

$$HP_{F2} = \frac{1490}{M3000} - 176. \tag{3}$$

This value is corrected for signal retardation with a height factor ($\Delta h$) equation [Ref. 15: p.26]

$$\Delta h = \left[ \frac{f}{f_c} \ln\left( \frac{f/f_c + 1}{f/f_c - 1} \right) - 2 \right] y_m, \tag{4}$$

where

$\Delta h$ = the height error,

$f_c$ = the critical frequency of the layer,

f = the transmitted frequency and

$y_m$ = the semithickness of the layer.

The $\Delta h$ factor is then subtracted from $HP_{F2}$ to produce a corrected height for the $F_2$ layer.

The $F_1$ layer parameters are not represented by ITS data but are calculated using the E and $F_2$ layer parameters. The $F_1$ layer must overlap the $F_2$ layer by half of its own semithickness with the bottom of the $F_1$ layer set at 130 km. The critical frequency of the $F_1$ layer is calculated based upon the critical frequency of the E layer ($f_oE$). In the event that the $F_2$ layer critical frequency is lower than that for $F_1$ $f_oF1$ is set to 0.695 $f_oF2$. [Ref. 15: p.27]

### 3. High-Latitude Corrections

Before any correction for high-latitude propagation paths can be made NATGEN must define the auroral oval using the Miller-Gibbs model [Ref. 15: pp. 28-30] with a value for the width of the oval in the path (X) and the location of the lower boundary of the oval ($\phi_A$). The lower boundary is

$$\phi_A = 71.9° - 2.5K_p - 5.1 \cos\left[\frac{2\pi}{24}(t_m - 1)\right] \tag{5}$$

and must lie between the boundaries

$$\phi_{\min} = 68.9° - K_p - 5.1 \cos\left[\frac{2\pi}{24}(t_m - 1)\right] \tag{6}$$

and

$$\phi_{\max} = 70.9° - K_p - 5.1 \cos\left[\frac{2\pi}{24}(t_m - 1)\right], \tag{7}$$

where

$t_m$ = geomagnetic time.

The width is calculated as

$$X = 7.0° - K_p. \tag{8}$$

The oval width is limited to between four and six degrees of latitude.

NATGEN is designed to accommodate propagation modeling at high latitudes by correcting critical frequencies for the $F_2$ layer ($f_oF2$) and the E layer ($f_oE$). Corrections are made to $f_oF2$ if the geographic latitude of the control point meets one of the following criteria:

- The point is located at greater than 45° North (corrected geomagnetic latitude ($\lambda_m$)).
- The point is located within the auroral oval.
- The point is in the nighttime midlatitude trough.

All the points used in this thesis are north of 45°N latitude and so the first criteria always applies. The correction applied to $f_oF2$ at high latitudes is a two step process. First $f_oF2$ is adjusted according to the first criteria above using

$$f_oF2_A = f_oF2_{ITS}\,[1 - \delta_{Kp}]\,, \tag{9}$$

where

$f_oF2_A$ = $f_oF2$ adjusted for high latitude,

$f_oF2_{ITS}$ = the F2 layer critical frequency from the ITS file and

$\delta_{Kp}$ is a function of $K_p$.

All other corrections are applied to this adjusted value. [Ref. 15: p. 29]

The second step is to adjust $f_oF2$ if the control point is in the midlatitude trough or the auroral oval. All control points that are north of the equatorward edge of the auroral oval are considered auroral oval corrections. Auroral oval adjustments are calculated based upon the location of the control point in reference to $\phi_A$ and X. The correction is calculated using the Miller-Gibbs equation [Ref. 15: p. 29]

$$f_oF2 = f_oF2_A\left[1 + 0.4946\,X_g\,e^{-1.125X_g^2}\right]\,, \tag{10}$$

where

$$X_g = \frac{|\,\lambda_m - \phi_A\,|}{X}\,. \tag{11}$$

This last parameter is the normalized distance referenced to the equatorward edge of the oval. [Ref. 15: pp.29-30]

The correction for the midlatitude trough accounts for the effect of this region on $f_oF2$. In this region the critical frequency can be as low as 1 to 2 MHz and a signal which enters this part of the ionosphere may penetrate into space. NATGEN makes corrections for the midlatitude trough only when the ionosphere is not sunlit, e.g., the solar zenith angle ($\chi$) is greater than 90° and the corrected geomagnetic time is between 1800 and 0600. Reference 15, pages 30 thru 31, provides complete details of the correction equations used by NATGEN.

The high-latitude correction to $f_oE$ is much different than that for $f_oF2$. This is due to the fact that E layer propagation at higher latitudes is dependent upon solar radiation and particle precipitation. The location of this auroral E zone will vary with the time of day and with magnetic activity. NATGEN compensates for this by first modeling the boundary of the auroral E zone and then calculating $f_oE$ based upon the separate values for the E layer critical frequency due to solar radiation ($f_oE(solar)$) and particle precipitation ($f_oE(auroral)$). [Ref. 15: p. 31-35]

The local K index is an indicator of particle precipitation which results in higher E layer ionization densities. The magnetic field at higher latitudes is much different from that at midlatitudes and is not well represented by $K_p$. The $K_p$ index reporting stations are mostly located in midlatitudes and therefore the index is weighted more heavily in favor of midlatitude values. Hatfield [Ref. 15: p.32-33] states that $K_p$ does not produce high latitude modeling results which correlate well with measured data, but using the local K index value does produce a stronger correlation to measured data. NATGEN has been adapted to estimate the local K index based upon the corrected geomagnetic latitude, the corrected geomagnetic time and the current $K_p$ index. This local K index value is used to calculate $f_oE(auroral)$.

The final step of the process is to combine the value for $f_oE(solar)$ with that for $f_oE(auroral)$. According to Hatfield [Ref. 15: p.35] the final value for $f_oE$ is given by the equation

$$f_oE = \sqrt[4]{1.5 f_oE(auroral)^4 + f_oE(solar)^4}\,. \tag{12}$$

The $f_oE(auroral)$ is given more weight than $f_oE(solar)$ since particle precipitation heavily influences the E layer at high latitudes.

## 4. NATGEN Input Variables

AMBCOM is a batch system in which the input stream which controls the execution of the system resembles a series of 80 column computer cards. AMBCOM was originally designed during the 1970s when card input systems still predominated [Ref. 15: p.15]. Figure 7 on page 18is an example of statements used to execute NATGEN. The ASSIGN statements provide NATGEN access to the ITS file (ESSABLU.DAT), the conversion tables for the geomagnetic coordinate system (RAGCOT.DAT), two output files (IONOS.DAT and NOISE.DAT), and execution control cards one through four.

AMBCOM provides a large amount of flexibility in the control of data production. NATGEN models the ionosphere along any propagation path at any hourly time increment specified by the numbered control cards. The AMBCOM user defines the problem by specifying the transmitter and receiver locations, the sunspot number, the $K_p$ index, the time increment, and the use of auroral layers.

Control parameters were chosen to model the ionosphere, as closely as possible, to the Project NONCENTRIC transmission paths. The intent was to execute the model from the perspective of a communicator who is attempting to estimate the possibility of communicating with another HF site under a given set of circumstances. Although the communicator does not have the advantage of using the sunspot number and $K_p$ index tables for a current month, he should have a rough estimate of the current sunspot number and K indices at any given time.

Figure 7 on page 18 shows the four control cards used to execute NATGEN. Card one is used to specify the use of auroral particle densities for all layer calculations, and card two causes NATGEN to run the ionspheric generator program. Card three defines the geographic latitude and longitude of the transmitter and receiver; negative numbers indicate a west longitude. Following the location information are the year, month, sunspot number, and $K_p$ index. Card four indicates the beginning hour, ending hour and time increment.

Input streams were divided into three hour periods over a 25 day period. This was for modeling the ionosphere during each of the three hour $K_p$ index periods throughout the day. The values for sunspot number and $K_p$ index were taken from the *Journal of Geophysical Research* [Ref. 5, 19, 20, and 21]. The days of the month and hourly time increments were derived from Project NONCENTRIC data.

```
$DEL OWINTEMP.DAT;*
$DEL COMOUT.DAT;*
$!3456789012345678901234567890123456789012345678901234567890123456789012345678901234567890
$!
$!  FREQUENCY MANAGEMENT BETWEEN A SPECIFIED TRANSMITTER AND RECEIVER
$!18 JANUARY 1989
$!****** BEGIN KP PERIOD 1 ************************************************************
$!  ****INPUT SETUP FOR NATGEN****
$!
$SET DEFAULT DKA0:[AMBCOM]
$ASSIGN DKA0:[AMBCOM]ESSABLU.DAT FOR001:
$ASSIGN DKA0:[AMBCOM]RAGCOT.DAT FOR075:
$ASSIGN DKA0:[AMBCOM]IONOS.DAT FOR002:
$ASSIGN DKA0:[AMBCOM]NOISE.DAT FOR004:
$ASSIGN SYS$INPUT: FOR058:
$ASSIGN DKA0:[WILSON]NATOUT.DAT FOR059:
$R DKA0:[AMBCOM]NATGEN
1         1          0          0          0          0
 BEGIN THESIS WORK WITH AMBCOM
2         1                                           1
3     70.00     -69.00      53.00     -01.00      1989      01.0      231.0       4.0
4       0.         2.         1.
```

Figure 7. NATGEN control cards used to model winter site O propagation data .

## D. RAYTRA

### 1. Overview

The raytracing program (RAYTRA) model is divided into two modes, point-to-point and radar. The point-to-point mode performs raytracing from a transmitter to a receiver and was used for this thesis. RAYTRA computes group times, phase time, signal losses, the effects of sporadic E and elevation angles at both points. These data are saved for each successful propagation path and are passed to COMEFF.

The raytracing algorithm computes the propagation path based data produced by NATGEN. A raytrace which ends within 1000 km of the receiver site is saved for further processing. When two rays bracket the receiver, the program interpolates a ray that falls within some preset value, in this case ten kilometers. The parameters describing this ray are saved for COMEFF. In the case where only a single ray is found, the program again interpolates until a ray close to the receiver is found. The AMBCOM

User's Guide For Engineers [Ref. 15: pp.35-56] provides an in-depth treatment of raytrace algorithms.

RAYTRA estimates the amount of absorption for each ray. The absorption calculations are divided into four parameters as follows:

- $L_D$ is the divergence, i.e. free space spreading loss.
- $L_A$ ionospheric absorption loss such as deviative, nondeviative, and auroral losses.
- $L_{Es}$ is the loss resulting from sporadic E.
- $L_G$ is the loss due to ground reflections along the path.

The total loss for a path is the summation of all of these factors. Only ionospheric absorption as it applies to auroral absorption will be described here. A full explanation of the RAYTRA path loss algorithms may be found in Reference 15, pages 56 thru 80.

**2. Auroral Absorption.**

RAYTRA models the auroral absorption using a modified Foppiano model [Ref. 15: pp. 64-71]. The adaptations made to this model by SRI provide the model with some dependence upon the $K_p$ index. Auroral absorption is related to particle precipitation which is, in turn, heavily influenced by the activity of the geomagnetic field and $K_p$ is a descriptor of the current state of the planetary magnetic field. The sunspot number (which is used by the Foppiano model) does not correlate well with changes in the magnetic field and it is not a good indicator of the amount of auroral absorption present.

The Foppiano model produces a median value for auroral absorption based upon the combined effects of substorm activity for a given hour of the day in a given month, and upon the level of solar activity. Solar activity is modeled with a 12 month running average of sunspot numbers which do not relate directly to geomagnetic field activity. Large variations in auroral absorption can be lost in the averaging process. On the other hand the addition of a large dependence upon $K_p$ could cause the model to produce incorrect results for quiet day predictions. SRI chose to include the $K_p$ index by the use of a normalized Gaussian distribution so that the location of the maximum amount of absorption is dependent upon $K_p$ but the magnitude of the maximum is not dependent upon $K_p$. [Ref. 15: pp. 64-65]

RAYTRA begins auroral absorption model by first calculating the factor $Q_1$ which is the one-way vertical absorption at 30 MHz that exceeds 1 dB. A riometer is used to measure changes in ionospheric absorption, at 30 MHz, in reference to quiet day

absorption levels. For RAYTRA the $Q_1$ factor is calculated from two other variables as

$$Q_1 = Q_{1d} + Q_{1s}, \tag{13}$$

$$Q_{1d} = 21\, d_\phi \times d_T \times d_R \times d_\theta \times d_m \tag{14}$$

and

$$Q_{1s} = 12\, s_\phi \times s_T \times s_R \times s_\theta \times s_m, \tag{15}$$

where

$d/s_\phi$ = the drizzle/splash precipitation latitudinal dependence,

$d/s_T$ = the drizzle/splash precipitation time dependence,

$d/s_R$ = the drizzle/splash precipitation sunspot dependence,

$d/s_\theta$ = drizzle/splash precipitation longitudinal dependence and

$d/s_m$ = the maximum latitude of drizzle/splash precipitation.

The term splash particle precipitation is associated with discrete ionospheric events that are limited spatially. Drizzle refers nearly constant and widespread particle precipitation that results from particle collisions in the upper atmosphere [Ref. 22: p.322]. The subscripts 1d and 1s refer to drizzle and splash precipitation, respectively. The only parameters modified for $K_p$ dependence are $d_\phi$, $s_\phi$, and $d_T$, which are the latitude of the drizzle component, the latitude of the splash component, and the time dependence. The remainder of the Foppiano model has not been modified. [Ref. 15 : pp. 64-66]

The latitude of the drizzle component of the model is calculated with the equation [Ref. 15: p. 66]

$$d_\phi = \exp\left[\frac{-[\phi - \phi_m]^2}{2\sigma_\phi^2}\right], \tag{16}$$

where $\phi_m$ is the latitude of maximum absorption and $\sigma_\phi$ is the latitudinal extent of the absorption zone. The $K_p$ influence is introduced with the equations [Ref. 15: p. 66]

$$\phi_m = \begin{cases} 67.864 - 0.6256K_p & ;K_p \le 5 \\ 75.616 - 2.176K_p & ;K_p > 5 \end{cases} \tag{17}$$

and

$$\sigma_\phi = \begin{cases} 3.06 + .2765K_p & ;K_p \le 5 \\ -.36 + .96K_p & ;K_p > 5 \end{cases}. \tag{18}$$

The $K_p$ influence for the time dependence is introduced similar to that for $\phi_m$. The time dependence is given by

$$d_T = \exp\left[ \frac{-[t_1 - T_m]^2}{15.7} \right], \tag{19}$$

where

$$T_m = \begin{cases} 9.9 - 0.46K_p & ;K_p > 5 \\ 15.6 - 1.6K_p & ;K_p \le 5 \end{cases}. \tag{20}$$

Both $d_\phi$ and $d_T$ are normalized Gaussian functions. [Ref. 15: p. 67]

The calculation of the splash component ($s_\phi$) is also performed with a normalized Gaussian equation as follows:

$$s_\phi = \exp\left[ \frac{-[\phi - \phi_{1m}]^2}{2\sigma_\phi^2} \right], \tag{21}$$

where

$$\phi_{1m} = \begin{cases} 66.799 - 0.9246K_p + (0.318 + 0.0828)\,|\,t\,| & ;K_p \le 5 \\ 78{,}256 - 3.216K_p + (.288K_p - .708)\,|\,t\,| & ;K_p > 5 \end{cases}, \tag{22}$$

$$t = \begin{cases} T - 3 & ;0 \le T \le 15 \\ T - 27 & ;15 < T < 24 \end{cases} \tag{23}$$

and T is the corrected geomagnetic time. This component value along with the others is used to produce $Q_1$. [Ref. 15: p.68]

$Q_\phi$ is used to calculate the median absorption value $A_m$, which must be adjusted from a monthly median value to one corresponding to $K_p$. The final value for absorption is obtained from

$$A_{Kp} = Y_{Kp}\, A_m, \tag{24}$$

where

$$Y_{Kp} = 1.8(0.17 + 0.14K_p). \quad (25)$$

The factor of 1.8 was included to scale the equation to match high latitude empirical data. [Ref. 15: pp.69-71]

### 3. Sporadic E Calculations

RAYTRA offers two choices for computing sporadic E ($E_s$). The first method computes the reflection of signals for frequencies below the blanketing frequency ($f_bE_s$). The blanketing frequency is computed based upon the location of the control point. The second method performs $E_s$ reflection calculations for all frequencies less than $f_oE_s$. The value for $f_oE_s$ is based upon the upper, median, or lower ITS $f_oE_s$ coefficients passed from NATGEN. The choice of value is specified by the user. RAYTRA calculates $f_oE_s$ dependent upon the percentage of $E_s$ specified by the AMBCOM user. If 90% $E_s$ is specified then RAYTRA uses the upper decile value of $f_oE_s$ from the ITS file. For 50% $E_s$ RAYTRA uses the median decile value. None of these $E_s$ models were designed to simulated sporadic E at high latitudes. [Ref. 15: pp.53-56]

RAYTRA offers two models for sporadic E ($E_s$) in reference to absorption loss, the Sinno model and the Phillips model. Based upon the work of Hunsucker [Ref. 7: p. 351], the author decided to examine the effect of differing amounts of $E_s$ on the generation of the model data. The Sinno model was chosen because it allows the user to choose which of the decile values to use for $f_oE_s$ for all sporadic E calculations. The Phillips model uses only the median decile value. [Ref. 15: pp.71-77]

### 4. RAYTRA Input Variables

RAYTRA, like NATGEN, provides the user with a number of options for controlling program execution. Options are specified with numbered control cards in-stream following the program execution statement. Figure 8 on page 23 is an example of the RAYTRA controlling statements used for this thesis.

Card two controls the amount of $E_s$ for a given execution. Three different types of input streams were chosen per campaign for comparing model accuracy as the percentage of $E_s$ is varied. Figure 8 on page 23 is an example of a modified sporadic E input stream. The number 70 in columns 49-50 indicates a value of 70% $f_oEs$ will be used for all raytracing and loss calculations for sporadic E during the time period specified by the preceding NATGEN program.

```
$!3456789012345678901234567890123456789012345678901234567890123456789012345678901234567890
$!
$! **** INPUT SETUP FOR RAYTRA ****
$!
$SET DEF DKA0:[AMBCOM]
$ASSIGN SYS$INPUT FOR060:
$ASSIGN DKA0:[WILSON]RAYOUT.DAT FOR059:
$ASSIGN DKA0:[AMBCOM]IONOS.DAT FOR002:
$ASSIGN DKA0:[AMBCOM]NOISE.DAT FOR004:
$ASSIGN DKA0:[AMBCOM]COMEFF.DAT FOR007:
$R DKA0:[AMBCOM]RAYTRA
1        0         0         0         0         0         0         0         0
2    70.00    -69.00     53.00    -01.00        70        0.       0.0       10.
3    -13.0       1.0       24.       2.0       2.0      60.0        .6        .6
4      3.2       4.5       6.8       6.9       9.9      10.2      13.9      14.4
4     17.5      18.2      20.3      20.9      23.2
5        1         0         4
8        0         0         0         0         0         0         0
0
0
0
0
0
0
0
0
0
0
0
0
1        0         1
```

**Figure 8. RAYTRA input stream used to model winter site O propagation data.**

Project NONCENTRIC Site O data was compared to data generated by AMBCOM using 0% sporadic E calculations, 50% sporadic E, and modified sporadic E. For modified $E_s$, the percentage was varied during the day. During the six hour period around midnight 90% $E_s$ was used, 70% during the three hour periods before and after the 90% window. RAYTRA was allowed to default to 50% for all other hours during the day. For the 50% sporadic E runs, RAYTRA was allowed to default to the median ITS $f_oE_s$ value. The sporadic E feature was turned off for the 0% $E_s$ input streams.

Frequencies for RAYTRA are specified by control card four. Frequencies from Project NONCENTRIC were used in RAYTRA to enable automated comparison of model and measured data. The automation of the comparison and statistical analysis process reduced the amount of time required to examine the results of a single execution and allowed more time for experimenting with the effects of changing control parameters.

## E. COMEFF

### 1. Overview

The communications effect (COMEFF) program evaluates the quality of a transmitted signal. Previously discussed programs, e.g., NATGEN and RAYTRA, dealt with the ionosphere and possible ionospheric effects along a given propagation path. The only site-dependent information required for those two programs were the site locations. COMEFF factors include transmit power, antenna configuration, signal bandwidth, and other communication site-dependent data. Based upon these local parameters and the data produced by RAYTRA, the performance of a particular communications link using given a frequency can be characterized in terms of the signal-to-noise ratio (SNR), field strengths and doppler spread.

### 2. Program Features

COMEFF uses the data generated by RAYTRA for all of the saved modes as the basis for evaluation of a particular communications link. The raytrace descriptive data, for each ray, includes:

- take-off angle,
- group time,
- phase time,
- path loss,
- noise power (per 1 Hz),
- arrival angle and
- transmitter frequency [Ref. 15: p.112].

Multiple raytraces may be described for each frequency. COMEFF combines the effects of multiple modes to produce a single reception statistic.

COMEFF allows the user to include the effects of the antenna configuration on the communications link. The antenna data is taken from ANTLIB.DAT, the AMBCOM antenna file. Unfortunately the antennas required for this thesis were not in the standard SRI antenna file. The antenna patterns for this thesis were taken from References 14 and 13 and adapted for use in AMBCOM. This is a manual process since AMBCOM does not provide the user with a program for entering the antenna data. Appendix A contains the antenna gain tables used for the summer and winter Clyde River-Leicester campaigns.

The communications effect program provides a variety of output options. COMEFF will calculate the signal-to-noise ratio (SNR), group time, doppler shift,

phase, and delay spread for all frequencies specified in RAYTRA. Other options provide field strengths or analysis of signal quality, e.g. the bit error rate. All requested data may be printed in several formats which include a listing of SNR, doppler shift, phase shift, and group times for each mode. COMEFF also produces a single report that sums the data for each frequency at a particular time. The SNR specified in the COMEFF summary report is a weighted accumulation of SNRs for all modes received from RAYTRA.

Weighted SNRs from the COMEFF summary report were compared to measured SNR values. This composite SNR is calculated by computing the power for each ray, combining these values and then subtracting the noise value. The power $A_i$ for each ray is computed with the equation

$$A_i = \frac{P_t G_t G_r c^2}{4\pi 10^{[L_i/10]} f^2 10^{12} 10^{[L_r/10]}}, \tag{26}$$

where

$P_t$ = transmitter power (W)

$G_t$ = transmitter antenna gain,

$G_r$ = receiver antenna gain,

$L_i$ = path loss for the ith ray,

$L_r$ = receiving antenna loss and

$f$ = frequency (MHz).

The composite SNR value is given by the equation

$$SNR = 10 \log_{10}\left(\sum A_i\right) - N_e, \tag{27}$$

where $N_e$ is the noise power density in dBW. [Ref. 15 : p.83]

### 3. COMEFF Input Variables

Figure 9 on page 26 is an example of the COMEFF input stream. Two control cards are used to control program execution. The first card specifies transmit power, path loss threshold, and the use of antennas. Transmit power is given in units of watts per hertz. A bandwidth of 50 Hz and a transmitter power output of 400 watts results in 8 W Hz. The path loss threshold is used to exclude modes with a path loss greater than the specified threshold. This parameter was set at 400 dB which effectively allowed

all modes to be included. The second COMEFF control statement is used to specify antennas.

```
$SET DEF DKA0:[AMBCOM]
$ASSIGN SYS$INPUT FOR055:
$ASSIGN DKA0:[WILSON]WAVEFORM.DAT FOR020:
$ASSIGN DKA0:[WILSON]COMOUT.DAT FOR059:
$ASSIGN DKA0:[AMBCOM]COMEFF.DAT FOR007:
$ASSIGN DKA0:[AMBCOM]ANTLIB.DAT FOR006:
$R DKA0:[AMBCOM]COMEFF
 NONCENTRIC 18 JANUARY 1988
    0   0. 1600    1     ,    0       8.0          0  400    1    0    0       0.0
WHIP      SLOPEVEE                                 1
```

Figure 9. COMEFF control input used to model winter site O propagation data .

# III. PROJECT NONCENTRIC

## A. SITES

### 1. Overview

Project NONCENTRIC was a study of communications at HF frequencies at high latitudes conducted by the University of Leicester, U.K. The concept of the project was to place a transmitter in the polar cap area and to transmit HF signals to receivers at several locations in polar cap and midlatitudes regions. Figure 10 shows approximate locations of transmitter and receiver sites. Table 1 on page 28 provides locations of sites in geographic latitude and longitude.

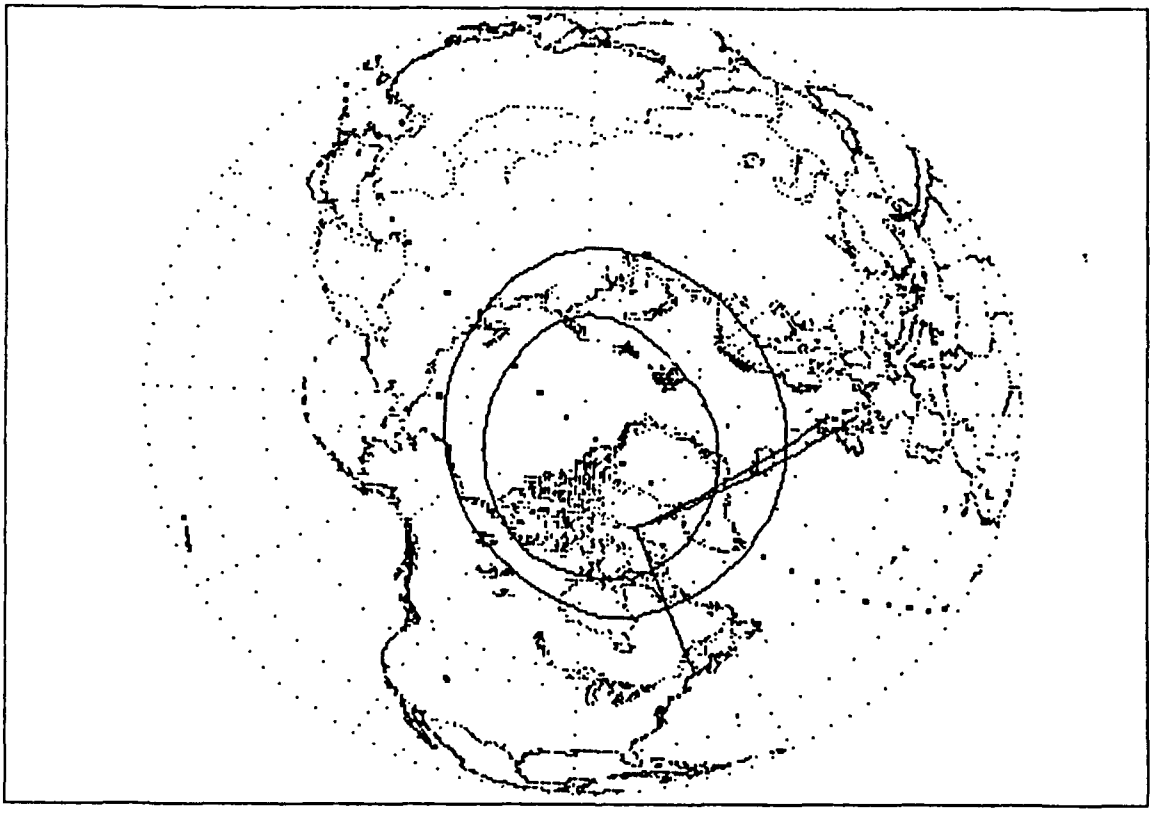

**Figure 10. The Project NONCENTRIC site locations and propagation paths.**

The equipment configuration used for Project NONCENTRIC receiver sites varied from site to site. No data are available which accurately describes the receiving equipment, distribution systems, or antennas in operating environments. Data produced

Table 1. RECEIVER SITE LOCATIONS

| SITE | LATITUDE | LONGITUDE |
|---|---|---|
| C | 57.10 N | 02.04 W |
| D | 44.48 N | 68.46 W |
| O | 53.00 N | 01.00 W |

by AMBCOM were not adjusted to account for site-dependent anomalies. The data produced for sites C and D exhibited large average errors at higher frequencies, i.e. 30-40 dB. It was assumed that site noise may have lowered the measured SNR, and the site C and D AMBCOM SNRs were adjusted down 15 dB to account for noise in the receiver system.

The geometry of all the Project NONCENTRIC antennas are recorded, but none of the antenna patterns were measured at their specific site. No measurements were taken of site noise levels, ground permitivities, or ground conductivities. All antenna patterns and local noise levels used to generate AMBCOM data are estimated.

**2. Transmitter Site**

The transmitter site was located at Clyde River, *Canada. Clyde River is located* within the polar cap region at 70° north latitude and 69° west longitude. Propagation data used for this thesis are from midlatitude receiver stations so paths from Clyde River must pass through the auroral oval region. The Clyde River site transmitter power output level was 400 watts.

Two different antenna configurations were used at the Clyde River site. During the summer campaign of 1988 a modified BUTTERNUT two-trap antenna (type HF6V-X) was used for all transmissions. The winter campaign employed a resistive whip antenna. These two antenna geometries were modeled by Tsolekas [Ref. 13: pp. 11-16] using descriptive data provided by the University of Leicester. The antenna models were created using the Numerical Electromagnetics Code, Version 3 (NEC-3) using the Sommerfield-Norton approximation for a finite ground plane. The results from this modeling process were used to construct antenna gain tables used by AMBCOM.

**3. Receiver Sites**

Site O (University of Leicester) files were the only sources used for the earlier works by Tsolekas [Ref. 13] and Gikas [Ref. 14]. In order to compare their results with

the data produced by AMBCOM the same site data and antenna configurations were employed. This thesis also includes some comparisons of data generated by AMBCOM for sites C and D.

Site O was equipped with a sloping vee antenna for all Project NONCENTRIC campaigns. This antenna was modeled by Gikas [Ref. 14: pp.10-16] using NEC-3. Gikas used the antenna geometry provided by the University of Leicester plus estimated values for permitivity and conductivity as inputs to NEC-3. The final form of the antenna gain tables for AMBCOM are interpolated from the results produced by Gikas for each of the Project NONCENTRIC frequencies.

## B. PROJECT NONCENTRIC DATA

### 1. Signal Format

Project NONCENTRIC data were taken from two of the four high latitude campaigns. The summer and winter campaigns were conducted 17 July-12 August 1988 and 18 January-12 February 1989 respectively. The data were collected from three sites which are labeled as sites C, D, and O.

Project NONCENTRIC signals were transmitted over a range of frequencies by stepping from 3.2 MHz to 23.9 MHz at preset time intervals. These transmissions were formatted to provide a repetitive pattern of signal forms which could easily be recognized; Figure 11 on page 30 is a diagram of the signal format. The call sign (CS) was sent in morse code at five second intervals. The Barker code sequence consisted of a bipolar code with bit length of $250\mu s$ repeated continuously during a 30 second interval. The Doppler signal represents 30 seconds of transmission with an unmodulated carrier. The call sign and Doppler signals were used for signal analysis by the automated signal recognition process used by the University of Leicester.

### 2. Project NONCENTRIC Data Analysis

An automated signal recognition program was used by the University of Leicester to validate the received transmissions and separated the data into the five files shown in Table 2 on page 30. The automated signal recognition process was validated by comparing the data from the five files with the results obtained by manual signal selection of a small subset of received transmissions. The automated signal recognition program was in agreement with manual selections about 80%-90% of the time [Ref. 23: p. 4].

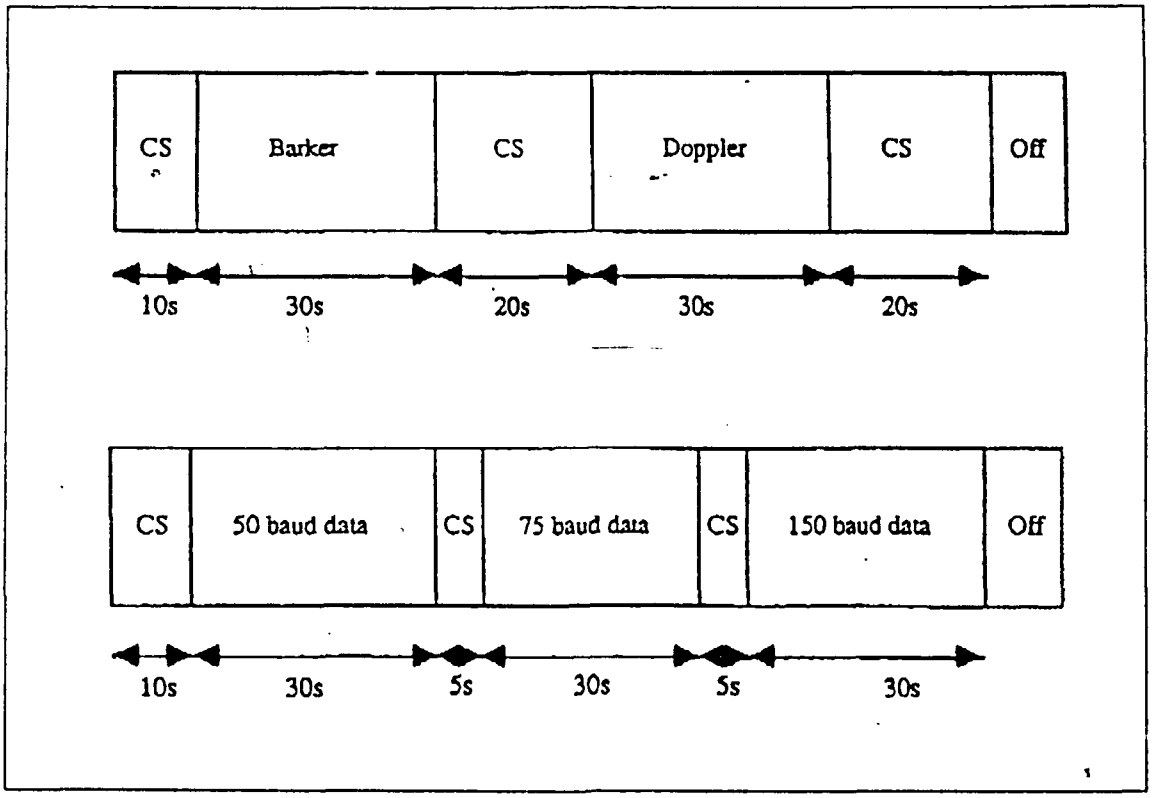


**Figure 11.** The time sequence of the Project NONCENTRIC signals showing Doppler and call sign sequences. [From Ref. 23]

**Table 2. PROJECT NONCENTRIC WINTER/SITE O FILES**

| FILE NAME | FILE DEFINITION |
|---|---|
| OWINTER.SIG | Passed all test; valid data |
| OWINTER.FCS | Passed only the call sign test |
| OWINTER.FSI | Passed only the spread index test |
| OWINTER.INT | Data judged to be interference |
| OWINTER.NOS | Data that failed all tests |

### 3. Spread Index Test

The spread index test provides a simple method for judging the amount of Doppler spreading for each signal. The method entails an analysis of the Doppler portion of the transmitted signal by observing the frequency shift of an unmodulated carrier

with time. The amount of Doppler spreading is indicated the observed frequency shift of the unmodulated carrier during a 30 second transmission. A noise spectrum, assuming a uniform noise distribution, would not be expected to exhibit the same spectrum as an unmodulated carrier with Doppler spreading. The spread index test takes advantage of this property to separate possible valid signal data from noise data. [Ref. 23: p. 1]

The spread index test is a multiple step process. The received signal's spectrum is first obtained from a 1000 point Fast Fourier Transform (FFT). Figure 12 on page 32 is an example of the resulting spectrum. The mean signal amplitude between -25 Hz and -12.5 Hz is taken as the mean noise level for the signal. This mean noise level value is subtracted from the spectrum to yield the form shown in Figure 13 on page 33. The area under the remaining signal is defined as the spread index. Since the spread index is proportional to the width of the remaining signal it is also proportional to the Doppler spreading of the signal.

The spread index is used in conjunction with the signal strength to determine signal validity. The selection criteria are as follows:

- A signal passes the spread index test if the spread index is large and the signal strength is greater than a preset threshold value.
- The signal is invalid if the spread index is negative.
- The signal is invalid if the spread index and signal strength are small.
- The signal is valid if the spread index is small and the signal strength is large.

All signals were passed to the call sign test regardless of the results of the spread index test.

**4. The Call Sign Test**

The call sign test provided a further means of validating data. The signal spectrum was produced with a 1000 point FFT. The mean noise level ($N_1$) was computed by examining the frequency spectrum from -50 Hz to -12.5 Hz. The value of the mean noise ($N_2$) used for the call sign test is increased to insure that a call sign signal mainlobe and sidelobes are present. The call sign mean noise value is given by

$$N_2 = 2.5\, N_1. \tag{28}$$

The value $N_2$ is subtracted from the signal spectrum to produce the call sign signal. Figure 14 on page 34 is an example of the call sign spectrum after the mean noise level

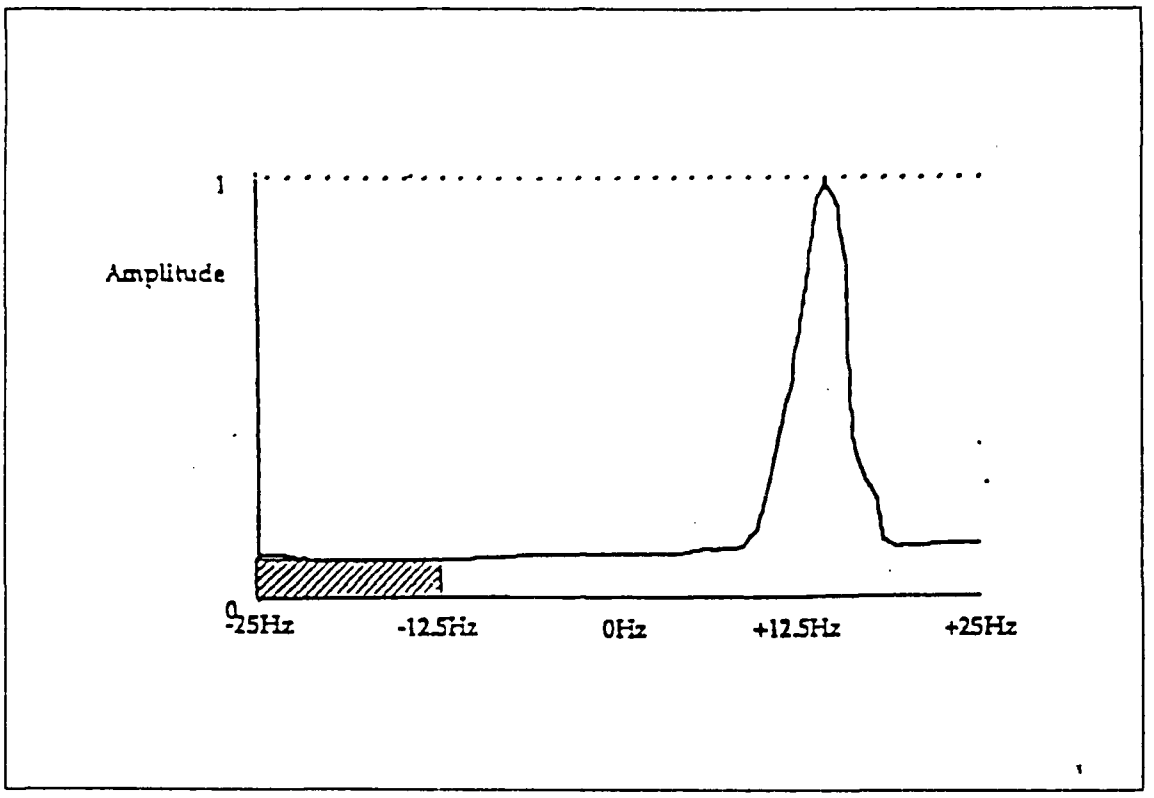


**Figure 12. The Project NONCENTRIC signal spectrum after the 1000 point FFT. [From Ref. 23]**

is removed. This signal is then examined to determine if it matches the call sign pattern. [Ref. 23: p. 2]

**5. Interference**

The automatic signal recognition process was designed to detect interfering signals and to mark the transmission data accordingly. A signal is considered interference if it passes the spread index test but fails the call sign test. A signal-to-noise ratio (SNR) greater than 10 dB should pass the call sign test. If it fails the call sign test then the signal is considered to be interference. A signal is considered invalid with a SNR less than 10 dB. [Ref. 23: p.3]

**6. Signal Categorization**

The tested data are categorized and stored in one of five files. The file categorization criteria is as follows:

- The data passes both tests and is written to the signal (SIG) file.

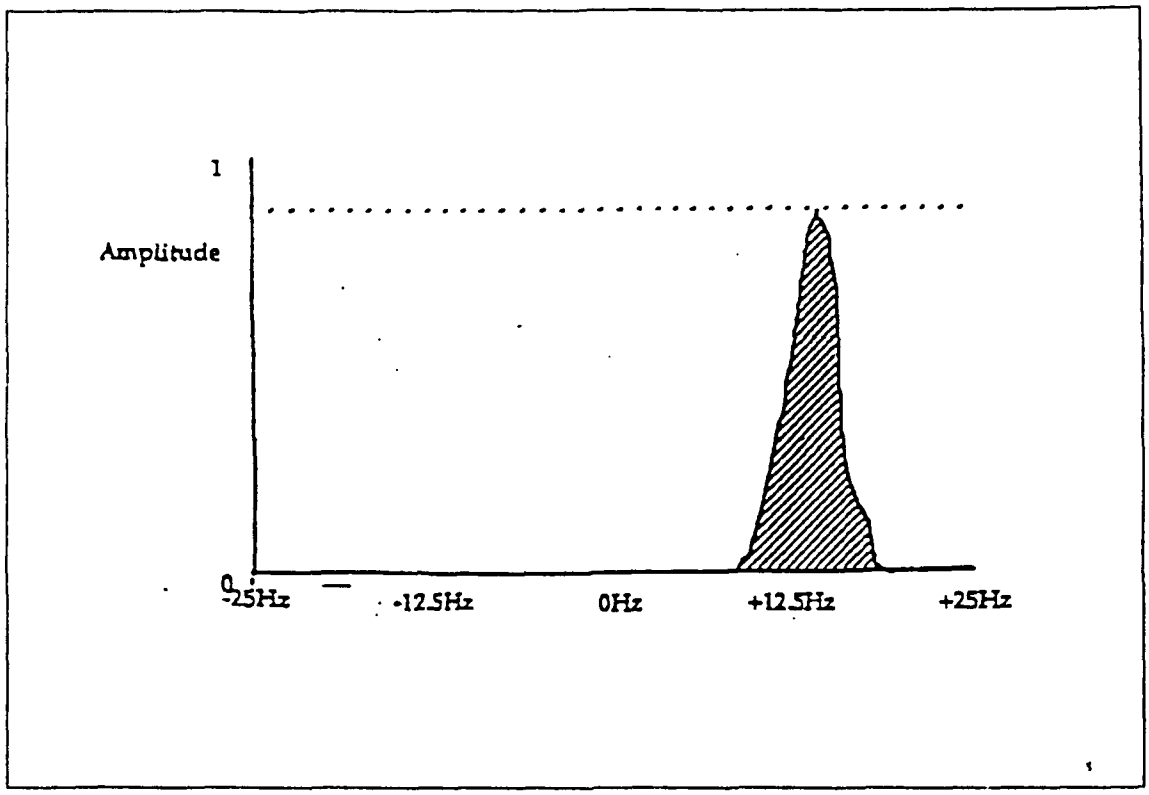


**Figure 13. The Project NONCENTRIC FFT Spectrum with the average noise removed. [From Ref. 23]**

- The data failed both tests and is written to the nonsignal (NOS) file.
- The data passes the spread index test only; the data is saved in the spread index file (FSI).
- The data passes the spread index test but is determined to be interference; the data is written to the interference (INT) file.
- The data passes the call sign test only; the data is written to the call sign (FCS) file.

The data from the SIG files were used to compare with the AMBCOM generated data. [Ref. 23: p. 3]

Each of the receiver sites used for this thesis produced its own set of five data files, e.g., SIG, NOS, FCS, FSI, and INT. The data are arranged in ascending order with respect to time. Table 3 on page 35 lists the attributes of each of the data elements.

The PEAK and NOISE units are one of the major problems with the Project NONCENTRIC data. The two values for these two elements are taken from the 1000 point FFT and they cannot be translated into the field strength and noise power values

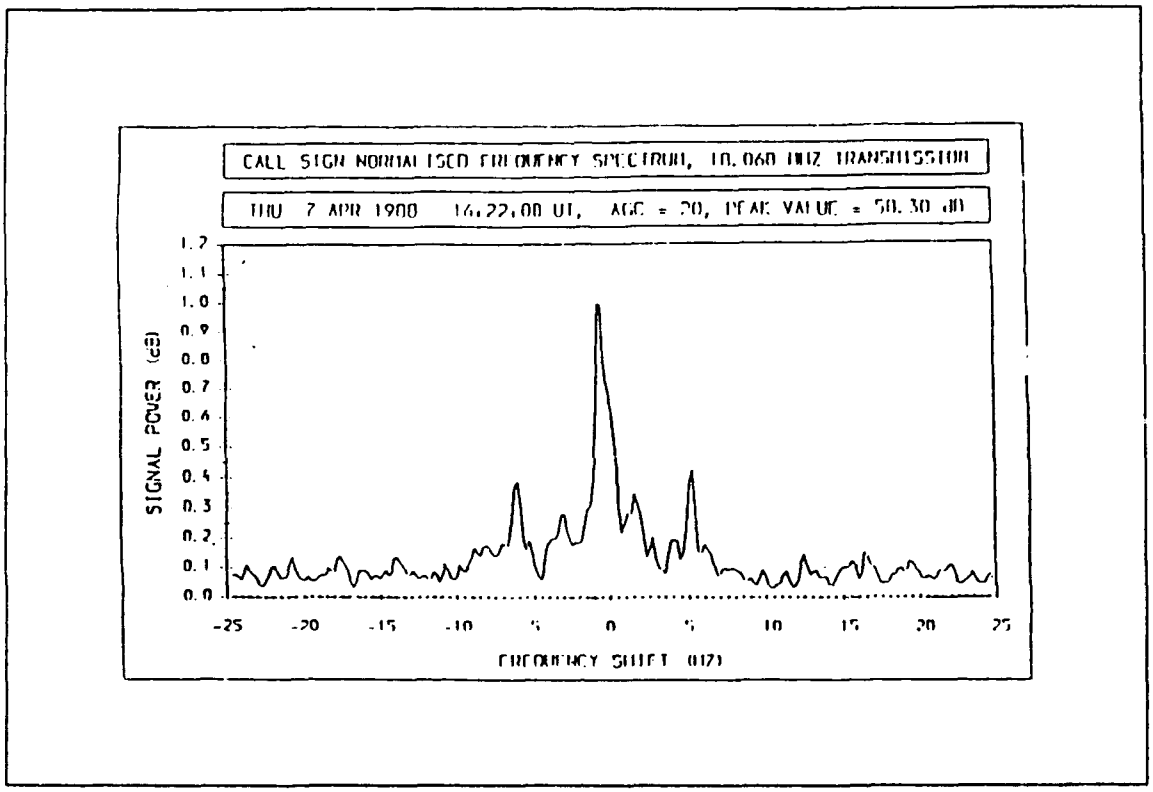


**Figure 14. The Project NONCENTRIC call sign spectrum produced by the 1000 point FFT. [From Ref. 23]**

present at the antenna. Fortunately PEAK and NOISE are both in units of dB/$\mu$V. The signal SNR is obtained by subtracting NOISE from PEAK. This SNR value was then compared to the AMBCOM SNR values produced for the COMEFF summary report.

### 7. The Signals File Data

The end product of this collection and analysis was the SIG file, which represents a very small portion of the total number of signals recorded during the Project NONCENTRIC campaigns. For example, the file OWINTER.SIG, the valid winter campaign signals received at site O, contains only 38 records out of a population of 609 received signals at 3.2 MHz. The highest number of records for a particular frequency is 266 out of a population of 609 at a frequency of 14.4 MHz. The signal files used for this thesis are a small sample in comparison to the total number of signals that were received.

**Table 3. PROJECT NONCENTRIC DATA ELEMENTS**

| NAME | Definition | UNITS |
|---|---|---|
| FREQ | Frequency | MHz |
| HOUR | Hour received | UT |
| MIN | Minute received | UT |
| DAY | Day of the week | none |
| DATE | Day of the month | |
| MONTH | Month of the year | |
| YEAR | Year | |
| PEAK | Signal amplitude | dB $\mu$V |
| NOISE | Mean noise level | dB $\mu$V |
| SPREAD | Spread index | dimensionless |

# IV. AMBCOM DATA ANALYSIS

## A. ANALYSIS METHODOLOGY

### 1. General

AMBCOM produces data which exhibits different trends as frequency is changed. Summary statistics, produced through manual analysis methods, tend to smooth over detail information about each frequency. An automated means of comparing AMBCOM data to measured data was designed to alleviate this problem. Computer programs compared AMBCOM data to Project NONCENTRIC data and accumulated statistics by frequency and sporadic E model. These statistics were then displayed graphically to highlight trends, by frequency, in AMBCOM's performance.

### 2. Data Synthesis

Project NONCENTRIC data is in a format that is easy to manipulate with a computer but AMBCOM data is not. AMBCOM SNR data used for comparison was taken from the summary report produced by COMEFF. The data must first be removed from the report and stored in a form which simplifies the comparison process. Originally this task was performed manually by reviewing each line of the COMEFF summary report and erasing those elements that were not needed. A simpler method was programming the VAX Workstation to perform this function which is one of the purposes of the modify data program (MODDAT).

MODDAT is called inside AMBCOM input streams which generate data for each campaign. It is executed once for each day or part of a day for which AMBCOM produces data. MODDAT concatenates all COMEFF summary reports for that day and then removes the data required for comparison with the Project NONCENTRIC data , e.g., the hour, frequency, and SNR. It also writes the month and day on each record. Files produced by MODDAT are allowed to accumulate until the end of AMBCOM input stream execution, when they are all concatenated and sorted for later processing.

### 3. Statistical Analysis

The statistical analysis is a two step process. The first step compares the AMBCOM data with the actual (Project NONCENTRIC) data. The matched records, actual records with no corresponding AMBCOM records, and AMBCOM records with no corresponding actual record are written to separate files for later processing. Statis-

tics regarding the average error, average SNR, number of matches, and number of misses of actual data are recorded. The final step accumulates statistics about the number of AMBCOM records which did not match an actual record.

The first step in the statistical analysis process is performed by the FORTRAN program WILSTAT. WILSTAT matches AMBCOM data with actual data by comparing the hour, month, day, and frequency of each record. Those AMBCOM records which do not match actual data are written to a file for later processing. Actual records which do not match AMBCOM records are accumulated by frequency as misses.

Each record that is matched is used to calculate, for each frequency, the average AMBCOM SNR and the number of matched records. All SNR values from AMBCOM matched data are accumulated in a table by frequency ($SNR_{freq}$) along with the total number of matched records ($TOT_{match}$) for that frequency. At the end of the program this table was used to calculate the average SNR per frequency ($SNR_{ave}$) using the equation,

$$SNR_{ave} = \frac{\sum SNR_{freq}}{TOT_{match}}. \tag{29}$$

A file, ordered by frequency, is produced which lists the average SNR, total number of matched records, and the average error.

The average error values are compiled from the error values recorded for each record. Once an AMBCOM record is matched to actual data, the error ($ERR_f$) is calculated by subtracting actual SNR ($SNR_{act}$) from AMBCOM SNR ($SNR_{ambcom}$). The frequency, month, day, hour, $SNR_{ambcom}$, $SNR_{actual}$, error, and spread index of all matched records are written to a file for processing with a graphics routine. The average error per frequency ($ERR_{ave}$) is given by

$$ERR_{ave} = \frac{\left(\sum ERR_f\right)}{TOT_f}, \tag{30}$$

where $TOT_f$ is the total number of records for that frequency.

WILSTAT also calculates the percentage of matched records ($P_{TOT}$). This value is the percentage of the total number of matched records (TOT) referenced to the total number of actual records ($TOT_{act}$). The percentage is given by

$$P_{TOT} = \left[ \frac{TOT}{TOT_{act}} \right] \times 100. \tag{31}$$

This equation was used by Gikas [Ref. 14 ] and Tsolekas [Ref. 13] to produce their percentage of matched records.

The second program of the statistical analysis process is called WILMAT.. The purpose of this routine is to accumulate the number of unmatched AMBCOM generated predictions which were of acceptable transmission quality, e.g. AMBCOM predicts a strong signal for a time and frequency for which no signal was received. The key to this procedure is to select a proper threshold SNR value for acceptable signal quality. WILMAT performs this function by using the $SNR_{ave}$ values calculated by WILSTAT as the transmission quality threshold for each frequency.

WILMAT calculates the percentage, by frequency, of matching AMBCOM data ($P_f$) referenced to the total number of AMBCOM predictions ($TOT_p$) for a given frequency. All of the AMBCOM records used for this statistic must have a SNR greater than or equal to the SNR threshold for exceptable transmission quality. $P_f$ is given by

$$P_f = \left[ \frac{TOT_f}{TOT_f + TOT_p} \right] \times 100. \tag{32}$$

This percentage was included in the model analysis to provide some basis for judging the reliability of a given AMBCOM prediction.

Using the data produced by WILSTAT, WILMAT produces the final summary report which lists by frequency

- the average SNR,
- the average error,
- the total number of matched records,
- the total number of unmatched actual records,
- the total number of unmatched AMBCOM records of acceptable transmission quality and
- $P_f$

Appendix C is the compilation of these statistics by site and campaign. All FORTRAN programs written to process the AMBCOM data are listed in Appendix B.

## B. AMBCOM INPUT STREAMS

The 90% $E_s$ AMBCOM input streams are designed to roughly emulate a pattern of $E_s$ frequency distributions that were described in Reference 7. The largest percentage of $E_s$ should occur at approximately midnight local time in the auroral oval, with less $E_s$ at later times. These conditions are very dependent on the location of the reflection points with respect to the auroral oval. $E_s$ is more intense within the auroral oval than at the lower latitudes. No attempt was made to manually adjust the percentage of $E_s$ at each of the reflection points. The percentage of $E_s$ was defined for the whole propagation path and AMBCOM adjusted for latitude and frequency differences.

The purpose of the 50% and 0% $E_s$ versions of the AMBCOM execution streams was to relate performance of the model with varying amounts of $E_s$ included in AMBCOM calculations. The 50% $E_s$ data were modeled with using the median decile value for $f_oE_s$. The 0% sporadic E data were created without using AMBCOM's $E_s$ model.

AMBCOM $E_s$ models are based on midlatitude $E_s$ critical frequencies from the ITS file. The resulting $E_s$ models are not specifically designed to describe high latitude sporadic E. The reason for this is that the original data produce by the Chatanika radar site, on which AMBCOM is based, did not have sufficient resolution to detect sporadic E [Ref. 24]. The addition of a high-latitude $E_s$ model to AMBCOM is feasible and may be undertaken in the future; however, the effect of using the current AMBCOM sporadic E model for high latitudes had not been examined before this thesis.

## C. WINTER DATA

### 1. Site O

AMBCOM Site O data showed a decrease in percentage of matched records as the percentage of $E_s$ was decreased to 0. The 90%, 50% and 0% $E_s$ data exhibited a $P_{TOT}$ of 88.9%, 80.5% and 68.3%, respectively. These percentages seem to indicate that the 90% $E_s$ model is much more accurate in this particular case, but this is not a complete statistical characterization. Figure 15 on page 40 shows the distribution of $P_f$ for all three sporadic E models. Between 14.4 and 18.2 MHz, the lower sporadic E models were able to match the actual data without predicting a large number of modes that had no Project NONCENTRIC equivalent. The 90% and 50% $E_s$ models showed a higher $P_f$ at lower frequencies, i.e., 6.9 to 9.9 MHz, than the data produced without sporadic E. The shapes of all three curves are approximately the same.

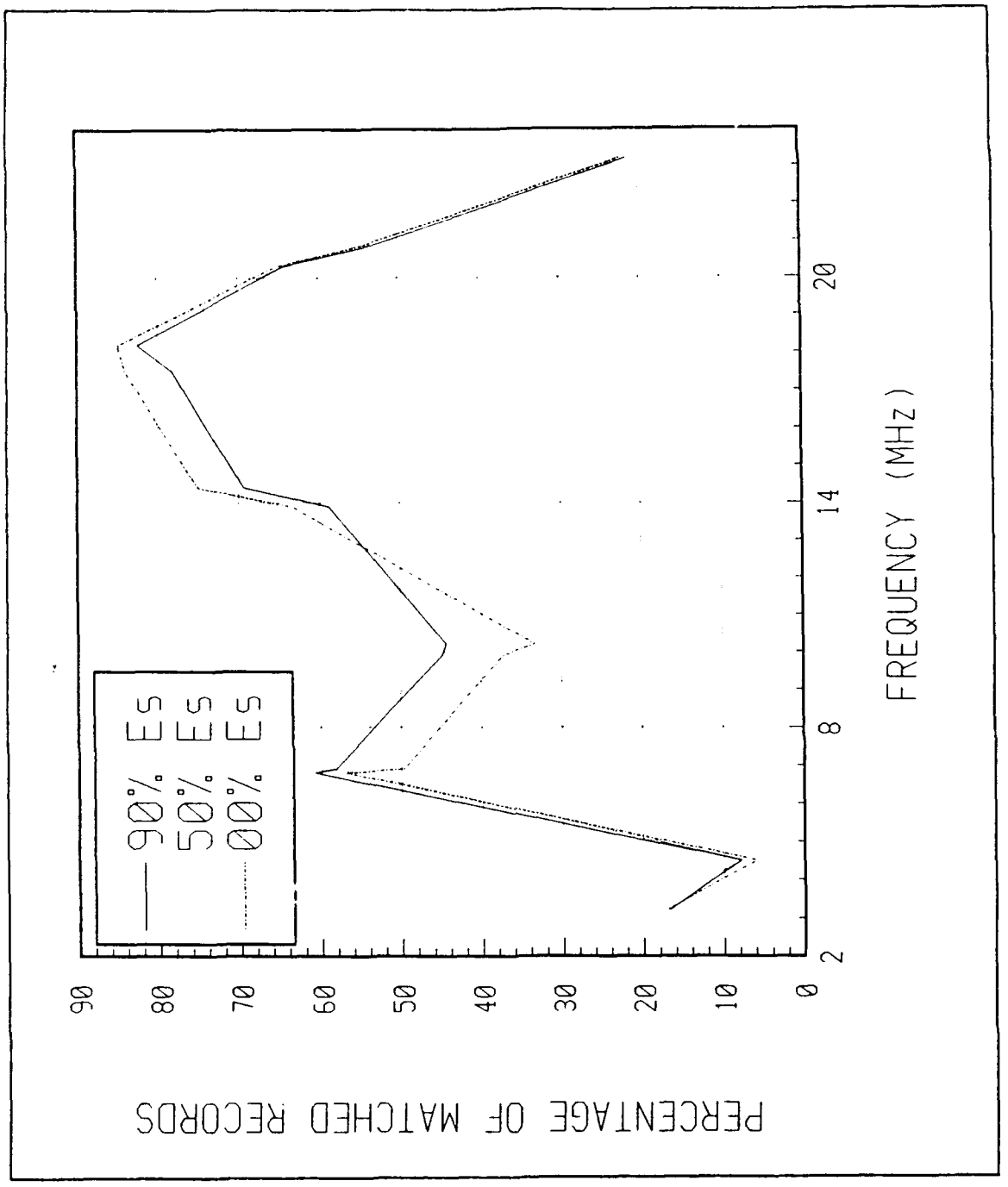


**Figure 15. The percentage of matching winter site O data relative to the total number of AMBCOM predictions (by frequency).**

The average error also varied with the percentage of sporadic E. The largest amount of average error was exhibited by the 50% $E_s$ model, i.e. -9.6 dB. The 90% and 0% $E_s$ data average error was -7.6 and -7.0 dB, respectively. Figure 16 on page 42 shows that a large precentage of the error is distributed between -20 and +20 dB, but the 50% sporadic E data shows a higher percentage of error outside of this range. Figure 17 on page 43 shows average error for all three models as it is distributed by frequency. The least amount of error is found in the frequency range between 9.9 and 20.9 MHz. This is not a clear indicator of the performance of AMBCOM since the accuracy of the antenna patterns used to produce the data is unknown.

**2. Site C**

Data generated by AMBCOM produced error patterns similar to site O. The percentage of matched records ($P_{TOT}$) was 91.7% (90% $E_s$), 87.3% (50% $E_s$) and 70.3% (0% $E_s$). The distribution of $P_f$ is very different from the pattern of the site O data (see Figure 18 on page 44). $P_f$ at higher frequencies did not greatly exceed those at lower frequencies and none of the percentages were larger than 55%. Some of these differences may be caused by different receiving antennas at the two sites.

The distribution of error (Figure 19 on page 45) exhibits that same skewed shape as site O data but the 50% $E_s$ curve does not have a second peak. The average error was -8.7 dB for 90% $E_s$, -12.6 dB for 50% $E_s$ and -10.6 dB for 0% $E_s$. The standard deviation of error for 90%, 50% and 0% $E_s$ models is 26.7 dB, 28.0 dB and 25.9 dB respectively. Figure 20 on page 46 shows the average error distributed by frequency. The average error is between -20 and +20 dB for frequencies between 6.8 and 23.2 MHz, roughly similar to the site O distribution. This is interesting since AMBCOM is producing a smaller average error at the higher frequency inspite of a change in the receive antenna.

**3. Site D**

The same trends continued for Site D data as were observed for Site O but the changes were not as dramatic. The overall percentage of matched records ($P_{TOT}$) does not vary by more than a decade for all three modeling methods. The percentages are 91.8%, 85.0%, and 81.8% for the 90%, 50% and 0% $E_s$ models respectively. The percentage of matching AMBCOM records (see Figure 21 on page 48) showed a similar two peak pattern seen in site C data but peak values were in the 80%-90% range. The 90% $E_s$ model (Figure 21 on page 48) demonstrated the lowest percentage of matches per frequency of the three models. A close examination of the tabular statistics in Appendix C indicates that the percentage of matches for 13.9 to 20.3 MHz improves with

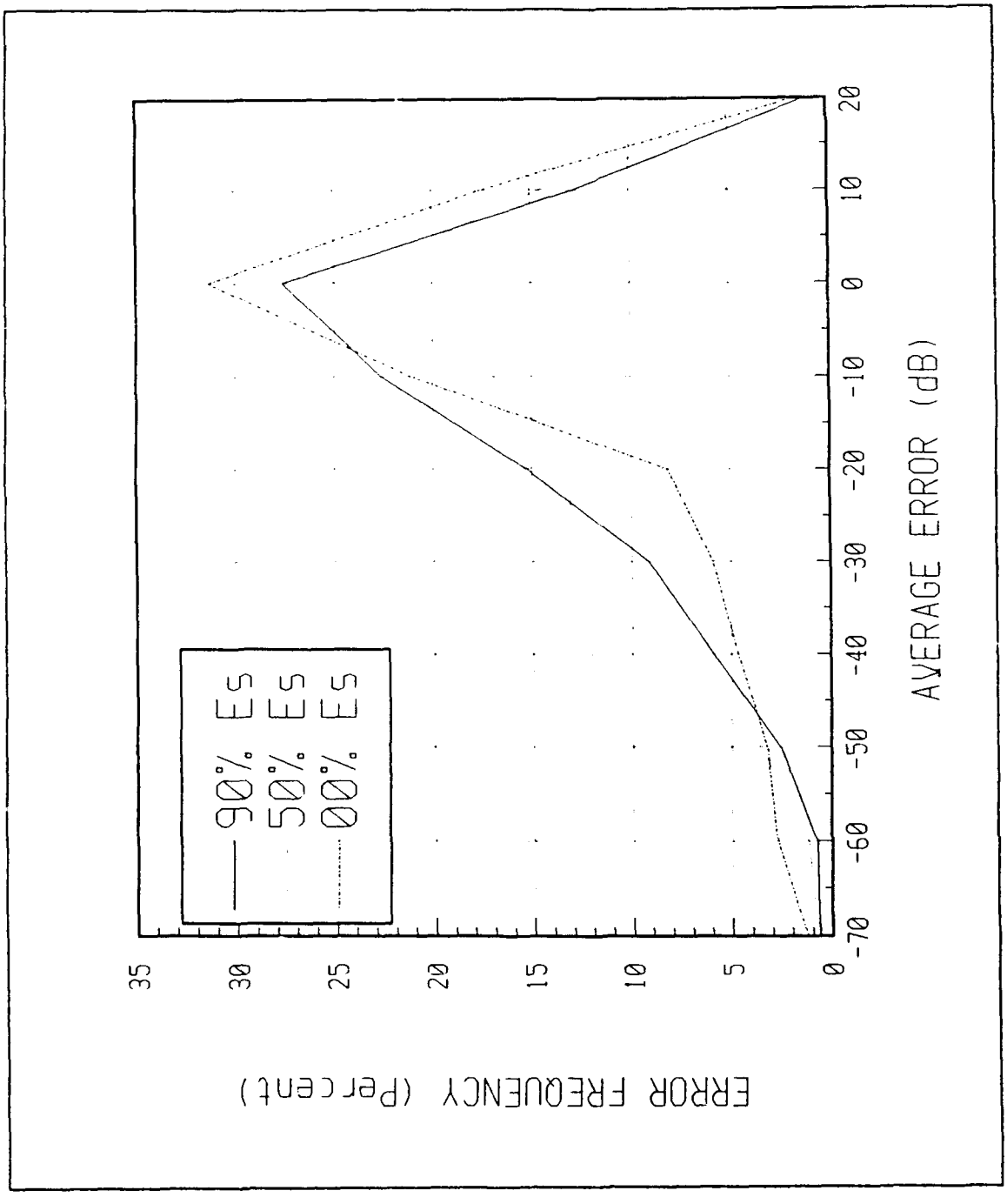


**Figure 16.** **The winter site O average error grouped in ten dB bins and plotted by percentage of error frequency.**

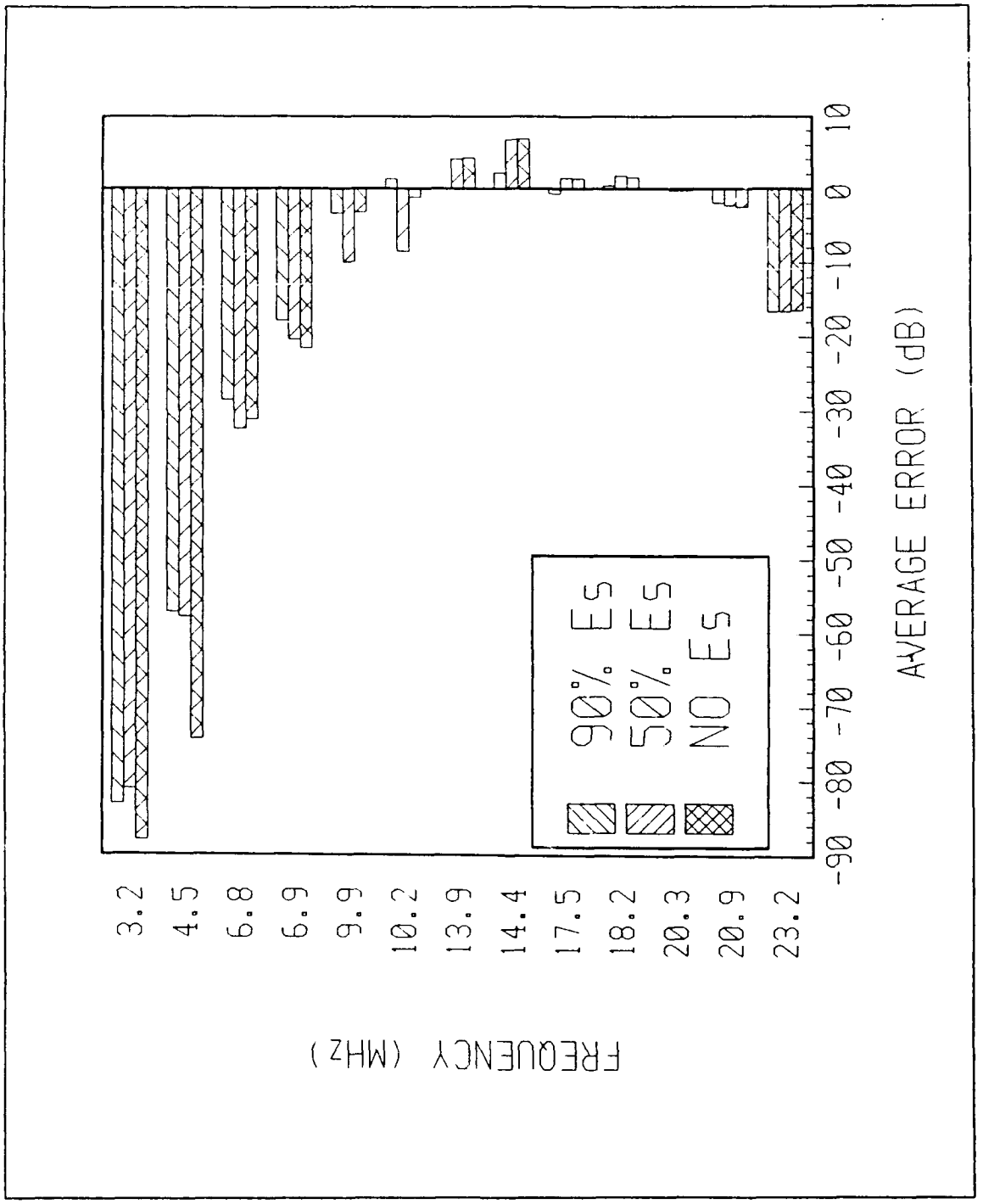


**Figure 17. The average error, for winter site O, listed by frequency.**

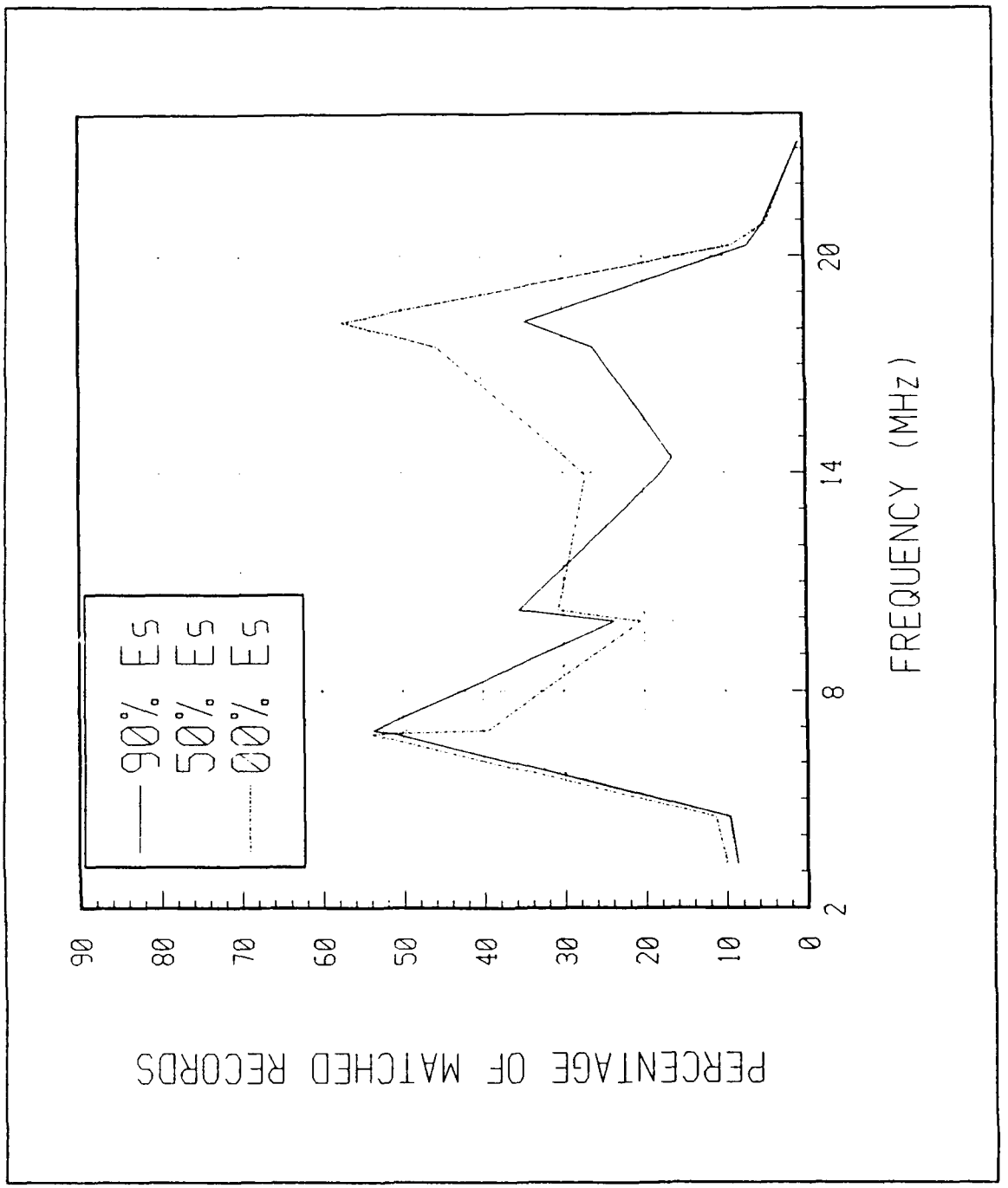


**Figure 18. The percentage of matching winter site C data relative to the total number of AMBCOM predictions (by frequency).**

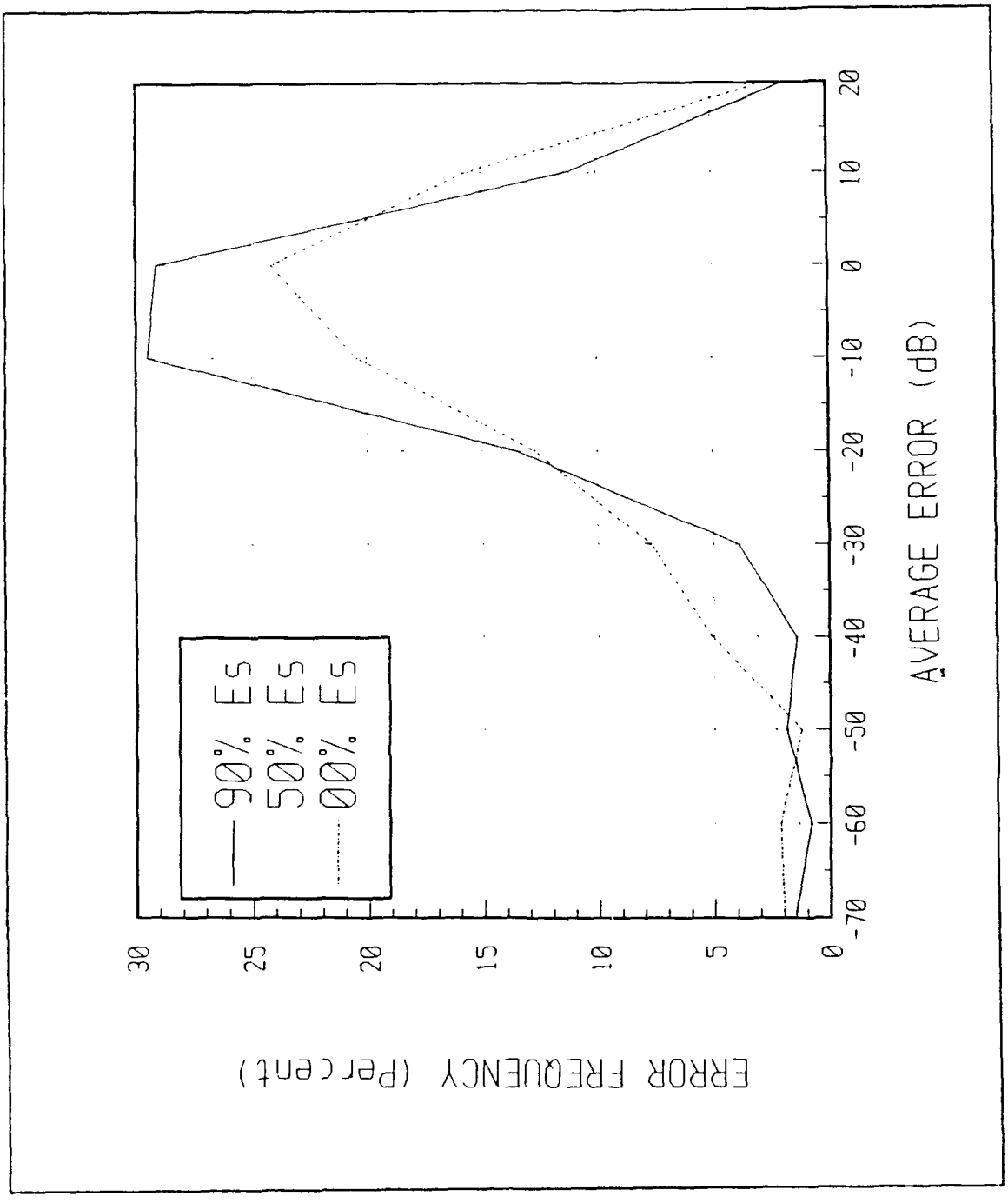


Figure 19. The winter site C average error grouped in ten dB bins and plotted by percentage of error frequency.

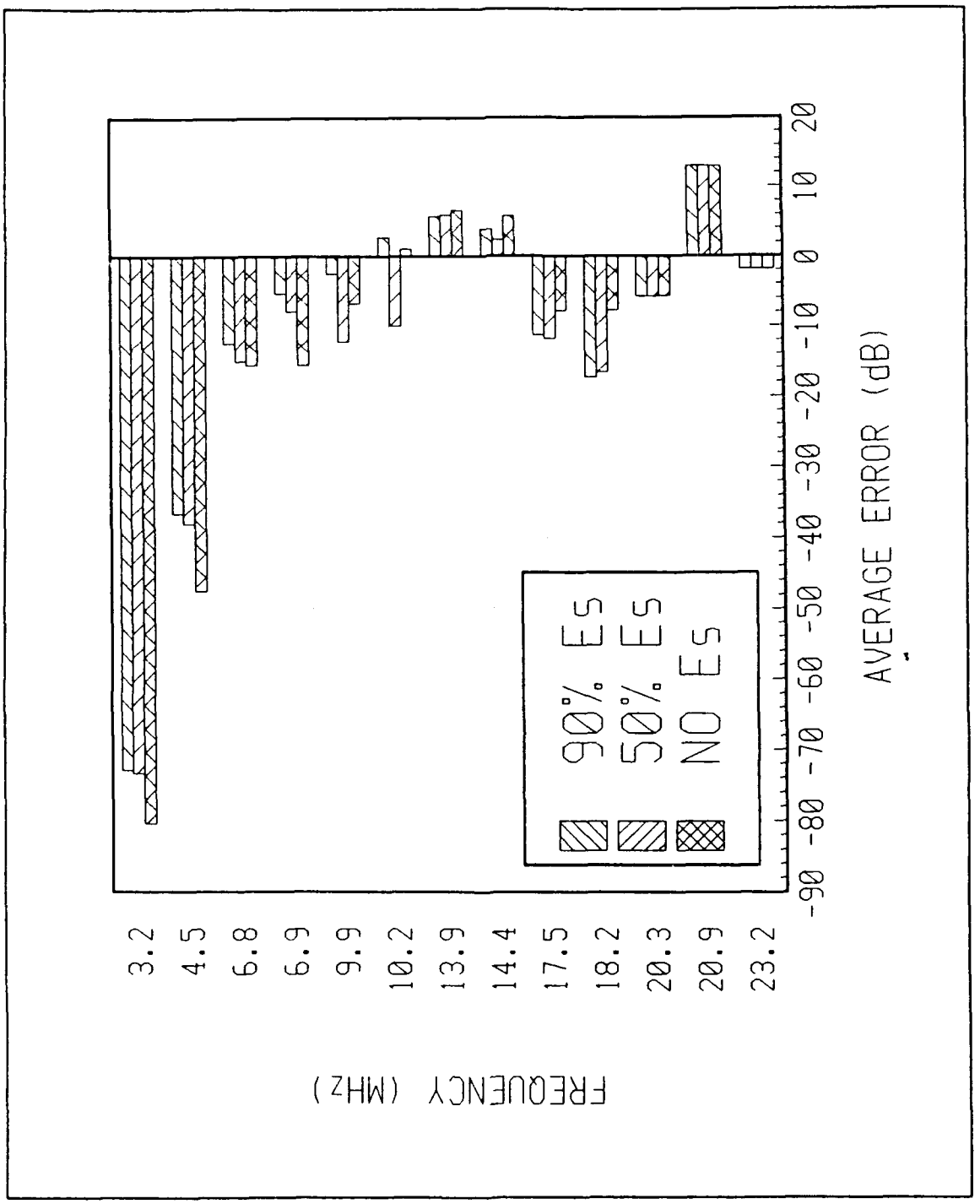


**Figure 20. The average error, for winter site C, listed by frequency.**

the 50% and 0% sporadic E models relative to the 90% $E_s$ version. It is particularly interesting to compare site C and D data, because they both used the same type of antenna but produce very different results. This may be attributed in part to the location of two sites and the possibility that the two antennas do not perform the same at their respective locations.

The average error for all three models displayed some variation. The 90% $E_s$ model produced an average error of -7.2 dB. The 50% model exhibited an average error of -9.3 dB while the 0% model produced an average error of -11.1 dB. Figure 22 on page 49 shows the distribution of the average error for all three models. The curves are similar in shape and in location along the average error axis. Figure 23 on page 50 is the average error versus frequency for site D. Clearly, the site D distribution is similar to that of site C, and both sites demonstrate, as in the case of site O, that the smallest absolute value for average error is found at higher frequencies.

## D. SUMMER DATA

### 1. Site O

The summer campaign data produced results that varied slightly with the amount of sporadic E included in the AMBCOM model. The percentage of matched records ($P_{TOT}$) was, respectively, 95.0%, 84.8% and 79.1% for 90%, 50% and 0% $E_s$. Figure 24 on page 51 is a plot of the percentage of matching AMBCOM ($P_f$) data for each of the sporadic E models. AMBCOM predicted a larger percentage of the measured data at high frequencies. The 90%, 50% and 0% $E_s$ results are similar below 13.9 MHz, but the 90% model exhibited lower $P_f$ from 14.4 to 23.2 MHz.

The average error of summer Site O data varied less than 3.5 dB between the three $E_s$ models. The 90% $E_s$ model produced an average error of -8.3 dB, but the 50% and 0% models exhibited an average error of -11.05 and -11.87 dB, respectively. Figure 25 on page 53 shows the error distributions for all sporadic E models for the summer campaign. The distribution is skewed in the direction of negative average error. The standard deviations for these distributions are 18.2 dB (90% $E_s$ ), 19.3 dB (50% $E_s$) and 23.0 dB (0% $E_s$). The distribution of average error by frequency (Figure 26 on page 54) is similar to the winter site O data. The lower frequency data exhibited larger absolute values of average error, but lower absolute error was the trend at higher frequencies, i.e., 13.9 to 20.9 MHz. There was very little variation in average error with $E_s$.

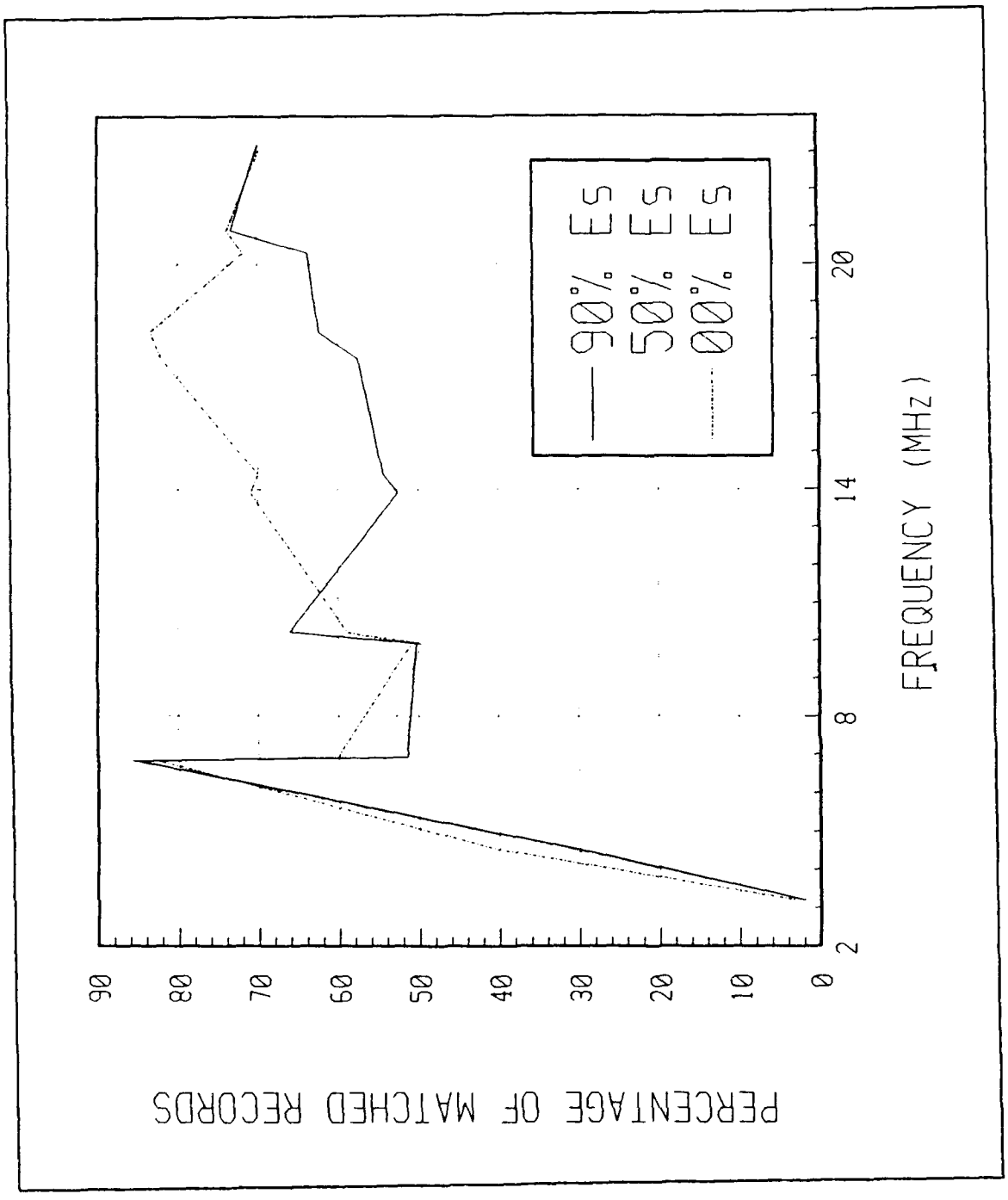


**Figure 21. The percentage of winter site D matching data referenced to the total number of AMBCOM predictions (by frequency).**

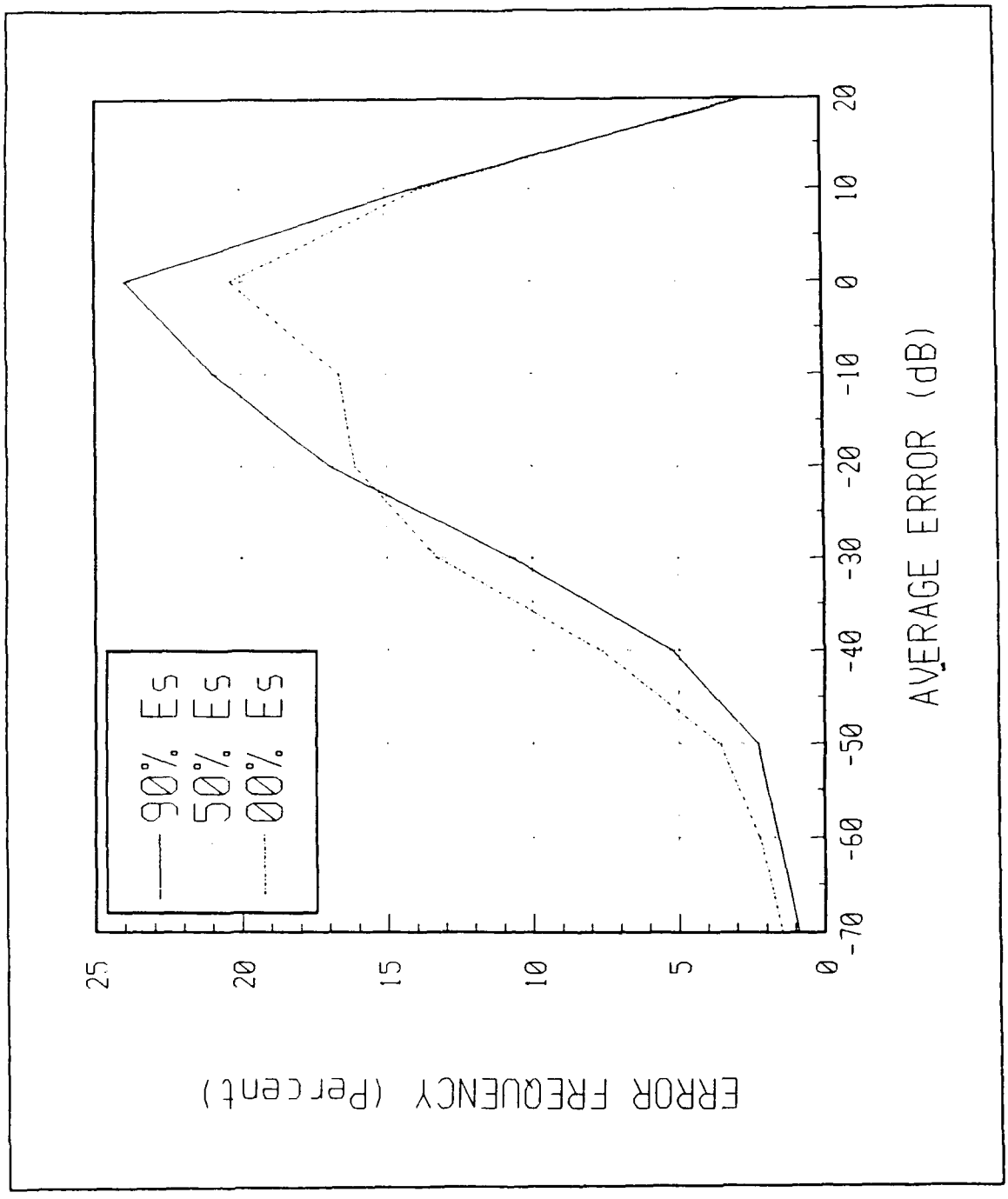


**Figure 22.** **The winter site D average error grouped in ten dB bins and plotted by percentage of error frequency.**

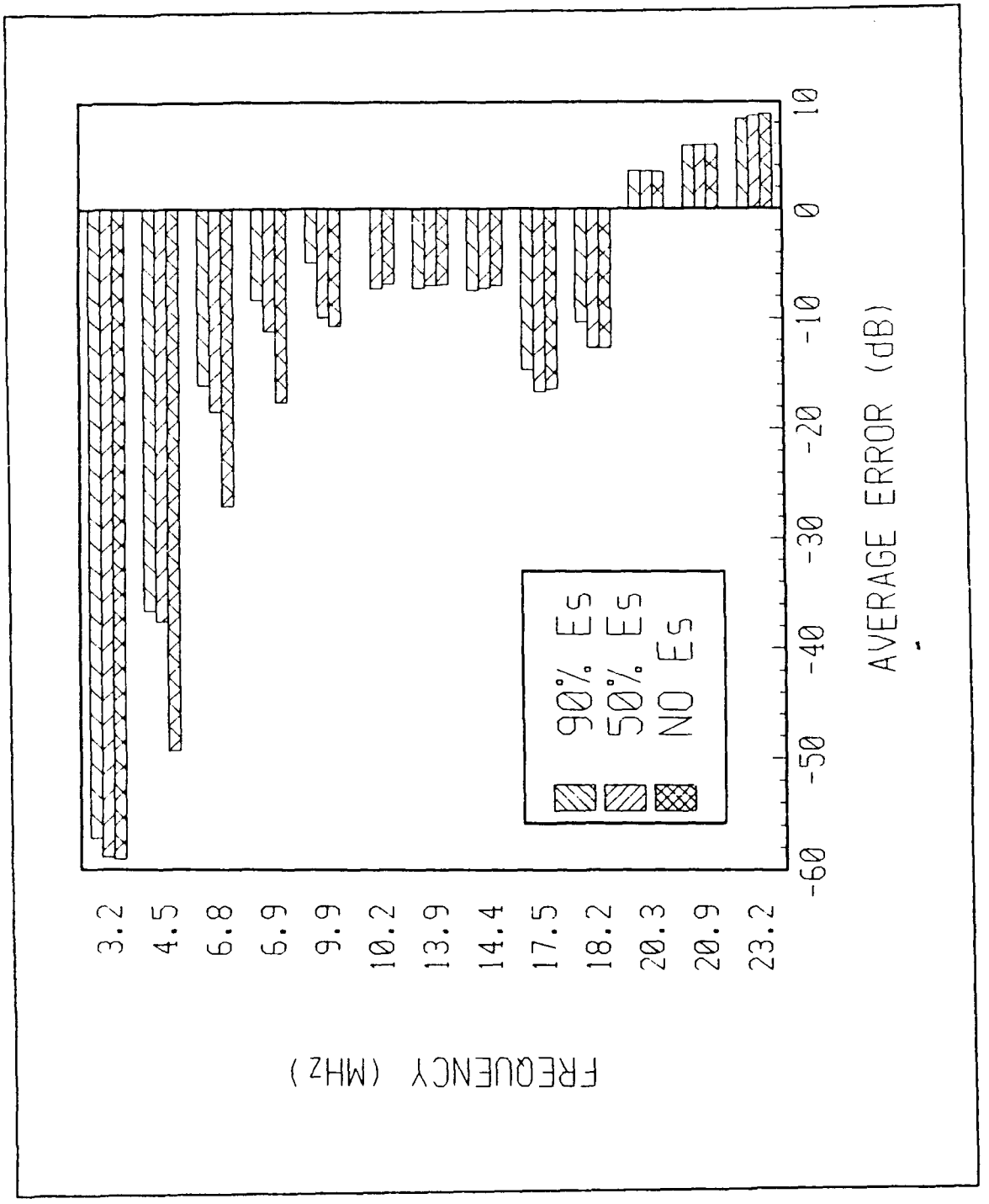


**Figure 23. The average error, for winter site D, listed by frequency.**

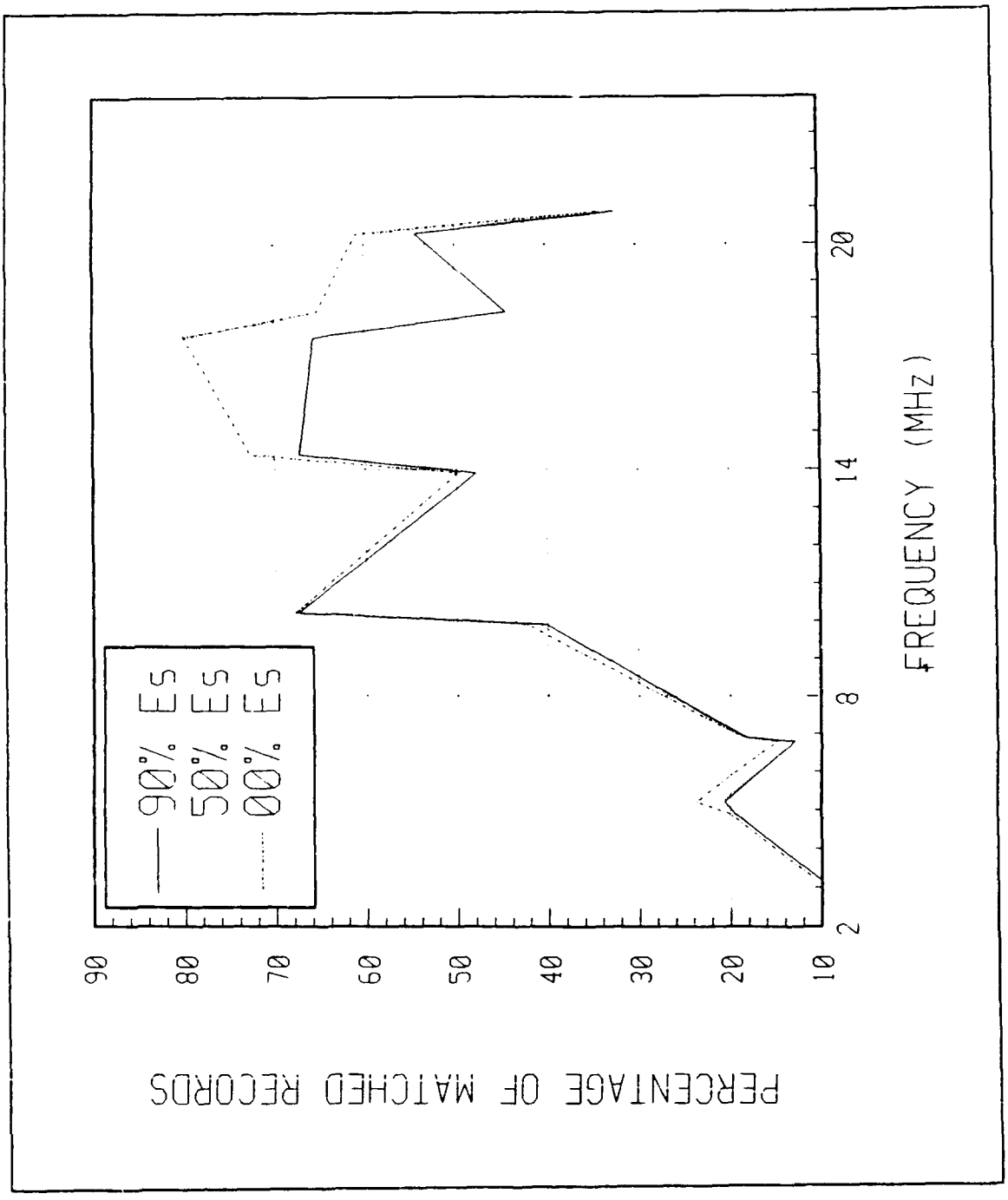


**Figure 24.** The percentage of matching summer site O data reference to the total number of AMBCOM predictions (by frequency).

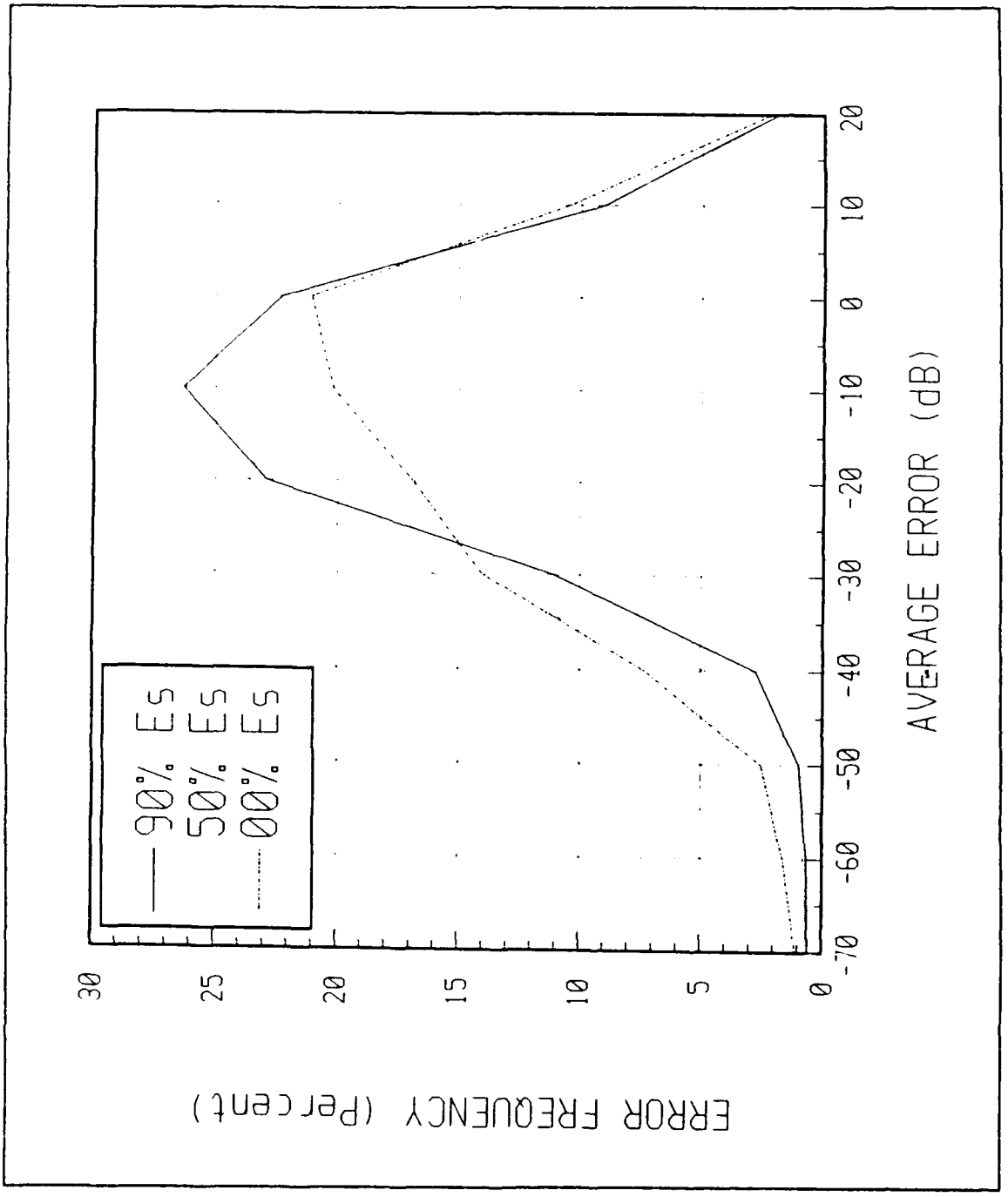


**Figure 25. Summer site O average error grouped in ten dB bins and plotted by percentage of error frequency.**

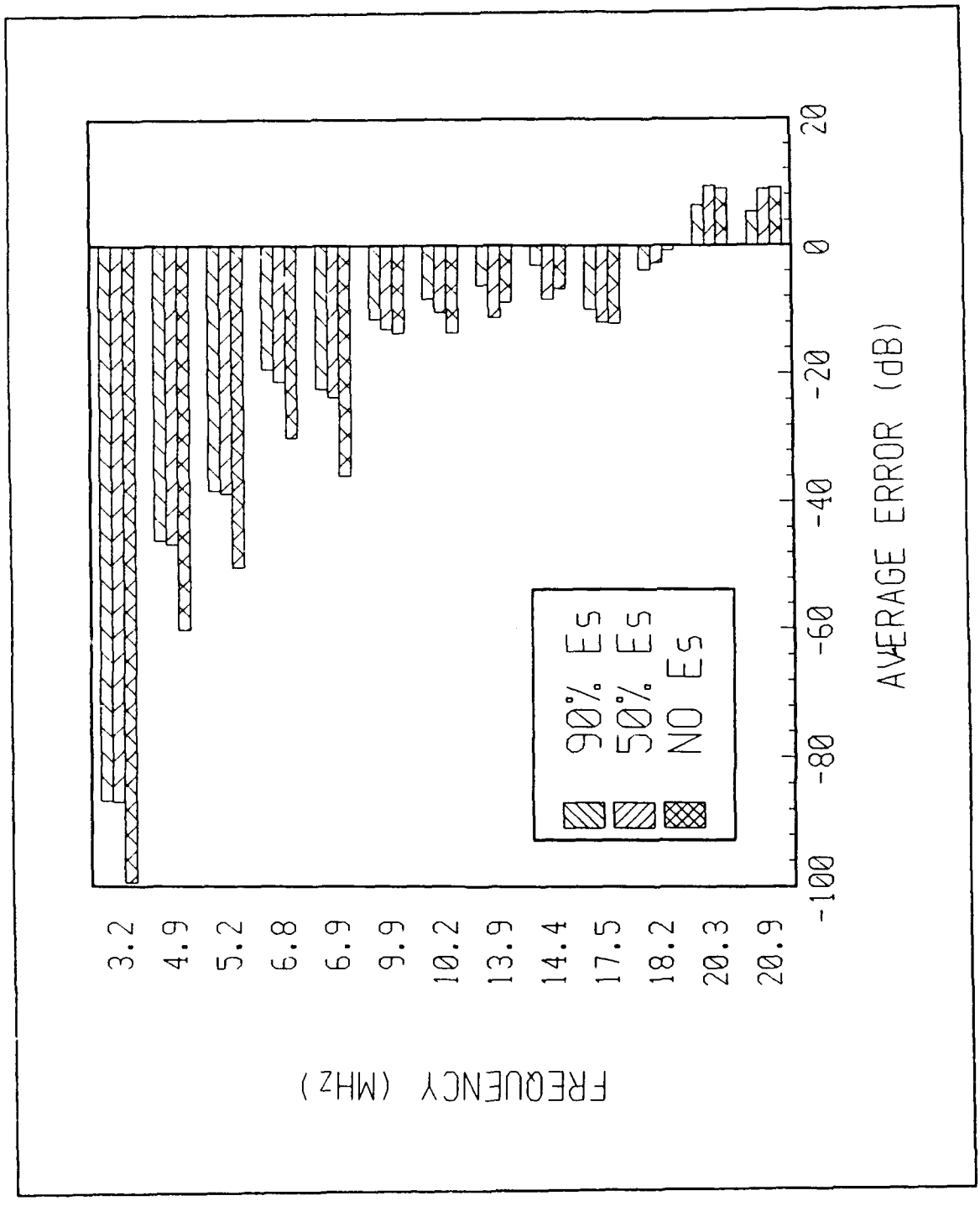


**Figure 26. The average error, for summer site O, listed by frequency.**

### 2. Site C

The summer site C data produced a high percentage of matched data ($P_{TOT}$) for all three $E_s$ models. The respective values for 90%, 50% and 0% $E_s$ are 95.8%, 90.8% and 81.8%. The distribution of $P_f$ was much different from that of the winter site C. Figure 27 on page 55 shows that $P_f$ was smaller at higher frequencies. This trend is the same for all three of the sporadic E models. For example, at 10.2 MHz all three of the models produced a high percentage of matching AMBCOM records. Peaks and valleys in this figure roughly agree with a similar distribution for summer site D. The common antenna model may be a major contributing factor.

Site C average error was obtained by subtracting 15 dB from the AMBCOM SNR to account for onsite noise at the receiving station. The average error is -6.2 dB, -8.9 dB and -13.3 dB for 90%, 50% and 0% $E_s$, respectively. Figure 28 on page 56 is the error distribution for site C. The distribution is skewed along the negative error axis. The 0% distribution is offset from the 90% and 50% curves. The standard deviations for these error data are 15.9 dB, 16.4 dB and 21.5 dB for 90%, 50% and 0% $E_s$.

### 3. Site D

Summer site D statistics were similar to those for summer site C. The percentage of matched records were, respectively, 89.1%, 80.4% and 76.0% for the 90%, 50% and 0% $E_s$ models. The distribution of $P_f$ is plotted in Figure 30 on page 58. This distribution exhibit a peak and valley pattern similar to that of summer site C. Values for $P_f$ for site D are, generally, much higher than for site C. It is reasonable that the peaks and valleys are in part attributable to the behavior of the site antenna at different frequencies, i.e. the antenna patterns used for the AMBCOM modeling of these sites may not be completely correct.

The average error for site D exhibited nearly the same pattern as for site C. The average error is -8.0 dB, -11.4 dB, and -17.0 dB for 90%, 50% and 0% $E_s$, respectively. Figure 31 on page 59 shows the distribution of average error is centered near -20 dB for the 90% and 50% models. The 0% $E_s$ error distribution curve was shifted in the negative direction along the average error axis with a peak value near -30 dB. The standard deviation of the error is 13.7 dB, 12.4 dB and 17.6 dB for the 90%, 50% and 0% models. Figure 32 on page 60 shows the distribution of average error by frequency.

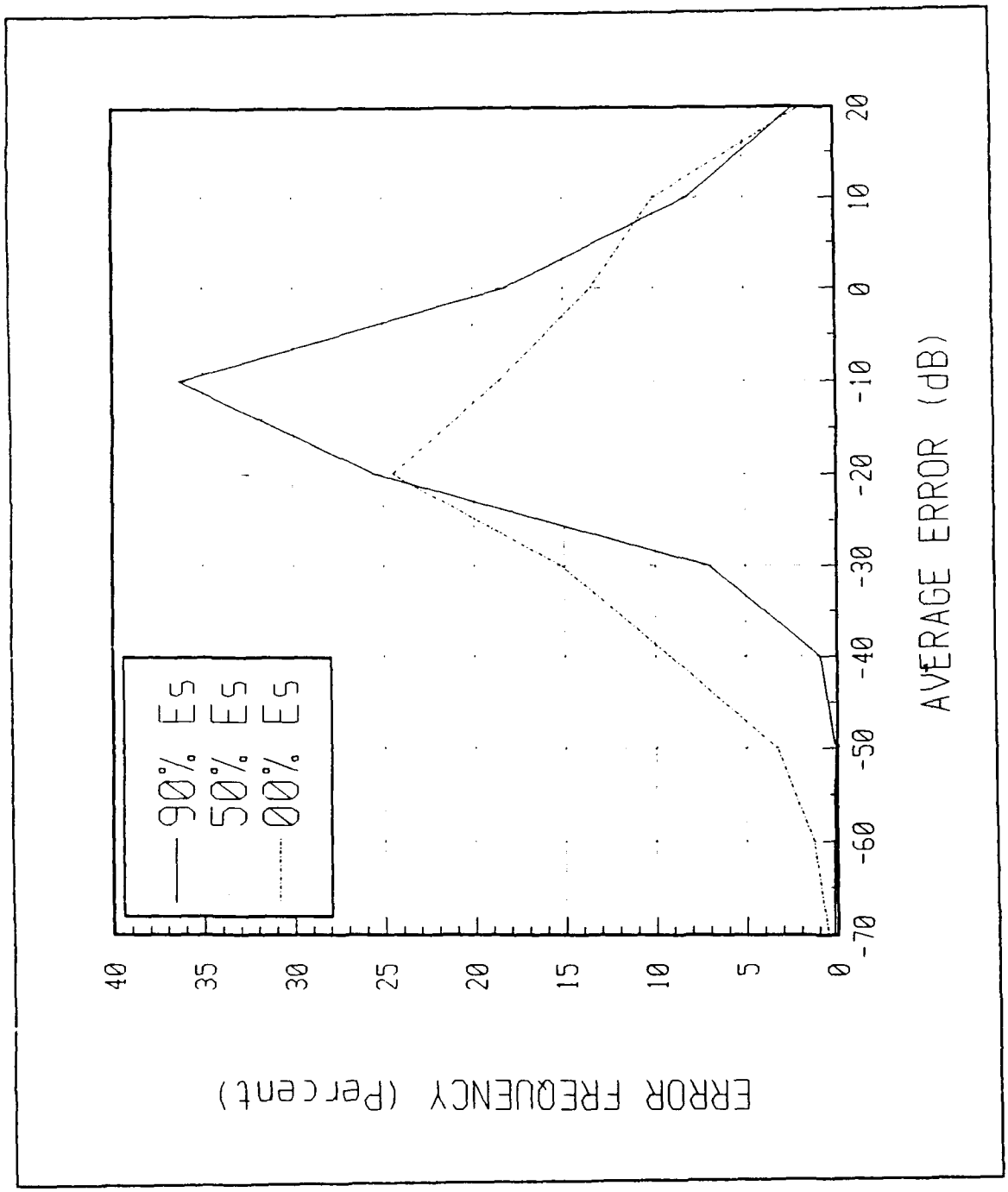


**Figure 27. The percentage of summer site C matching data reference to the total number of AMBCOM predictions (by frequency).**

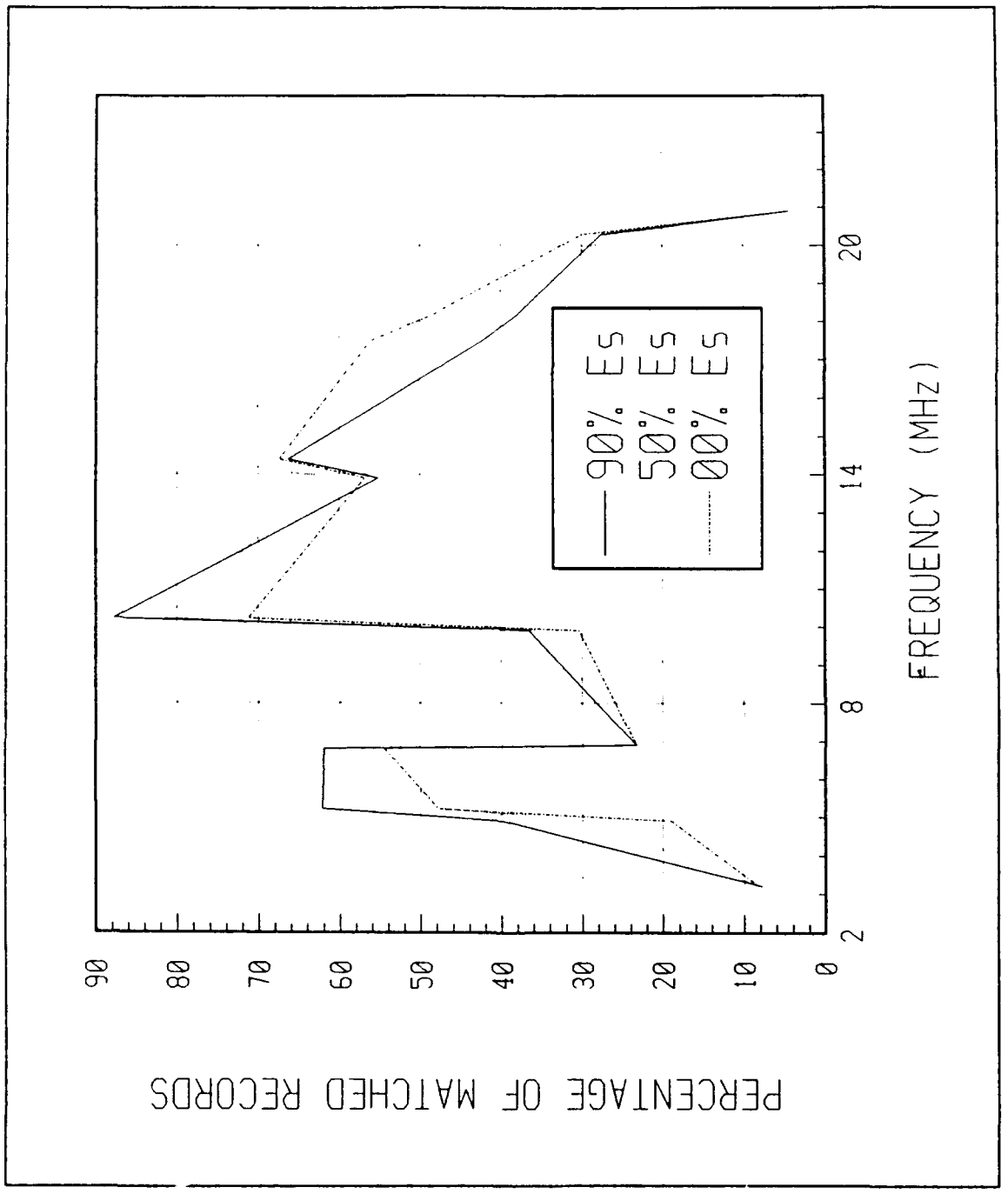


**Figure 28.** The summer site C average error grouped in ten dB bins and plotted by percentage of error frequency.

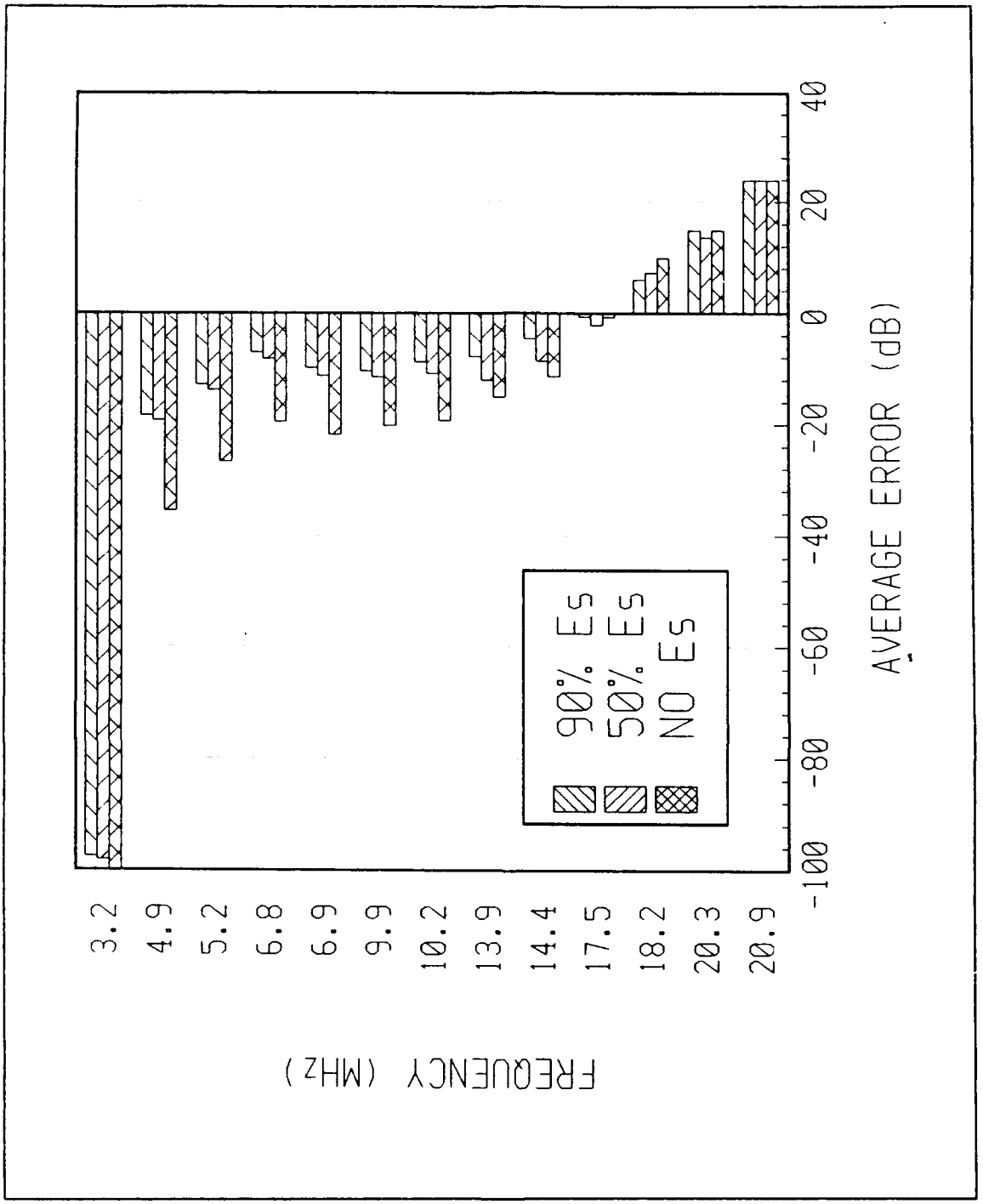


**Figure 29. The average error, for summer site C, listed by frequency.**

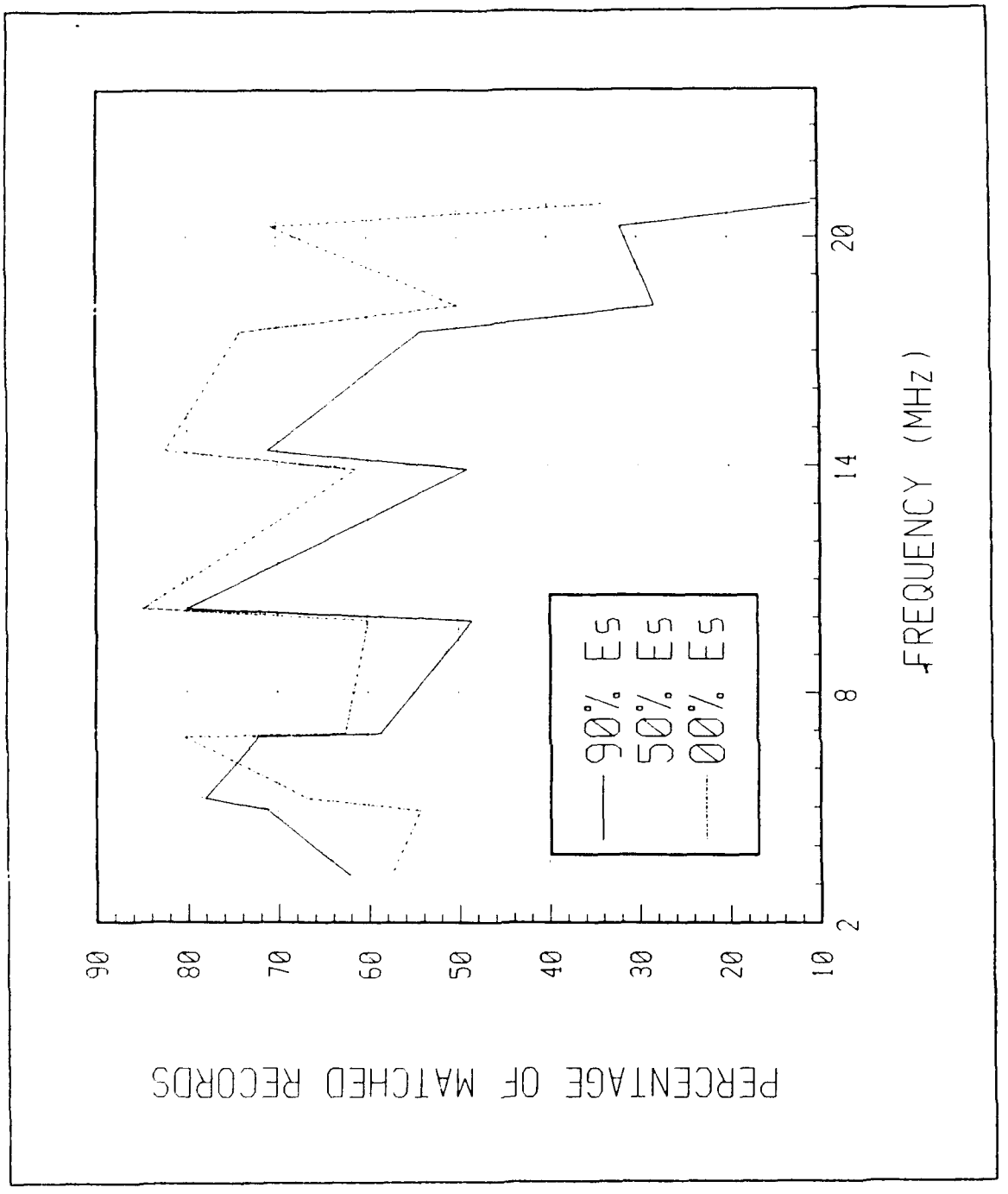


**Figure 30.** The percentage of summer site D matching data reference to the total number of AMBCOM predictions (by frequency).

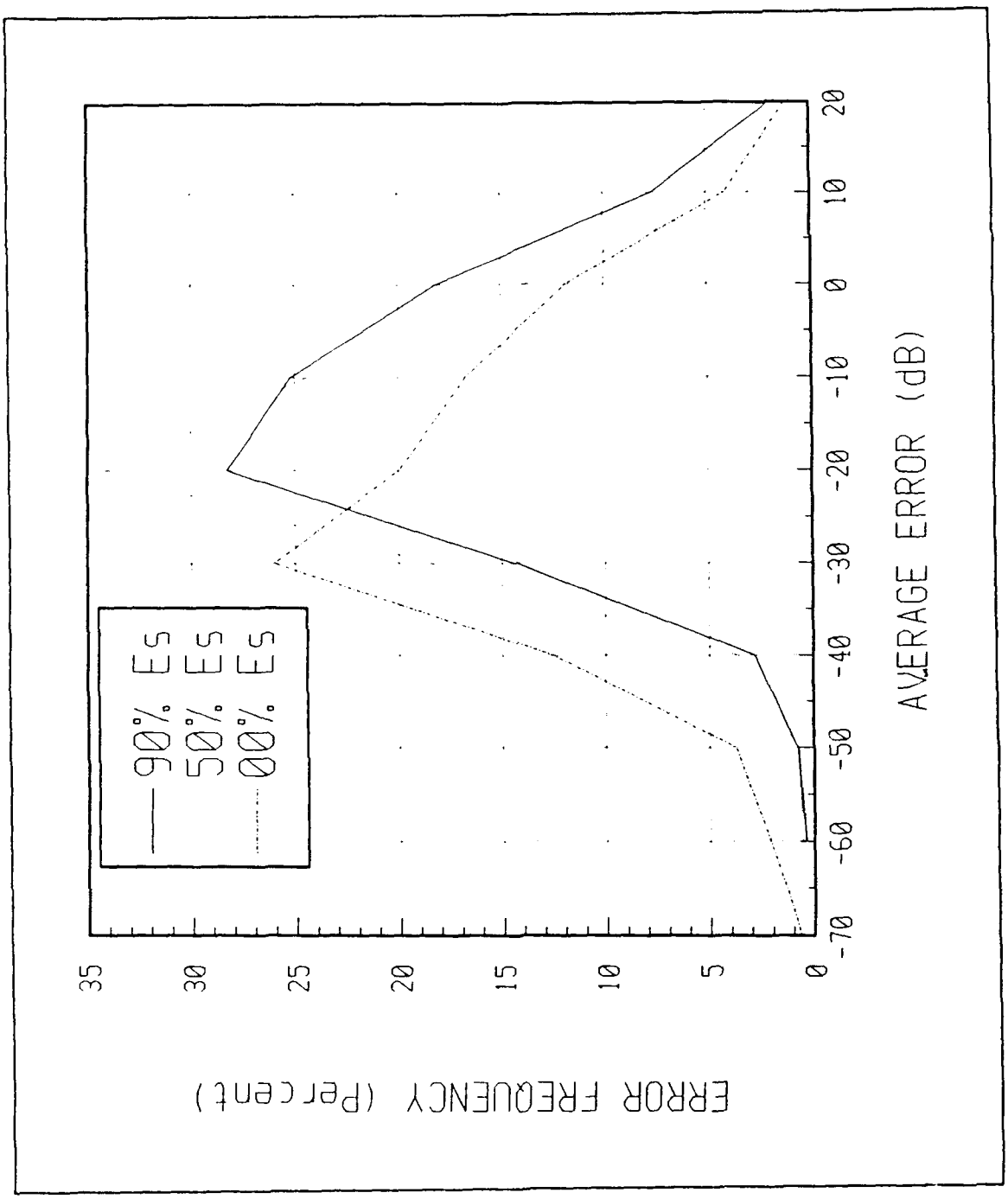


Figure 31. The summer site D average error grouped in ten dB bins and plotted by percentage of error frequency.

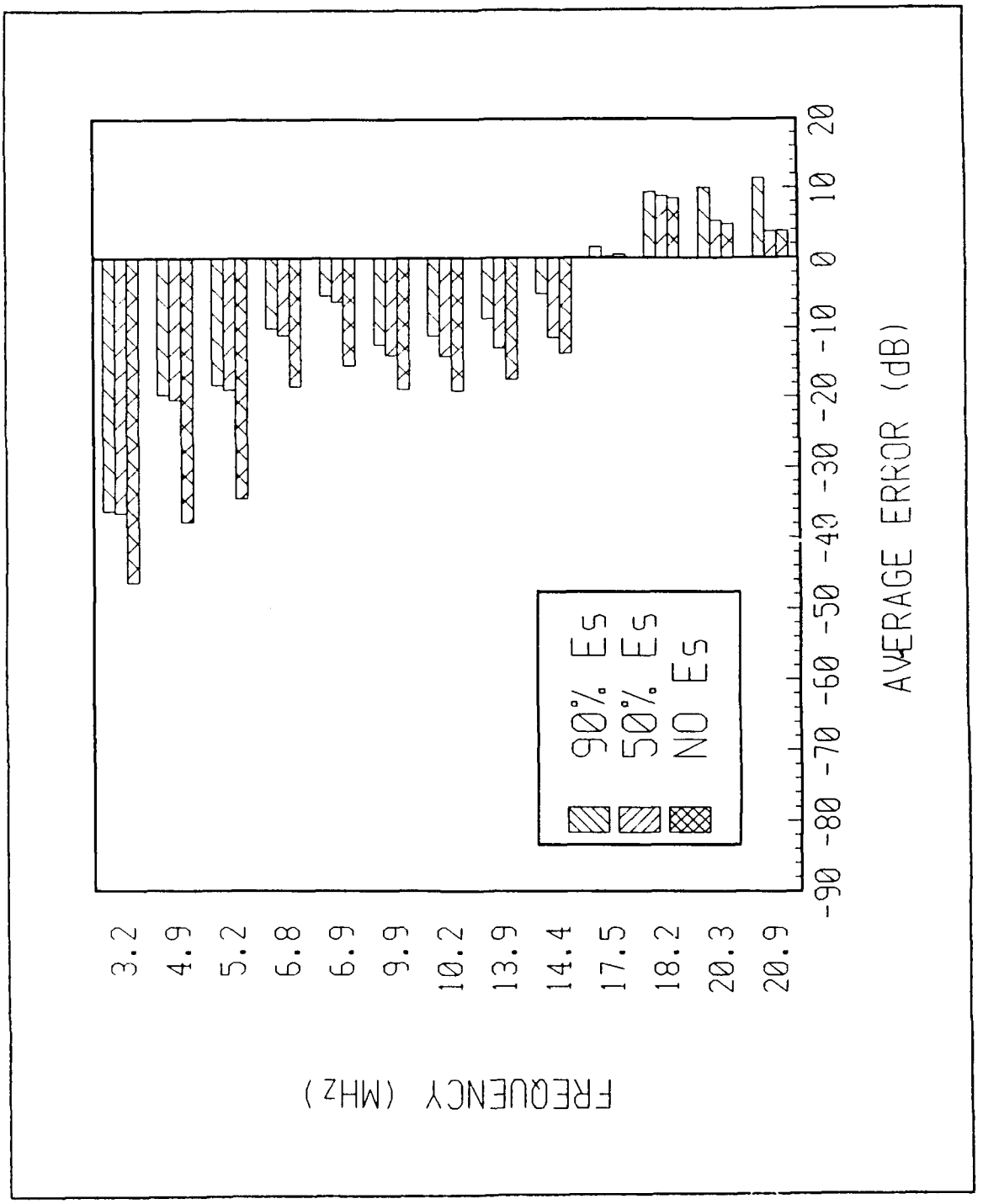


**Figure 32. The average error, for summer site D, listed by frequency.**

# V. CONCLUSIONS AND RECOMMENDATIONS

## A. CONCLUSIONS

### 1. The Project NONCENTRIC Data

Project NONCENTRIC data were not designed for the validation of computer-based propagation prediction models. For example, data did not contain necessary information such as

- measured or computed antenna patterns,
- measured received field strengths at the antenna,
- measured signal and noise levels at the receiver,
- ground constands at receiver sites,
- measured receiver site noise levels and
- periodic ionospheric data.

For example, the antenna gain tables used by AMBCOM were modeled using estimated values of ground permitivity and conductivity for each receiver site. It is likely that these estimated parameters resulted in errors in the computation of AMBCOM SNRs. AMBCOM's validity as a high-latitude propagation prediction model cannot be fully established by Project NONCENTRIC data since the impact of these errors on AMBCOM's accuracy cannot be evaluated.

Project NONCENTRIC files were useful as a standard data base for comparing computer-based models. IONCAP, PROPHET and AMBCOM were executed using the same antenna gain tables, sunspot numbers, $K_p$ indices and frequencies. The data produced by these models were then compared to the same Project NONCENTRIC data using standardized analysis procedures. The results of these studies were comparable since errors introduced by estimated input parameters were the same for each model.

### 2. AMBCOM

The results from this thesis fully evaluate the usefullness of AMBCOM for high-latitude propagation modeling, but AMBCOM does perform well when compared to IONCAP and PROPHET. As may be observed in Appendix D, the normalized median error for AMBCOM, for the winter campaign, ranged from -.2 dB to 5.8 dB. The winter campaign normalized error for IONCAP [Ref. 13: p. 24] and PROPHET [Ref. 14: p. 39] were 4.6 dB and .77 dB, respectively. AMBCOM produced winter campaign

error distributions having standard deviations, depending upon $E_s$ model, ranging from 15.9 dB to almost 20 dB. IONCAP's standard deviation for the winter campaign error distribution was 18.5 dB [Ref. 13: p. 24]. PROPHET produced a standard deviation of 14.7 dB for a similar distribution [Ref. 14: p. 24]. Similar results were obtained for the site O summer campaign.

AMBCOM's batch input mode and operational flexibility make it ideal for automated data analysis and communication link modeling with unique antenna configurations. AMBCOM allows the user to

- create large input streams representing several campaign days,
- save data and report files for further processing,
- add unique antenna patterns to AMBCOM's antenna library,
- include user written programs within the AMBCOM batch input stream and
- review data produced by program modules (e.g., review the NATGEN data passed to RAYTRA).

IONCAP and PROPHET do not have all of these capabilities. IONCAP does not allow the user to easily add new antenna patterns to its antenna library. Tsolekas [Ref. 13] accounted for antenna effects by manually adjusting the IONCAP output. PROPHET does not provide a batch input mode, but PROPHET is an example of a interactive computer-based model with online editor features and both graphical and numerical output. Gikas [Ref. 14] found it necessary to produce the PROPHET model data one hour and one frequency at a time for a 25 day campaign.

AMBCOM also has its limitations. AMBCOM is difficult to use because it provides the user with little online support. Some of AMBCOM's shortcomings noted during this thesis are

- input control parameters must be located in specified columns,
- there are no data entry programs to assist the user in entering control parameters or antenna data,
- there are no graphic output displays and
- the programs run only on VAX VMS-based systems or a mainframe computer systems.

Data produced by AMBCOM were displayed using a COMPAQ-386 and GRAPHTOOL because statistical trends are not easily visualized using numerical reports.

### 3. Statistics

The accumulation of propagation prediction model statistics, by frequency, are useful for highlighting patterns in model performance. The analysis of IONCAP and PROPHET did not include statistics by frequency [Ref. 13 and 14]; however, the results from this thesis point to the importance of examining the performance of the model at each frequency. The general statistics and distributions of error provide only part of the picture of how well a model performs. For example, the 90% $E_s$ model for winter site O showed a $P_{TOT}$ of nearly 90% and a low absolute value of average error. An examination of the average error by frequency reveals that the absolute value of low frequency average error was very large. The distribution of $P_f$ showed that a small percentage of AMBCOM predictions matched the measured data at low frequency. None of these trends may be observed with general statistics.

## B. RECOMMENDATIONS

### 1. Comparison Data

A new set of high-latitude data should be produced. This data should include

- measured field strengths at the antenna and receiver,
- measured noise levels throughout the receive site,
- measured or, at least, carefully modeled antenna patterns and
- periodic ionospheric data from the WWV broadcast and other solar-terrestrial sources.

This will provide the model user with a standard set of transmission data and the background information needed to create input for his computer-based model.

### 2. AMBCOM

AMBCOM should be updated. The model should be redesigned with such features as

- a menu-driven input editor,
- a choice of operation modes, i.e., interactive or batch,
- the capability to maintain a library of transmitter/receiver sites and
- graphic output displays.

One proposal is to use PROPHET's user-friendly editor and graphic displays as a shell for the AMBCOM software. The user would have the interactive features of PROPHET but would have access to the powerful AMBCOM propagation prediction models.

AMBCOM should be downsized to run on PC-type microcomputers. The majority of the military user community has access to Zenith 248 type microcomputers. Placing AMBCOM on a microcomputer will make it available to a larger segment of this user population. In addition, the microcomputer's graphics capability would provide AMBCOM with a means of changing from numerical reports to graphical representations of the data. The trends noted in this thesis were not dramatically noticeable until the data was graphed with PC-based software. AMBCOM provides no graphical displays.

### 3. Statistics

All computer-based model examinations should use the same analysis methodology. Statistics should include detailed information by frequency to include the average error and the percentage of matched records $P_f$ This will provide some insight regarding the behavior of the model at various frequencies.

# APPENDIX A. ANTENNA GAIN TABLES

## Table 4. RESISTIVE WHIP GAIN TABLE

WHIP

| ELEVATION | FREQUENCY, MHz | | | | | | | | | | | | | | | |
|---|---|---|---|---|---|---|---|---|---|---|---|---|---|---|---|---|
| | 2 | 4 | 6 | 8 | 10 | 12 | 14 | 16 | 18 | 20 | 22 | 24 | 26 | 28 | 30 |
| 2.0 | -52.2 | -39.7 | -31.7 | -24.6 | -17.4 | -15.6 | -16.8 | -17.9 | -18.4 | -17.4 | -16.5 | -16.6 | -17.6 | -17.3 | -17.0 |
| 4.0 | -47.2 | -34.7 | -26.6 | -19.5 | -12.3 | -10.5 | -11.7 | -12.9 | -13.3 | -12.7 | -11.4 | -11.5 | -12.5 | -12.2 | -11.9 |
| 6.0 | -44.2 | -32.1 | -24.0 | -16.8 | -9.7 | -7.8 | -9.1 | -10.2 | -10.7 | -10.1 | -10.0 | -8.9 | -9.8 | -9.6 | -9.4 |
| 8.0 | -43.1 | -30.5 | -22.4 | -15.1 | -8.9 | -6.2 | -7.4 | -8.7 | -9.2 | -8.6 | -7.3 | -7.3 | -8.2 | -8.0 | -8.0 |
| 10.0 | -42.0 | -29.4 | -21.2 | -14.0 | -6.8 | -5.1 | -6.4 | -7.6 | -8.2 | -7.7 | -6.3 | -6.2 | -7.2 | -7.2 | -7.2 |
| 12.0 | -41.2 | -28.6 | -20.4 | -13.1 | -6.0 | -4.3 | -5.7 | -7.0 | -7.6 | -7.1 | -5.7 | -5.5 | -6.5 | -6.6 | -6.8 |
| 14.0 | -40.6 | -28.0 | -19.8 | -12.6 | -5.5 | -3.8 | -5.2 | -6.6 | -7.3 | -6.9 | -5.4 | -5.0 | -6.0 | -6.4 | -6.8 |
| 16.0 | -40.2 | -27.6 | -19.3 | -12.1 | -5.1 | -3.4 | -4.9 | -6.4 | -7.2 | -6.9 | -5.2 | -4.6 | -5.7 | -6.3 | -6.9 |
| 18.0 | -39.8 | -27.2 | -19.0 | -11.8 | -4.8 | -3.2 | -4.8 | -6.4 | -7.3 | -7.0 | -5.1 | -4.4 | -5.6 | -6.4 | -7.3 |
| 20.0 | -39.6 | -27.6 | -18.8 | -11.6 | -4.7 | -3.2 | -4.8 | -6.5 | -7.5 | -7.2 | -5.1 | -4.2 | -5.5 | -6.7 | -7.8 |
| 22.0 | -39.4 | -26.8 | -18.6 | -11.5 | -4.6 | -3.2 | -4.9 | -6.8 | -7.9 | -7.6 | -5.2 | -4.1 | -5.6 | -7.0 | -8.4 |
| 24.0 | -39.3 | -26.7 | -18.5 | -11.4 | -4.6 | -3.3 | -5.1 | -7.1 | -8.3 | -7.9 | -5.2 | -4.0 | -5.7 | -7.5 | -9.2 |
| 26.0 | -39.2 | -26.6 | -18.5 | -11.5 | -4.7 | -3.5 | -5.4 | -7.5 | -8.8 | -8.3 | -5.3 | -4.0 | -5.9 | -8.0 | -10.2 |
| 28.0 | -39.2 | -26.6 | -18.5 | -11.5 | -4.9 | -3.7 | -5.8 | -8.0 | -9.4 | -8.7 | -5.4 | -3.9 | -6.2 | -8.7 | -11.3 |
| 30.0 | -39.2 | -26.6 | -18.6 | -11.6 | -5.1 | -4.0 | -6.3 | -8.6 | -10.0 | -9.0 | -5.5 | -4.0 | -6.5 | -9.5 | -12.6 |
| 35.0 | -39.3 | -26.9 | -18.9 | -12.1 | -5.8 | -5.1 | -7.6 | -10.3 | -11.5 | -9.5 | -5.7 | -4.3 | -7.9 | -12.3 | -16.8 |
| 40.0 | -39.7 | -27.3 | -19.4 | -12.8 | -6.8 | -6.4 | -9.4 | -12.2 | -12.6 | -9.7 | -6.0 | -5.1 | -9.7 | -15.4 | -21.1 |
| 45.0 | -40.2 | -27.8 | -20.1 | -13.8 | -8.0 | -8.0 | -11.3 | -13.9 | -13.3 | -9.9 | -7.0 | -6.3 | -10.6 | -14.8 | -19.0 |
| 50.0 | -40.9 | -28.6 | -21.0 | -14.9 | -9.4 | -9.7 | -13.3 | -15.3 | -13.6 | -10.4 | -7.6 | -8.0 | -11.7 | -13.8 | -16.0 |
| 55.0 | -41.8 | -29.6 | -22.1 | -16.2 | -11.0 | -11.7 | -15.2 | -16.2 | -14.1 | -11.2 | -9.0 | -10.3 | -13.6 | -14.0 | -14.5 |
| 60.0 | -42.9 | -30.7 | -23.4 | -17.7 | -12.9 | -13.7 | -17.0 | -17.1 | -14.9 | -12.4 | -10.9 | -13.0 | -16.1 | -15.2 | -15.2 |
| 65.0 | -44.3 | -32.2 | -25.0 | -19.5 | -15.0 | -15.9 | -18.7 | -18.1 | -16.1 | -14.0 | -13.1 | -16.2 | -19.4 | -17.1 | -14.8 |
| 70.0 | -46.1 | -34.1 | -27.0 | -21.6 | -17.3 | -18.3 | -20.6 | -19.6 | -17.8 | -16.1 | -15.8 | -19.8 | -23.1 | -19.7 | -16.3 |
| 75.0 | -48.5 | -36.5 | -29.5 | -24.3 | -20.2 | -21.1 | -22.9 | -21.7 | -20.1 | -18.8 | -19.0 | -23.8 | -27.0 | -22.9 | -18.5 |
| 80.0 | -51.9 | -40.0 | -33.0 | -28.0 | -24.0 | -24.8 | -26.2 | -25.0 | -23.6 | -22.5 | -23.1 | -28.4 | -32.0 | -27.9 | -22.0 |
| 85.0 | -57.9 | -46.0 | -39.1 | -34.1 | -30.2 | -30.9 | -32.1 | -30.8 | -29.5 | -28.6 | -29.4 | -35.0 | -38.3 | -33.3 | -28.0 |
| 90.0 | -99.9 | -99.9 | -99.9 | -99.9 | -99.9 | -99.9 | -99.9 | -99.9 | -99.9 | -99.9 | -99.9 | -99.9 | -99.9 | -99.9 | -99.9 |
| BWIDTH | 360.0 | 360.0 | 360.0 | 360.0 | 360.0 | 360.0 | 360.0 | 360.0 | 360.0 | 360.0 | 360.0 | 360.0 | 360.0 | 360.0 | 360.0 |
| LOSS | 0.0 | 0.0 | 0.0 | 0.0 | 0.0 | 0.0 | 0.0 | 0.0 | 0.0 | 0.0 | 0.0 | 0.0 | 0.0 | 0.0 | 0.0 |

Table 5. BUTTERNUT HF6V GAIN TABLE

BUTTERNUT

| | FREQUENCY, MHZ | | | | | | | | | | | | | | |
|---|---|---|---|---|---|---|---|---|---|---|---|---|---|---|---|
| | 2 | 4 | 6 | 8 | 10 | 12 | 14 | 16 | 18 | 20 | 22 | 24 | 26 | 28 | 30 |
| E | 2.0 -28.1 | -24.3 | -21.9 | -19.9 | -18.1 | -16.0 | -15.0 | -14.1 | -13.3 | -12.7 | -12.2 | -11.8 | -11.2 | -10.7 | -10.1 |
| L | 4.0 -23.9 | -19.7 | -17.1 | -15.0 | -13.1 | -11.0 | -10.0 | -9.1 | -8.2 | -7.7 | -7.2 | -6.7 | -6.2 | -5.6 | -5.1 |
| E | 6.0 -22.0 | -17.5 | -14.7 | -12.5 | -10.6 | -8.4 | -7.4 | -6.5 | -5.6 | -5.1 | -4.6 | -4.1 | -3.6 | -3.1 | -2.5 |
| V | 8.0 -20.9 | -16.1 | -13.3 | -11.0 | -9.0 | -6.8 | -5.8 | -4.9 | -4.0 | -3.5 | -3.0 | -2.6 | -2.1 | -1.6 | -1.0 |
| A | 10.0 -20.2 | -15.3 | -12.3 | -10.0 | -8.0 | -5.8 | -4.8 | -3.8 | -3.0 | -2.4 | -2.0 | -1.6 | -1.1 | -0.6 | -0.1 |
| T | 12.0 -19.7 | -14.6 | -11.6 | -9.3 | -7.2 | -4.7 | -4.0 | -3.0 | -2.2 | -1.7 | -1.3 | -0.9 | -0.5 | -0.1 | 0.4 |
| I | 14.0 -19.4 | -14.2 | -11.1 | -8.7 | -6.7 | -4.4 | -3.4 | -2.5 | -1.7 | -1.2 | -0.9 | -0.4 | -0.2 | 0.2 | 0.7 |
| O | 16.0 -19.2 | -13.9 | -10.7 | -8.3 | -6.3 | -4.0 | -3.1 | -2.2 | -1.4 | -1.0 | -0.6 | -0.3 | 0.0 | 0.4 | 0.7 |
| N | 18.0 -19.0 | -13.7 | -10.5 | -8.1 | -6.0 | -3.8 | -2.8 | -1.9 | -1.2 | -0.8 | -0.5 | -0.3 | 0.0 | 0.3 | 0.6 |
| | 20.0 -18.9 | -13.5 | -10.3 | -7.9 | -5.8 | -3.6 | -2.6 | -1.8 | -1.1 | -0.8 | -0.5 | -0.4 | -0.1 | 0.1 | 0.3 |
| A | 22.0 -18.9 | -13.5 | -10.2 | -7.8 | -5.7 | -3.4 | -2.5 | -1.7 | -1.1 | -0.8 | -0.7 | -0.5 | -0.4 | -0.2 | -0.1 |
| N | 24.0 -18.9 | -13.4 | -10.2 | -7.7 | -5.7 | -3.4 | -2.5 | -1.7 | -1.2 | -0.9 | -0.9 | -0.8 | -0.7 | -0.6 | -0.6 |
| G | 26.0 -18.9 | -13.4 | -10.1 | -7.7 | -5.7 | -3.4 | -2.5 | -1.8 | -1.3 | -1.2 | -1.2 | -1.2 | -1.2 | -1.2 | -1.1 |
| L | 28.0 -19.0 | -13.4 | -10.1 | -7.7 | -5.7 | -3.4 | -2.6 | -1.9 | -1.5 | -1.4 | -1.5 | -1.6 | -1.7 | -1.7 | -1.8 |
| E | 30.0 -19.1 | -13.5 | -10.2 | -7.7 | -5.8 | -3.5 | -2.7 | -2.1 | -1.8 | -1.8 | -2.0 | -2.1 | -2.3 | -2.3 | -2.4 |
| | 35.0 -19.4 | -13.8 | -10.5 | -8.0 | -6.1 | -3.9 | -3.2 | -2.8 | -2.6 | -2.9 | -3.3 | -3.7 | -3.9 | -3.9 | -3.9 |
| I | 40.0 -19.9 | -14.2 | -10.9 | -8.6 | -6.7 | -4.5 | -3.9 | -3.6 | -3.7 | -4.2 | -4.9 | -5.6 | -5.7 | -5.3 | -4.0 |
| N | 45.0 -20.5 | -14.8 | -11.5 | -9.2 | -7.4 | -5.3 | -4.8 | -4.7 | -5.1 | -6.0 | -6.8 | -7.6 | -7.4 | -6.4 | -5.4 |
| | 50.0 -21.2 | -15.6 | -12.3 | -10.0 | -8.3 | -6.2 | -5.9 | -6.0 | -6.6 | -7.9 | -8.7 | -9.4 | -8.9 | -7.2 | -5.5 |
| D | 55.0 -22.2 | -16.5 | -13.3 | -11.0 | -8.4 | -7.4 | -7.2 | -7.5 | -8.3 | -10.0 | -10.6 | -10.9 | -10.1 | -8.0 | -5.9 |
| E | 60.0 -23.3 | -17.7 | -14.4 | -12.2 | -10.7 | -8.7 | -8.7 | -9.1 | -10.3 | -12.3 | -12.4 | -12.3 | -11.1 | -8.8 | -6.5 |
| G | 65.0 -24.8 | -19.1 | -15.9 | -13.7 | -12.2 | -10.4 | -10.5 | -11.1 | -12.4 | -14.7 | -14.4 | -13.6 | -12.2 | -9.9 | -7.6 |
| R | 70.0 -26.6 | -20.9 | -17.7 | -15.6 | -14.2 | -12.3 | -12.6 | -13.3 | -14.8 | -17.2 | -16.5 | -15.2 | -13.5 | -11.4 | -9.3 |
| E | 75.0 -29.0 | -23.3 | -20.2 | -18.1 | -16.7 | -13.9 | -15.2 | -16.1 | -17.7 | -20.2 | -19.1 | -17.4 | -14.6 | -13.6 | -11.6 |
| E | 80.0 -32.4 | -26.8 | -23.6 | -21.6 | -20.2 | -18.5 | -18.8 | -19.8 | -21.5 | -24.0 | -22.7 | -20.7 | -18.8 | -16.9 | -15.0 |
| S | 85.0 -38.4 | -32.8 | -29.6 | -37.6 | -26.3 | -24.5 | -24.9 | -24.9 | -27.6 | -30.1 | -28.7 | -26.6 | -24.7 | -22.8 | -20.9 |
| | 90.0 -99.9 | -99.9 | -99.9 | -99.9 | -99.9 | -99.9 | -99.9 | -99.9 | -99.9 | -99.9 | -99.9 | -99.9 | -99.9 | -99.9 | -99.9 |
| BWIDTH | 360.0 | 360.0 | 360.0 | 360.0 | 360.0 | 360.0 | 360.0 | 360.0 | 360.0 | 360.0 | 360.0 | 360.0 | 360.0 | 360.0 | 360.0 |
| LOSS | 0.0 | 0.0 | 0.0 | 0.0 | 0.0 | 0.0 | 0.0 | 0.0 | 0.0 | 0.0 | 0.0 | 0.0 | 0.0 | 0.0 | 0.0 |

Table 6. SLOPING VEE GAIN TABLE

SLOPING VEE

| | | FREQUENCY, MHZ | | | | | | | | | | | | | | |
|---|---|---|---|---|---|---|---|---|---|---|---|---|---|---|---|---|
| | | 2 | 4 | 6 | 8 | 10 | 12 | 14 | 16 | 18 | 20 | 22 | 24 | 26 | 28 | 30 |
| E | 2.0 | -31.8 | -21.9 | -17.7 | -15.9 | -14.7 | -12.9 | -11.0 | -9.5 | -8.7 | -8.7 | -7.3 | -6.0 | -5.1 | -4.6 | -4.2 |
| L | 4.0 | -25.8 | -15.9 | -11.8 | -10.1 | -8.8 | -7.0 | -5.2 | -3.7 | -3.1 | -3.1 | -1.8 | -0.5 | 0.3 | 0.7 | 1.0 |
| E | 6.0 | -22.4 | -12.5 | -8.4 | -6.8 | -5.6 | -3.8 | -2.0 | -0.6 | -0.1 | -0.2 | 0.9 | 2.1 | 2.8 | 3.0 | 3.2 |
| V | 8.0 | -19.9 | -10.1 | -6.1 | -4.6 | -3.4 | -1.6 | 0.0 | 1.3 | 1.6 | 1.3 | 2.4 | 3.4 | 3.9 | 3.8 | 3.6 |
| A | 10.0 | -18.0 | -8.3 | -5.5 | -3.0 | -1.9 | -0.1 | 1.4 | 2.4 | 2.5 | 2.0 | 2.9 | 3.8 | 3.9 | 3.3 | 2.7 |
| T | 12.0 | -16.5 | -6.9 | -3.1 | -1.8 | -0.8 | 0.9 | 2.4 | 3.1 | 2.8 | 2.0 | 2.6 | 3.2 | 2.8 | 1.4 | 0.0 |
| I | 14.0 | -15.3 | -5.7 | -2.1 | -1.0 | -0.1 | 1.7 | 2.9 | 3.3 | 2.5 | 1.4 | 1.6 | 1.7 | 0.3 | -2.8 | -5.9 |
| O | 16.0 | -14.2 | -5.8 | -1.3 | -0.4 | 0.4 | 2.1 | 3.2 | 3.0 | 1.6 | 0.2 | -0.4 | -1.1 | -7.9 | -21.1 | -34.2 |
| N | 18.0 | -13.3 | -5.0 | -0.6 | 0.0 | 0.7 | 2.4 | 3.1 | 2.3 | 0.2 | -1.8 | -3.9 | -6.1 | -7.0 | -6.5 | -6.0 |
| | 20.0 | -12.5 | -3.3 | -0.2 | 0.2 | 0.9 | 2.5 | 2.8 | 1.2 | -2.1 | -4.6 | -6.9 | -9.1 | -8.5 | -4.8 | -1.2 |
| A | 22.0 | -11.8 | -2.7 | 0.1 | 0.2 | 0.9 | 2.4 | 2.2 | -0.5 | -5.6 | -9.0 | -6.9 | -4.7 | -2.8 | -1.0 | 0.8 |
| N | 24.0 | -11.2 | -2.3 | 0.3 | 0.1 | 0.8 | 2.2 | 1.3 | -3.0 | -11.6 | -17.6 | -10.6 | -3.5 | 0.3 | 1.0 | 1.5 |
| G | 26.0 | -10.6 | -1.9 | 0.4 | -0.1 | 0.7 | 1.8 | 0.0 | -6.6 | -29.4 | -20.3 | -11.5 | -2.7 | 1.7 | 1.7 | 1.6 |
| L | 28.0 | -10.1 | -1.6 | 0.4 | -0.4 | 0.4 | 1.2 | -1.8 | -12.1 | -15.8 | -10.2 | -5.2 | -0.3 | 1.9 | 1.4 | 0.8 |
| E | 30.0 | -9.7 | -1.4 | -0.3 | -0.8 | 0.2 | 0.3 | -4.2 | -15.8 | -10.1 | -5.6 | -2.3 | 0.2 | 1.0 | -0.1 | -1.2 |
| | 35.0 | -8.8 | -1.1 | -0.4 | -1.9 | -0.8 | -3.1 | -11.8 | -7.4 | -4.4 | 0.1 | -1.5 | -3.0 | -4.7 | -6.7 | -8.6 |
| I | 40.0 | -8.2 | -1.3 | -1.5 | -2.7 | -2.5 | -9.4 | -8.2 | -5.4 | -0.7 | 0.8 | -3.7 | -8.3 | -8.4 | -3.9 | 0.5 |
| N | 45.0 | -7.7 | -1.7 | -3.0 | -3.3 | -5.8 | -12.3 | -6.8 | -2.9 | 0.4 | -3.5 | -4.9 | -6.3 | -5.9 | -3.8 | -1.6 |
| | 50.0 | -7.5 | -2.5 | -4.2 | -4.2 | -11.6 | -9.1 | -6.3 | -1.1 | -2.7 | -10.0 | -6.5 | -2.9 | -1.2 | -1.3 | -1.4 |
| D | 55.0 | -7.4 | -3.6 | -4.8 | -5.8 | -17.6 | -9.0 | -3.7 | -2.6 | -7.9 | -12.5 | -9.1 | -5.7 | -9.8 | -21.2 | -32.7 |
| E | 60.0 | -7.5 | -4.9 | -4.9 | -8.8 | -15.8 | -7.8 | -2.9 | -7.1 | -8.0 | -10.8 | -7.1 | -3.3 | -4.7 | -11.4 | -18.0 |
| G | 65.0 | -7.8 | -6.1 | -5.1 | -13.8 | -16.6 | -5.1 | -5.2 | -6.8 | -15.3 | -8.3 | -8.3 | -8.3 | -7.2 | -5.0 | -2.8 |
| R | 70.0 | -8.2 | -7.1 | -5.7 | -21.2 | -15.0 | -4.4 | -7.7 | -7.7 | -15.4 | -9.8 | -8.6 | -7.3 | -6.2 | -5.2 | -4.3 |
| E | 75.0 | -8.7 | -7.6 | -6.9 | -21.3 | -10.7 | -6.2 | -6.0 | -16.6 | -22.4 | -4.8 | -10.8 | -16.8 | -16.3 | -9.5 | -2.6 |
| E | 80.0 | -9.4 | -7.6 | -8.6 | -18.7 | -9.0 | -6.8 | -6.7 | -16.1 | -10.9 | -8.5 | -10.5 | -12.4 | -11.3 | -6.9 | -2.5 |
| S | 85.0 | -10.3 | -7.5 | -10.4 | -18.7 | -10.1 | -6.2 | -10.8 | -14.0 | -8.8 | -6.3 | -10.9 | -15.5 | -15.5 | -10.8 | -6.2 |
| | 90.0 | -11.3 | -7.5 | -11.0 | -20.6 | -13.3 | -5.8 | -9.4 | -25.9 | -15.7 | -6.7 | -11.2 | -15.7 | -14.9 | -8.9 | -2.8 |
| BWIDTH | | 30.0 | 30.0 | 30.0 | 30.0 | 30.0 | 30.0 | 30.0 | 30.0 | 30.0 | 30.0 | 30.0 | 30.0 | 30.0 | 30.0 | 30.0 |
| LOSS | | 0.0 | 0.0 | 0.0 | 0.0 | 0.0 | 0.0 | 0.0 | 0.0 | 0.0 | 0.0 | 0.0 | 0.0 | 0.0 | 0.0 | 0.0 |

# APPENDIX B. STATISTICAL ANAYLSIS PROGRAMS

## A. MODDAT

```
C*************************************************************************
c*  PROGRAM: MODDAT                                    DATE: DEC 1990
c*  PROGRAMMER: D.J.WILSON
c*  MODDAT READS THE SUMMARY REPORT PRODUCED BY COMEFF AND STRIPS OUT THE
c*  THE TIME, FREQUENCY, AND SNR FOR LATER PROCESSING.  THE DAY
c*  AND THE MONTH FOR WHICH THIS DATA WAS GENERATED IS
c*  ALSO RECORDED ON EACH OUTPUT RECORD.
C*************************************************************************
      REAL YFREQ,SNRIN                    ;SET UP REAL VARIABLES
      INTEGER MONTH,DAY,YHR               ;SET UP INTEGER VARIABLES
      READ(58,2) MONTH,DAY                ;READ IN THE MONTH AND DAY
2     FORMAT(I2,1X,I2)
3     READ(5,10,ERR=300,END=500) YHR,YFREQ,SNRIN  ;READ COMEFF LINE
10    FORMAT(6X,I2,12X,F4.1,49X,E11.4)          ;IF ERROR GO TO 300
      IF (YFREQ.LT.3.OR.YFREQ.GT.24) GO TO 3  ;FREQ BETWEEN 3 / 24 MHz
                                          ; NO - THEN  GO TO 3
      IF (SNRIN.EQ.0) GO TO 3             ; YES - THEN IS SNR EQUAL TO 0
                                          ; YES - THEN GO TO 3
      WRITE(4,20) YHR,YFREQ,SNRIN,MONTH,DAY   ; NO - WRITE RECORD FOR
                                          ; LATER PROCESSING
20    FORMAT(1X,I2,2X,F4.1,2X,F7.2,2X,I2,2X,I2)
      GO TO 3                             ;GO GET ANOTHER RECORD
300   GO TO 3   ;IN THE EVENT A FORMAT ERROR IS DETECTED DURING A READ
                ;THE PROGRAM TRANSFERS CONTROL TO STATEMENT 300 WHICH
                ;IN CAUSES THE PROGRAM TO GO BACK AND READ ANOTHER
                ;RECORD.  THE ERROR RECORD IS EFFECTIVELY IGNORED.  BY
                ;DOING THIS THE PROGRAM ONLY USES THOSE INPUT RECORDS
                ;WHICH MEET THE INPUT CRITERIA FOR A LINE OF INFORMATION
                ;FROM THE BODY OF THE COMEFF SUMMARY REPORT AND IGNORES
                ;THE REPORT HEADER AND TRAILERS.
500   END
```

## B. WILSTAT

```
C*************************************************************************
c* PROGRAM: WILSTAT                                    DATE: DEC 1990
c* PROGRAMMER: D.J.WILSON
c* THIS PROGRAM COMPARES THE AMBCOM DATA WITH THE PROJECT NONCENTRIC
c* DATA.  IF THE DATA MATCHES THEN THE SNR FOR BOTH RECORDS, ERROR,
c* SPREAD INDEX, FREQUENCY, TIME, MONTH AND HOUR ARE WRITTEN TO
c* FILE FOR LATER PROCESSING.  THE FREQUENCY AND SNR FOR UNMATCHED AMBCOM
c* DATA ARE WRITTEN TO A FILE FOR FURTHER PROCESS BY THE PROGRAM WILMAT.
c* THE UNMATCHED NONCENTRIC RECORDS ARE COUNTED AND THE TOTAL IS
c* MAINTAINED IN A TABLE BY FREQUENCY.  ADDITIONALLY THE AVERAGE SNR BY
C* FREQUENCY AND HOUR IS ACCUMULATED.
C*************************************************************************
c************ DATA SETUP ***********************************************
      REAL*8 SNRTAB(16,24,3),ERRTAB(16,5),RECTOT(16)   ; SET UP DOUBLE
      REAL*8 ACTEMP,MODTEMP,TOAVERR,TOTREC,PRCNT,TOTMOD ; PRECISION
                                          ; VARIABLES.
```

```
      REAL*4 MFREQ,MSNR                          ; SET UP SINGLE PRECISION
                                                 ; VARIALBLES.
      REAL*4 FREQ,SNR,SPI
      INTEGER MHR,MMON,MDAY,DOM,MON,XHR,HOUR ; IDENTIFY INTEGER VARIALBES
      ACTEMP=0.                                  ; INITIALIZE
C********** READ IN THE COMPARISON DATA **********************************
      READ(2,10,END=1400) FREQ,SNR,SPI,DOM,MON,XHR  ; NONCENTRIC DATA
   10 FORMAT(1X,F4.1,1X,F7.2,1X,F7.2,1X,I2,2X,I1,2X,I2)
   20 READ(3,30,END=1500) MHR,MFREQ,MSNR,MMON,MDAY ; AMBCOM DATA
   30 FORMAT(1X,I2,2X,F4.1,2X,F7.2,2X,I2,2X,I2)
C*****************************************************************************
c       MSNR=MSNR - 15.0                   ; USED TO ADD 15 dB OF NOISE TO
                                           ; SITES C AND D DATA.
      MODTEMP=0.                           ; INITIALIZE TEMP SPACE
      L=1                                  ; INITIAILIZE INDICES
      I=1
      J=1
   40 IF(MFREQ.EQ.SNRTAB(I,J,L)) THEN ; IS THE AMBCOM FREQ IN THE TABLE?
           GO TO 100                       ; YES - GO PROCESS
      ELSE                                 ; NO - FIND AN EMPTY SPOT
           IF(SNRTAB(I,J,L).EQ. 0) THEN    ; IS THIS AN EMPTY LINE?
               SNRTAB(I,J,L)=MFREQ         ; YES - SAVE FREQ
               GO TO 100                   ; GO PROCESS
           ELSE                            ; NO -
               I=I+1                       ; INCREMENT BY 1
               GO TO 40                    ; GO LOOK AT NEXT LINE OF TABLE
           ENDIF
      ENDIF
C ***** ADD SNR TO ACCUM SNR BY FREQ ***************************************
  100 J=MHR+1
      SNRTAB(I,J,2)=MSNR + SNRTAB(I,J,2)
      SNRTAB(I,J,3)=SNRTAB(I,J,3)+1
c****** MATCH THE RECORDS  ************************************************
  105 ACTEMP=(MON*1E5)+(DOM* 1E2) + XHR
      MODTEMP= (MMON*1E5)+(MDAY*1E2)+MHR
  110 IF(ACTEMP-MODTEMP) 200,150,300 ;DO THE MONTHS, DAYS AND HOURS
  150 I=1                            ;MATCH?
      IF(FREQ-MFREQ) 200,155,300     ;YES - DO THE FREQ MATCH?
  155 ERR=MSNR-SNR                   ;YES - CALCULATE ERROR AND PRINT
      WRITE(4,160) MFREQ,MSNR,SNR,ERR,SPI,MON,MDAY,MHR
  160 FORMAT(1X,F4.1,1X,F7.2,1X,F7.2,1X,F7.2,1X,F7.2,1X,I2,1X,I2,1X,I2)
C******** INCREMENT THE ERROR TABLE AT THE CORRECT FREQ ********************
  170 IF(MFREQ.EQ.ERRTAB(I,1)) THEN ;DOES THE AMBCOM FREQ  = TABLE FREQ?
           GO TO 180                 ;YES - GO PROCESS
      ELSE                           ;NO -
           IF(ERRTAB(I,1).EQ.0) THEN  ;IS THIS AN EMPTY SLOT IN TABLE?
                ERRTAB(I,1)=MFREQ    ;YES - SAVE FREQ AND GO PROCESS
           ELSE
                I=I+1                ;NO - INCREMENT AND GO TRY AGAIN
                GO TO 170
           ENDIF
      ENDIF
  180 ERRTAB(I,2)=ERRTAB(I,2)+ERR    ;ADD ERROR FOR AVERAGE ERROR
                                     ;CALCULATION LATER
      ERRTAB(I,3)=ERRTAB(I,3)+1      ;ADD ONE TO MATCH RECORD COUNT
      ERRTAB(I,4)=ERRTAB(I,4)+ MSNR ;ADD SNR FOR AVERAGE SNR CALCULATION
```

```
      READ(2,10,END=1400) FREQ,SNR,SPI,DOM,MON,XHR ;GET MORE ACTUAL DATA
      GO TO 20                        ;GO GET MORE AMBCOM DATA
C **** NO MATCH - GET ANOTHER ACTUAL DATA RECORD ********************
 200  I=1                             ;LIST MISS FOR ACTUAL RECORD IN TABLE
 210  IF(FREQ.EQ.ERRTAB(I,1)) THEN    ;DOES ACTUAL FREQ EQ TABLE?
           GO TO 250                  ;YES - GO PROCESS
      ELSE                             ;NO -
           IF(ERRTAB(I,1).EQ.0) THEN  ;IS THIS SLOT EMPTY?
                ERRTAB(I,1)=FREQ      ;YES - SAVE ACTUAL FREQ IN TABLE
                GO TO 250             ;GO PROCESS
           ELSE
                I=I+1                 ;INCREMENT BY ONE GO GET MORE
                GO TO 210             ;DATA
           ENDIF
      ENDIF
 250  ERRTAB(I,5)=ERRTAB(I,5)+1             ;ADD ONE TO ACTUAL MISSES
      WRITE(9,10) FREQ,SNR,SPI,DOM,MON,XHR ;FOR THAT FREQUENCY
      READ(2,10,END=1400) FREQ,SNR,SPI,DOM,MON,XHR  ;GET ANOTHER ACTUAL
      ACTEMP=0                               ;RECORD AND GO AGAIN
      GO TO 105
C ****** NO MATCH - GET MORE MORE MODEL DATA  ******************************
  300 WRITE(7,1450) MFREQ,MSNR     ;SAVE AMBCOM DATA FOR WILMAT
  360 GO TO 20                     ;GET ANOTHER AMBCOM RECORD
C
C*** OUT OF ACTUAL DATA READ ALL REMAINING MODEL RECORDS TO NO MATCH TABLE
 1400 WRITE(7,1450) MFREQ,MSNR
 1450 FORMAT(1X,F4.1,2X,F7.2)
 1460 READ(3,30,END=2000) MHR,MFREQ,MSNR,MON,MDAY
C      MSNR=MSNR-15.0
      GO TO 1400

C
C*** OUT OF MODEL DATA READ ALL REMAINING ACTUAL RECORDS TO NO MATCH TABLE
 1500 I=1
 1510 IF (FREQ.EQ.ERRTAB(I,1)) THEN  ;IS THIS ACTUAL FREQ THE CURRENT
           GO TO 1550                ;TABLE FREQ - YES THEN GO PROCESS
      ELSE
           IF(ERRTAB(I,1).EQ.0) THEN ;NO - IS THIS AN EMPTY SPOT?
                ERRTAB(I,1)=FREQ     ;YES - SAVE THE ACTUAL FREQ
           ELSE
                I=I+1                   ;NO - INCREMENT BY ONE AND GO
                GO TO 1510              ;LOOK AGAIN.
           ENDIF
      ENDIF
 1550 ERRTAB(I,5)=ERRTAB(I,5)+1          ;INCREMENT ACTUAL MISS COUNT FOR
      WRITE(9,10) FREQ,SNR,SPI,DOM,MON,XHR ;THIS FREQ THEN WRITE THE
      READ(2,10,END=2000) FREQ,SNR,SPI,DOM,MON,XHR ;ACTUAL RECORD AND
      GO TO 1500                              ;READ A NEW ACTUAL RECORD
C
C
C*** THE END ROUTINE - SPIT OUT ALL THE ACCUM DATA FROM THE TABLES
C
C
 2000 DO 2100 I=1,16
      IF(ERRTAB(I,1).EQ.0) THEN
          CONTINUE
```

```
      ELSE
           IF (ERRTAB(I,3).GT.0) THEN
             AVEERR=(ERRTAB(I,2)/ERRTAB(I,3))
             AVESNR1=(ERRTAB(I,4)/ERRTAB(I,3))
             TOAVERR= (AVEERR * ERRTAB(I,3))+TOAVERR
             TOTMOD = ERRTAB(I,3)+TOTMOD
             TOTREC= TOTREC + ERRTAB(I,5)
             WRITE(5,2010) ERRTAB(I,1),ERRTAB(I,3),AVEERR,AVESNR1,
     C       ERRTAB(I,5)
 2010        FORMAT(1X,F4.1,2X,F7.0,2X,F7.2,2X,F10.2,2X,F7.0)
           ELSE
             AVERR=0.0
             AVESNR1=0.0
             TOTREC = TOTREC + ERRTAB(I,5)
             WRITE(5,2010) ERRTAB(I,1),ERRTAB(I,3),AVEERR,AVESNR1,
     C       ERRTAB(I,5)
           ENDIF
      ENDIF
      DO 2170 J =1,24
      IF (SNRTAB(I,J,3).GT. 0) THEN
           SNRTAB(I,J,2)= (SNRTAB(I,J,2)/SNRTAB(I,J,3))
           RECTOT(I)= RECTOT(I) + SNRTAB(I,J,3)
      ELSE
           SNRTAB(I,J,2)= -999.
      ENDIF
 2170 CONTINUE
 2100 CONTINUE
 2200 DO 2500 I=1,16
      IF (SNRTAB(I,1,1).GT.0) THEN
         WRITE(8,2040) SNRTAB(I,1,1),(SNRTAB(I,J,2), J=1,12)
 2040    FORMAT('1',F4.1,12(1X,F4.0))
         WRITE(8,2050) SNRTAB(I,1,1),(SNRTAB(I,J,3),J=1,12)
 2050    FORMAT('2',F4.1,12(1X,F4.0))
         WRITE(8,2042) SNRTAB(I,1,1),(SNRTAB(I,J,2), J=13,24)
 2042    FORMAT('3',F4.1,12(1X,F4.0))
         WRITE(8,2052) SNRTAB(I,1,1),(SNRTAB(I,J,3),J=13,24)
 2052    FORMAT('4',F4.1,12(1X,F4.0))
         WRITE(8,2045) SNRTAB(I,1,1),RECTOT(I)
 2045    FORMAT('5',F4.1,1X,'TOTAL NUMBER OF RECORDS',2X,F7.2)
      ELSE
         CONTINUE
      ENDIF
2500  CONTINUE
      TOAVERR= (TOAVERR/TOTMOD)
      PRCNT= (TOTMOD/(TOTMOD+TOTREC))*100
      WRITE(6,2600) PRCNT, TOAVERR
2600  FORMAT(1X,F5.2,1X,F7.2)
      END
```

## C. WILMAT

```
c*************************************************************************
c* PROGRAM: WILMAT                                    DATE: DEC 1990
c* PROGRAMMER: D.J.WILSON
c* THIS PROGRAM EXAMINES THE UNMATCHED AMBCOM PREDICTIONS AND DETERMINES
c* IF THEY ARE SIGNAL QUALITY TRANSMISSIONS.  IF THE AMBCOMB PREDICTION
c* PASSES THIS TEST, THEN THE COUNTER FOR THE TOTAL NUMBER OF AMBCOM
```

```
c* PREDICTIONS FOR THAT FREQUENCY IS INCREASED BY ONE.  ONCE ALL THE
c* AMBCOM PREDICTIONS ARE PROCESSED A REPORT CONTAINING, BY FREQUENCY,
c* AVERAGE SNR, AVERAGE ERROR, NUMBER OF MATCHED RECORDS, NUMBER OF
c* UNMATCHED ACTUAL RECORDS, NUMBER OF UNMATCHED AMBCOM RECORDS AND THE
C* PERCENTAGE OF MATCHED AMBCOM RECORDS REFERENCED TO THE TOTAL NUMBER
c* OF AMBCOM RECORDS FOR A GIVEN FREQUENCY.
C*********************************************************************************
      REAL*8 SNRTAB(16,6)           ; SET UP DOUBLE PRECISION TABLE
      REAL*4 MFREQ,NOSNR,NOMAT      ; RESERVE SPACE FOR REAL VARIABLES
      I=1                           ; INITIALIZE INDICES
      J=1
C**********   BUILD UP TABLE OF AVERAGE FREQUENCY DATA  **************
 10   READ(3,50,END=100) FREQ,NOMAT,AVEERR,AVESNR1,ACTNOMAT ; READ
                                    ; AVERAGE ERROR, AVERAGE SNR,
                                    ; NUMBER OF MATCHES, NUMBER OF
                                    ; ACTUAL MISSES.
 50   FORMAT(1X,F4.1,2X,F7.0,2X,F7.2,2X,F10.2,2X,F7.0)
 60   IF(FREQ.EQ.SNRTAB(I,1)) THEN ; IS THIS FREQ IN THE TABLE?
          GO TO 10                  ; YES - GO PROCESS
      ELSE                          ; NO -  FIND AN EMPTY SPACE
          IF(SNRTAB(I,1).EQ.0) THEN ; IS THIS SPACE EMPTY?
              SNRTAB(I,1)=FREQ      ; YES - MOVE FREQ TO FIRST SPOT OF
              SNRTAB(I,2)=AVESNR1   ; THIS LINE OF THE TABLE AND THEN
              SNRTAB(I,3)=AVEERR    ; MOVE THE AVERAGE SNR, AVERAGE ERROR,
              SNRTAB(I,4)=NOMAT     ; NUMBER OF MATCHES PER FREQ, AND THE
              SNRTAB(I,5)=ACTNOMAT  ; NUMBER OF UNMATCHE NONCENTRIC RECS
              GO TO 10              ; GO PROCESS
           ELSE                     ; NO - THIS SPACE IS NOT EMPTY
              I=I+1                 ; INCREMENT INDEX BY 1
              GO TO 60              ; GO LOOK AGAIN
           ENDIF
      ENDIF
C****** USE TABLE OF AVERAGE DATA TO SIFT UNMATCHED AMBCOM DATA *******
100   READ(4,150,END=380) MFREQ,NOSNR ; READ AN UNMATCHED AMBCOM RECORD
150   FORMAT(1X,F4.1,2X,F7.2)
      I=1                           ; INITIALIZE THE INDICES
      J=1
200   IF(SNRTAB(I,1).EQ.MFREQ) THEN ; DOES THE UNMATCHED AMBCOM FREQ
                                    ; EQUAL THE FREQ IN THIS LINE
                                    ; OF THE AVERAGE DATA TABLE?
          GO TO 300                 ; YES - GO PROCESS
      ELSE                          ; NO
          IF(I.EQ.16) THEN          ; HAVE WE EXHAUSTED THE TABLE?
               GO TO 100            ; YES - GO GET ANOTHER RECORD
          ELSE                      ; NO - INCREMENT THE INDEX AND
               I=I+1                ; SEARCH NEXT LINE OF THE TABLE.
               GO TO 200
          ENDIF
      ENDIF
300   IF(SNRTAB(I,2).GT.NOSNR) THEN ; IS AVERAGE SNR GREATER THAN
                                    ; UNMATCHED AMBCOM RECORD SNR?
          GO TO 100                 ; YES - THROWAWAY, GET A NEW REC.
      ELSE                          ; NO - GO PROCESS
          CONTINUE
      ENDIF
350   SNRTAB(I,6)= SNRTAB(I,6)+1    ; ADD ONE TO THE COUNT OF UNMATCHED
```

```
                                        ; AMBCOM PREDICTIONS WHICH HAVE NO
                                        ; CORRESPONDING NONCENTRIC REC.
      GO TO 100                         ; GET ANOTHER UNMATCHED AMBCOM REC.
C **** OUTPUT THE TOTAL MISSES ***********************************************
380   DO 400 I=1,16             ; WRITE THE TABLE WHICH CONTAINS FOR EACH
                                ; FREQUENCY THE AVERAGE SNR, AVERAGE ERROR,
                                ; NUMBER OF MATCHED RECORDS, NUMBER OF
                                ; NONCENTRIC RECORDS WITHOUT MATCHES, AND
                                ; NUMBER UNMATCHED AMBCOM RECORDS.
      IF (SNRTAB(I,1).GT.0) THEN
           WRITE(5,2030) SNRTAB(I,1),SNRTAB(I,2),SNRTAB(I,3),
     C     SNRTAB(I,4),SNRTAB(I,5),SNRTAB(I,6)
 2030      FORMAT(1X,F4.1,2X,F7.2,2X,F7.2,2X,F7.0,2X,F7.0,
     C     2X,F10.2)
      ELSE
           CONTINUE
      ENDIF
400   CONTINUE
      END
```

# APPENDIX C. TABLES OF SITE STATISTICS

**Table 7. WINTER SITE O - 90% ES**

| FREQ (MHz) | SNR (dB) | ERR (dB) | NUMBER MATCHED | ACTUAL MISSES | AMBCOM MISSES | % |
|---|---|---|---|---|---|---|
| 3.2 | -63.4 | -83.2 | 38.0 | 0.0 | 187.00 | 16.9 |
| 4.5 | -27.4 | -57.3 | 17.0 | 4.0 | 202.00 | 07.6 |
| 6.8 | -3.6 | -28.6 | 208.0 | 0.0 | 134.00 | 60.8 |
| 6.9 | 3.3 | -17.8 | 167.0 | 0.0 | 120.00 | 58.2 |
| 9.9 | 18.0 | -3.3 | 149.0 | 0.0 | 183.00 | 44.9 |
| 10.2 | 21.4 | 1.3 | 167.0 | 1.0 | 209.00 | 44.4 |
| 13.9 | 24.3 | 0.0 | 200.0 | 28.0 | 140.00 | 58.8 |
| 14.4 | 26.5 | 2.2 | 238.0 | 28.0 | 105.00 | 69.3 |
| 17.5 | 28.1 | -0.6 | 169.0 | 57.0 | 47.00 | 78.2 |
| 18.2 | 29.1 | 0.4 | 170.0 | 56.0 | 36.00 | 82.5 |
| 20.3 | 26.8 | 0.2 | 119.0 | 30.0 | 66.00 | 64.3 |
| 20.9 | 24.3 | -1.9 | 96.0 | 11.0 | 86.00 | 52.7 |
| 23.2 | 16.4 | -16.6 | 22.0 | 4.0 | 81.00 | 21.4 |
| PERCENTAGE MATCHED 88.93% AVERAGE ERROR -7.6dB | | | | | | |

**Table 8. WINTER SITE O - 50% ES**

| FREQ (MHz) | SNR (dB) | ERR (dB) | NUMBER MATCHED | ACTUAL MISSES | AMBCOM MISSES | % |
|---|---|---|---|---|---|---|
| 3.2 | -61.4 | -81.2 | 38.0 | 0.0 | 167.00 | 18.5 |
| 4.5 | -28.0 | -57.8 | 17.0 | 4.0 | 198.00 | 7.9 |
| 6.8 | -7.5 | -32.5 | 208.0 | 0.0 | 167.00 | 55.5 |
| 6.9 | 0.7 | -20.4 | 167.0 | 0.0 | 118.00 | 58.6 |
| 9.9 | 11.7 | -10.0 | 141.0 | 8.0 | 167.00 | 45.8 |
| 10.2 | 11.9 | -8.5 | 157.0 | 11.0 | 228.00 | 40.8 |
| 13.9 | 28.8 | 4.1 | 144.0 | 84.0 | 79.00 | 64.6 |
| 14.4 | 31.4 | 6.8 | 176.0 | 90.0 | 59.00 | 74.9 |
| 17.5 | 30.2 | 1.5 | 150.0 | 76.0 | 25.00 | 85.7 |
| 18.2 | 30.4 | 1.7 | 160.0 | 66.0 | 29.00 | 84.7 |
| 20.3 | 26.4 | -0.3 | 118.0 | 31.0 | 65.00 | 64.5 |
| 20.9 | 24.0 | -2.3 | 96.0 | 11.0 | 81.00 | 54.2 |
| 23.2 | 16.4 | -16.6 | 22.0 | 4.0 | 76.00 | 22.4 |
| PERCENTAGE MATCHED 80.55% AVERAGE ERROR -9.61 dB | | | | | | |

**Table 9. WINTER SITE O - 0% ES**

| FREQ | SNR | ERR | NUMBER | ACTUAL | AMBCOM | % |
|---|---|---|---|---|---|---|
| (MHz) | (dB) | (dB) | MATCHED | MISSES | MISSES | |
| 3.2 | -67.9 | -88.0 | 37.0 | 1.0 | 178.00 | 17.2 |
| 4.5 | -44.0 | -74.5 | 14.0 | 7.0 | 224.00 | 5.9 |
| 6.8 | -5.5 | -31.1 | 132.0 | 76.0 | 100.00 | 56.9 |
| 6.9 | 0.1 | -21.6 | 108.0 | 59.0 | 109.00 | 49.8 |
| 9.9 | 17.8 | -3.2 | 96.0 | 53.0 | 161.00 | 37.4 |
| 10.2 | 19.2 | -1.1 | 93.0 | 75.0 | 186.00 | 33.3 |
| 13.9 | 29.1 | 4.2 | 144.0 | 84.0 | 83.00 | 63.4 |
| 14.4 | 31.6 | 6.9 | 175.0 | 91.0 | 58.00 | 75.1 |
| 17.5 | 30.0 | 1.4 | 152.0 | 74.0 | 29.00 | 84.0 |
| 18.2 | 30.2 | 1.5 | 164.0 | 62.0 | 29.00 | 85.0 |
| 20.3 | 26.4 | -0.3 | 118.0 | 31.0 | 63.00 | 65.2 |
| 20.9 | 23.8 | -2.4 | 97.0 | 10.0 | 83.00 | 53.9 |
| 23.2 | 16.6 | -16.4 | 22.0 | 4.0 | 77.00 | 22.2 |
| PERCENTAGE MATCHED 68.32% AVERAGE ERROR -7.04 dB | | | | | | |

**Table 10. WINTER SITE C - 90% ES**

| FREQ (MHz) | SNR (dB) | ERR (dB) | NUMBER MATCHED | ACTUAL MISSES | AMBCOM MISSES | % |
|---|---|---|---|---|---|---|
| 3.2 | -54.6 | -73.0 | 22.0 | 0.0 | 234.00 | 8.6 |
| 4.5 | -14.8 | -36.6 | 19.0 | 3.0 | 180.00 | 9.5 |
| 6.8 | 8.7 | -12.5 | 138.0 | 0.0 | 133.00 | 50.9 |
| 6.9 | 13.5 | -5.3 | 161.0 | 0.0 | 139.00 | 53.7 |
| 9.9 | 17.7 | -2.5 | 80.0 | 1.0 | 259.00 | 23.6 |
| 10.2 | 22.6 | 2.7 | 98.0 | 2.0 | 178.00 | 35.5 |
| 13.9 | 26.9 | 5.7 | 43.0 | 4.0 | 194.00 | 18.1 |
| 14.4 | 24.2 | 3.9 | 57.0 | 7.0 | 290.00 | 16.4 |
| 17.5 | 12.4 | -11.3 | 90.0 | 23.0 | 254.00 | 26.2 |
| 18.2 | 7.9 | -17.3 | 118.0 | 34.0 | 223.00 | 34.6 |
| 20.3 | 15.7 | -5.8 | 15.0 | 2.0 | 199.00 | 7.0 |
| 20.9 | 32.9 | 13.0 | 6.0 | 0.0 | 116.00 | 4.9 |
| 23.2 | 12.7 | -1.9 | 1.0 | 1.0 | 169.00 | 0.6 |
| PERCENTAGE MATCHED 91.68% AVERAGE ERROR -8.75 dB | | | | | | |

Table 11. WINTER SITE C - 50% ES

| FREQ | SNR | ERR | NUMBER | ACTUAL | AMBCOM | % |
|---|---|---|---|---|---|---|
| (MHz) | (dB) | (dB) | MATCHED | MISSES | MISSES | |
| 3.2 | -55.5 | -71.8 | 11.0 | 11.0 | 85.00 | 11.5 |
| 4.5 | -20.4 | -41.1 | 7.0 | 15.0 | 88.00 | 7.4 |
| 6.8 | 5.6 | -14.8 | 58.0 | 80.0 | 63.00 | 47.9 |
| 6.9 | 8.8 | -9.2 | 72.0 | 89.0 | 87.00 | 45.3 |
| 9.9 | 3.7 | -16.5 | 27.0 | 54.0 | 226.00 | 10.7 |
| 10.2 | 8.2 | -10.5 | 30.0 | 70.0 | 189.00 | 13.7 |
| 13.9 | 25.7 | 4.3 | 16.0 | 31.0 | 39.00 | 29.1 |
| 14.4 | 23.7 | 3.3 | 13.0 | 51.0 | 61.00 | 17.6 |
| 17.5 | 9.6 | -13.6 | 35.0 | 78.0 | 59.00 | 37.2 |
| 18.2 | 10.6 | -14.7 | 54.0 | 98.0 | 43.00 | 55.7 |
| 20.3 | 11.3 | -11.3 | 7.0 | 10.0 | 72.00 | 8.9 |
| 20.9 | 15.7 | -3.6 | 2.0 | 4.0 | 64.00 | 3.0 |
| 23.2 | 0.00 | -3.57 | 0.0 | 2.0 | 89.00 | 0.0 |
| PERCENTAGE MATCHED 35.89% AVERAGE ERROR -13.87 dB | | | | | | |

**Table 12. WINTER SITE C - 0% ES**

| FREQ | SNR | ERR | NUMBER | ACTUAL | AMBCOM | % |
|---|---|---|---|---|---|---|
| (MHz) | (dB) | (dB) | MATCHED | MISSES | MISSES | |
| 3.2 | -61.7 | -80.4 | 21.0 | 1.0 | 191.00 | 9.9 |
| 4.5 | -25.0 | -47.6 | 17.0 | 5.0 | 134.00 | 11.3 |
| 6.8 | 5.5 | -15.6 | 86.0 | 52.0 | 73.00 | 54.1 |
| 6.9 | 2.7 | -15.6 | 105.0 | 56.0 | 161.00 | 39.5 |
| 9.9 | 13.9 | -6.7 | 56.0 | 25.0 | 218.00 | 20.4 |
| 10.2 | 21.0 | 1.0 | 59.0 | 41.0 | 134.00 | 30.6 |
| 13.9 | 27.6 | 6.6 | 32.0 | 15.0 | 86.00 | 27.1 |
| 14.4 | 25.2 | 5.7 | 50.0 | 14.0 | 119.00 | 29.6 |
| 17.5 | 15.7 | -7.8 | 86.0 | 27.0 | 103.00 | 45.5 |
| 18.2 | 17.7 | -7.8 | 116.0 | 36.0 | 86.00 | 57.4 |
| 20.3 | 15.8 | -5.7 | 15.0 | 2.0 | 151.00 | 9.0 |
| 20.9 | 32.9 | 13.0 | 6.0 | 0.0 | 121.00 | 4.7 |
| 23.2 | 12.7 | -1.9 | 1.0 | 1.0 | 175.00 | 0.6 |
| PERCENTAGE MATCHED 70.27% AVERAGE ERROR -10.59 dB | | | | | | |

**Table 13. WINTER SITE D - 90% ES**

| FREQ (MHz) | SNR (dB) | ERR (dB) | NUMBER MATCHED | ACTUAL MISSES | AMBCOM MISSES | % |
|---|---|---|---|---|---|---|
| 3.2 | -36.2 | -57.1 | 3.0 | 0.0 | 160.00 | 1.8 |
| 4.5 | -17.8 | -36.6 | 107.0 | 30.0 | 255.00 | 29.6 |
| 6.8 | 9.2 | -16.0 | 371.0 | 0.0 | 65.00 | 85.1 |
| 6.9 | 14.1 | -8.3 | 195.0 | 0.0 | 184.00 | 51.5 |
| 9.9 | 17.7 | -4.9 | 206.0 | 5.0 | 204.00 | 50.2 |
| 10.2 | 22.7 | 0.1 | 250.0 | 2.0 | 128.00 | 66.1 |
| 13.9 | 18.3 | -7.3 | 220.0 | 27.0 | 199.00 | 52.5 |
| 14.4 | 19.6 | -7.4 | 231.0 | 42.0 | 194.00 | 54.4 |
| 17.5 | 17.7 | -14.6 | 250.0 | 44.0 | 185.00 | 57.5 |
| 18.2 | 22.1 | -10.3 | 286.0 | 31.0 | 173.00 | 62.3 |
| 20.3 | 33.9 | 3.5 | 192.0 | 27.0 | 109.00 | 63.8 |
| 20.9 | 37.4 | 5.9 | 197.0 | 14.0 | 72.00 | 73.2 |
| 23.2 | 42.6 | 8.4 | 172.0 | 17.0 | 74.00 | 69.9 |
| PERCENTAGE MATCHED 91.81% AVERAGE ERROR -7.20 dB | | | | | | |

**Table 14. WINTER SITE D - 50% ES**

| FREQ (MHz) | SNR (dB) | ERR (dB) | NUMBER MATCHED | ACTUAL MISSES | AMBCOM MISSES | % |
|---|---|---|---|---|---|---|
| 3.2 | -37.9 | -58.8 | 3.0 | 0.0 | 152.00 | 1.9 |
| 4.5 | -18.8 | -37.6 | 107.0 | 30.0 | 242.00 | 30.7 |
| 6.8 | 6.9 | -18.4 | 368.0 | 3.0 | 61.00 | 85.8 |
| 6.9 | 11.3 | -11.1 | 194.0 | 1.0 | 162.00 | 54.5 |
| 9.9 | 12.3 | -9.9 | 174.0 | 37.0 | 177.00 | 49.6 |
| 10.2 | 14.6 | -7.3 | 190.0 | 62.0 | 144.00 | 56.9 |
| 13.9 | 18.3 | -7.0 | 199.0 | 48.0 | 86.00 | 69.8 |
| 14.4 | 19.7 | -7.2 | 214.0 | 59.0 | 94.00 | 69.5 |
| 17.5 | 16.2 | -16.6 | 228.0 | 66.0 | 51.00 | 81.7 |
| 18.2 | 20.1 | -12.7 | 254.0 | 63.0 | 50.00 | 83.6 |
| 20.3 | 34.0 | 3.4 | 188.0 | 31.0 | 74.00 | 71.8 |
| 20.9 | 37.5 | 5.9 | 192.0 | 19.0 | 69.00 | 73.6 |
| 23.2 | 43.0 | 8.6 | 169.0 | 20.0 | 73.00 | 69.8 |
| PERCENTAGE MATCHED 84.96% AVERAGE ERROR -9.26 dB | | | | | | |

**Table 15. WINTER SITE D - 0% ES**

| FREQ (MHz) | SNR (dB) | ERR (dB) | NUMBER MATCHED | ACTUAL MISSES | AMBCOM MISSES | % |
|---|---|---|---|---|---|---|
| 3.2 | -38.2 | -59.1 | 3.0 | 0.0 | 93.00 | 3.1 |
| 4.5 | -30.6 | -49.4 | 99.0 | 38.0 | 150.00 | 39.8 |
| 6.8 | -1.9 | -27.1 | 329.0 | 42.0 | 70.00 | 82.5 |
| 6.9 | 4.9 | -17.5 | 175.0 | 20.0 | 116.00 | 60.1 |
| 9.9 | 11.4 | -10.7 | 157.0 | 54.0 | 152.00 | 50.8 |
| 10.2 | 14.8 | -6.8 | 179.0 | 73.0 | 125.00 | 58.9 |
| 13.9 | 18.4 | -7.0 | 200.0 | 47.0 | 82.00 | 70.9 |
| 14.4 | 20.0 | -7.0 | 215.0 | 58.0 | 92.00 | 70.0 |
| 17.5 | 16.4 | -16.4 | 228.0 | 66.0 | 50.00 | 82.0 |
| 18.2 | 20.1 | -12.6 | 254.0 | 63.0 | 51.00 | 83.3 |
| 20.3 | 34.0 | 3.4 | 188.0 | 31.0 | 74.00 | 71.8 |
| 20.9 | 37.6 | 6.0 | 192.0 | 19.0 | 68.00 | 73.8 |
| 23.2 | 43.2 | 8.8 | 169.0 | 20.0 | 74.00 | 69.5 |
| PERCENTAGE MATCHED 81.81% AVERAGE ERROR -11.10 dB | | | | | | |

**Table 16. SUMMER SITE O - 90% ES**

| FREQ | SNR | ERR | NUMBER | ACTUAL | AMBCOM | % |
|---|---|---|---|---|---|---|
| (MHz) | (dB) | (dB) | MATCHED | MISSES | MISSES | |
| 3.2 | -66.3 | -86.8 | 21.0 | 0.0 | 184.00 | 10.2 |
| 4.9 | -24.7 | -46.2 | 41.0 | 0.0 | 169.00 | 19.5 |
| 5.2 | -15.9 | -38.3 | 43.0 | 0.0 | 166.00 | 20.6 |
| 6.8 | 2.2 | -19.4 | 22.0 | 0.0 | 148.00 | 12.9 |
| 6.9 | 0.9 | -22.4 | 45.0 | 0.0 | 202.00 | 18.2 |
| 9.9 | 14.1 | -11.5 | 120.0 | 0.0 | 179.00 | 40.1 |
| 10.2 | 19.2 | -8.4 | 251.0 | 0.0 | 121.00 | 67.5 |
| 13.9 | 23.1 | -6.3 | 255.0 | 4.0 | 278.00 | 47.8 |
| 14.4 | 27.8 | -3.1 | 334.0 | 7.0 | 162.00 | 67.3 |
| 17.5 | 22.6 | -10.0 | 327.0 | 17.0 | 171.00 | 65.7 |
| 18.2 | 27.5 | -3.9 | 157.0 | 17.0 | 197.00 | 44.4 |
| 20.3 | 33.6 | 6.4 | 153.0 | 27.0 | 128.00 | 54.4 |
| 20.9 | 33.4 | 5.3 | 81.0 | 26.0 | 168.00 | 32.5 |
| PERCENTAGE MATCHED 94.97% AVERAGE ERROR -8.33 dB | | | | | | |

**Table 17. SUMMER SITE O - 50% ES**

| FREQ (MHz) | SNR (dB) | ERR (dB) | NUMBER MATCHED | ACTUAL MISSES | AMBCOM MISSES | % |
|---|---|---|---|---|---|---|
| 3.2 | -66.5 | -87.0 | 21.0 | 0.0 | 184.00 | 10.2 |
| 4.9 | -25.2 | -46.7 | 41.0 | 0.0 | 170.00 | 19.4 |
| 5.2 | -16.3 | -38.7 | 43.0 | 0.0 | 162.00 | 21.0 |
| 6.8 | 0.3 | -21.2 | 22.0 | 0.0 | 148.00 | 12.9 |
| 6.9 | -0.3 | -23.7 | 45.0 | 0.0 | 200.00 | 18.4 |
| 9.9 | 12.6 | -13.1 | 120.0 | 0.0 | 173.00 | 41.0 |
| 10.2 | 17.1 | -10.5 | 251.0 | 0.0 | 111.00 | 69.3 |
| 13.9 | 18.2 | -11.3 | 243.0 | 16.0 | 196.00 | 55.4 |
| 14.4 | 22.6 | -8.5 | 304.0 | 37.0 | 100.00 | 75.2 |
| 17.5 | 21.5 | -12.0 | 258.0 | 86.0 | 60.00 | 81.1 |
| 18.2 | 29.1 | -2.8 | 125.0 | 49.0 | 73.00 | 63.1 |
| 20.3 | 37.8 | 9.3 | 124.0 | 56.0 | 87.00 | 58.8 |
| 20.9 | 39.5 | 8.9 | 55.0 | 52.0 | 120.00 | 31.4 |
| PERCENTAGE MATCHED 84.80% AVERAGE ERROR -11.05 dB | | | | | | |

**Table 18. SUMMER SITE O - 0% ES**

| FREQ (MHz) | SNR (dB) | ERR (dB) | NUMBER MATCHED | ACTUAL MISSES | AMBCOM MISSES | % |
|---|---|---|---|---|---|---|
| 3.2 | -78.9 | -99.4 | 21.0 | 0.0 | 176.00 | 10.7 |
| 4.9 | -38.8 | -60.3 | 41.0 | 0.0 | 163.00 | 20.1 |
| 5.2 | -28.0 | -50.4 | 41.0 | 2.0 | 132.00 | 23.7 |
| 6.8 | -8.4 | -30.0 | 21.0 | 1.0 | 120.00 | 14.9 |
| 6.9 | -12.7 | -35.9 | 41.0 | 4.0 | 179.00 | 18.6 |
| 9.9 | 12.4 | -13.7 | 99.0 | 21.0 | 135.00 | 42.3 |
| 10.2 | 14.0 | -13.6 | 204.0 | 47.0 | 97.00 | 67.8 |
| 13.9 | 20.7 | -8.9 | 219.0 | 40.0 | 221.00 | 49.8 |
| 14.4 | 24.6 | -6.8 | 288.0 | 53.0 | 108.00 | 72.7 |
| 17.5 | 21.4 | -12.1 | 255.0 | 89.0 | 64.00 | 79.9 |
| 18.2 | 30.6 | -0.7 | 124.0 | 50.0 | 66.00 | 65.3 |
| 20.3 | 37.3 | 8.9 | 131.0 | 49.0 | 84.00 | 60.9 |
| 20.9 | 39.7 | 9.0 | 56.0 | 51.0 | 108.00 | 34.1 |
| PERCENTAGE MATCHED 79.11% AVERAGE ERROR -11.87 dB | | | | | | |

**Table 19. SUMMER SITE C - 90% ES**

| FREQ (MHz) | SNR (dB) | ERR (dB) | NUMBER MATCHED | ACTUAL MISSES | AMBCOM MISSES | % |
|---|---|---|---|---|---|---|
| 3.2 | -72.2 | -97.5 | 15.0 | 0.0 | 177.00 | 7.8 |
| 4.9 | 5.5 | -18.4 | 12.0 | 0.0 | 18.00 | 40.0 |
| 5.2 | 10.6 | -12.8 | 23.0 | 1.0 | 14.00 | 62.2 |
| 6.8 | 16.9 | -7.0 | 52.0 | 2.0 | 32.00 | 61.9 |
| 6.9 | 10.7 | -9.8 | 42.0 | 1.0 | 138.00 | 23.3 |
| 9.9 | 15.7 | -10.4 | 59.0 | 2.0 | 102.00 | 36.6 |
| 10.2 | 19.7 | -8.7 | 215.0 | 5.0 | 30.00 | 87.8 |
| 13.9 | 21.8 | -7.8 | 192.0 | 3.0 | 156.00 | 55.2 |
| 14.4 | 26.1 | -4.6 | 230.0 | 2.0 | 117.00 | 66.3 |
| 17.5 | 32.3 | -0.6 | 139.0 | 10.0 | 190.00 | 42.2 |
| 18.2 | 38.4 | 6.0 | 81.0 | 12.0 | 133.00 | 37.9 |
| 20.3 | 44.0 | 14.8 | 34.0 | 5.0 | 89.00 | 27.6 |
| 20.9 | 48.7 | 23.9 | 2.0 | 5.0 | 43.00 | 4.4 |
| PERCENTAGE MATCHED 95.80% AVERAGE ERROR -6.23 dB | | | | | | |

**Table 20. SUMMER SITE C - 50% ES**

| FREQ (MHz) | SNR (dB) | ERR (dB) | NUMBER MATCHED | ACTUAL MISSES | AMBCOM MISSES | % |
|---|---|---|---|---|---|---|
| 3.2 | -72.8 | -98.1 | 15.0 | 0.0 | 170.00 | 8.1 |
| 4.9 | 4.2 | -19.2 | 11.0 | 1.0 | 27.00 | 28.9 |
| 5.2 | 9.5 | -13.8 | 22.0 | 2.0 | 25.00 | 46.8 |
| 6.8 | 15.9 | -8.1 | 51.0 | 3.0 | 38.00 | 57.3 |
| 6.9 | 9.2 | -11.2 | 41.0 | 2.0 | 145.00 | 22.0 |
| 9.9 | 14.7 | -11.4 | 59.0 | 2.0 | 106.00 | 35.8 |
| 10.2 | 17.5 | -10.8 | 212.0 | 8.0 | 48.00 | 81.5 |
| 13.9 | 17.6 | -12.0 | 190.0 | 5.0 | 119.00 | 61.5 |
| 14.4 | 22.3 | -8.5 | 216.0 | 16.0 | 67.00 | 76.3 |
| 17.5 | 31.2 | -2.2 | 116.0 | 33.0 | 70.00 | 62.4 |
| 18.2 | 39.8 | 7.3 | 75.0 | 18.0 | 89.00 | 45.7 |
| 20.3 | 45.6 | 13.5 | 29.0 | 10.0 | 83.00 | 25.9 |
| 20.9 | 48.7 | 23.9 | 2.0 | 5.0 | 42.00 | 4.5 |
| PERCENTAGE MATCHED 90.82% AVERAGE ERROR -8.88 dB | | | | | | |

**Table 21. SUMMER SITE C - 0% ES**

| FREQ (MHz) | SNR (dB) | ERR (dB) | NUMBER MATCHED | ACTUAL MISSES | AMBCOM MISSES | % |
|---|---|---|---|---|---|---|
| 3.2 | -83.7 | -109.1 | 15.0 | 0.0 | 169.00 | 8.2 |
| 4.9 | -12.2 | -35.6 | 11.0 | 1.0 | 47.00 | 19.0 |
| 5.2 | -3.5 | -26.7 | 22.0 | 2.0 | 24.00 | 47.8 |
| 6.8 | 4.4 | -19.5 | 48.0 | 6.0 | 40.00 | 54.5 |
| 6.9 | -1.3 | -21.8 | 41.0 | 2.0 | 135.00 | 23.3 |
| 9.9 | 5.8 | -20.1 | 50.0 | 11.0 | 115.00 | 30.3 |
| 10.2 | 9.1 | -19.3 | 178.0 | 42.0 | 72.00 | 71.2 |
| 13.9 | 14.67 | -15.0 | 166.0 | 29.0 | 126.00 | 56.8 |
| 14.4 | 19.6 | -11.3 | 196.0 | 36.0 | 95.00 | 67.4 |
| 17.5 | 32.9 | -0.7 | 105.0 | 44.0 | 82.00 | 56.1 |
| 18.2 | 42.3 | 9.9 | 73.0 | 20.0 | 78.00 | 48.3 |
| 20.3 | 46.9 | 14.8 | 29.0 | 10.0 | 68.00 | 29.9 |
| 20.9 | 48.7 | 23.9 | 2.0 | 5.0 | 42.00 | 4.5 |
| PERCENTAGE MATCHED 81.82% AVERAGE ERROR -13.33 dB | | | | | | |

**Table 22. SUMMER SITE D - 90% ES**

| FREQ (MHz) | SNR (dB) | ERR (dB) | NUMBER MATCHED | ACTUAL MISSES | AMBCOM MISSES | % |
|---|---|---|---|---|---|---|
| 3.2 | -4.2 | -36.3 | 36.0 | 7.0 | 22.00 | 62.1 |
| 4.9 | 5.1 | -19.6 | 109.0 | 0.0 | 44.00 | 71.2 |
| 5.2 | 10.8 | -18.3 | 128.0 | 0.0 | 36.00 | 78.0 |
| 6.8 | 16.2 | -10.0 | 178.0 | 0.0 | 69.00 | 72.1 |
| 6.9 | 21.9 | -5.3 | 133.0 | 0.0 | 94.00 | 58.6 |
| 9.9 | 15.6 | -12.4 | 164.0 | 0.0 | 175.00 | 48.4 |
| 10.2 | 20.5 | -11.1 | 359.0 | 0.0 | 90.00 | 80.0 |
| 13.9 | 28.4 | -8.7 | 198.0 | 1.0 | 206.00 | 49.0 |
| 14.4 | 32.8 | -5.1 | 340.0 | 0.0 | 138.00 | 71.1 |
| 17.5 | 42.6 | 1.6 | 231.0 | 44.0 | 196.00 | 54.1 |
| 18.2 | 48.2 | 9.3 | 74.0 | 55.0 | 189.00 | 28.1 |
| 20.3 | 48.2 | 10.0 | 46.0 | 107.0 | 98.00 | 31.9 |
| 20.9 | 47.0 | 11.4 | 15.0 | 31.0 | 125.00 | 10.7 |
| PERCENTAGE MATCHED 89.14% AVERAGE ERROR -8.02 dB | | | | | | |

**Table 23. SUMMER SITE D - 50% ES**

| FREQ (MHz) | SNR (dB) | ERR (dB) | NUMBER MATCHED | ACTUAL MISSES | AMBCOM MISSES | % |
|---|---|---|---|---|---|---|
| 3.2 | -4.6 | -36.7 | 36.0 | 7.0 | 22.00 | 62.1 |
| 4.9 | 4.4 | -20.4 | 109.0 | 0.0 | 46.00 | 70.3 |
| 5.2 | 10.1 | -18.9 | 128.0 | 0.0 | 35.00 | 78.5 |
| 6.8 | 15.2 | -11.1 | 178.0 | 0.0 | 67.00 | 72.7 |
| 6.9 | 21.0 | -6.3 | 133.0 | 0.0 | 101.00 | 56.8 |
| 9.9 | 14.1 | -14.0 | 163.0 | 1.0 | 167.00 | 49.4 |
| 10.2 | 17.6 | -14.1 | 356.0 | 3.0 | 63.00 | 85.0 |
| 13.9 | 25.1 | -13.0 | 171.0 | 28.0 | 103.00 | 62.4 |
| 14.4 | 27.6 | -11.4 | 273.0 | 67.0 | 64.00 | 81.0 |
| 17.5 | 43.1 | 0.2 | 184.0 | 91.0 | 64.00 | 74.2 |
| 18.2 | 49.0 | 8.8 | 53.0 | 76.0 | 53.00 | 70.0 |
| 20.3 | 49.8 | 5.3 | 26.0 | 127.0 | 8.00 | 76.5 |
| 20.9 | 46.9 | 3.8 | 5.0 | 41.0 | 8.00 | 38.5 |
| PERCENTAGE MATCHED 80.45% AVERAGE ERROR -11.44 dB | | | | | | |

**Table 24. SUMMER SITE D - 0% ES**

| FREQ | SNR | ERR | NUMBER | ACTUAL | AMBCOM | % |
|---|---|---|---|---|---|---|
| (MHz) | (dB) | (dB) | MATCHED | MISSES | MISSES | |
| 3.2 | -14.7 | -46.4 | 34.0 | 9.0 | 25.00 | 57.6 |
| 4.9 | -13.1 | -37.8 | 100.0 | 9.0 | 84.00 | 54.3 |
| 5.2 | -5.2 | -34.5 | 121.0 | 7.0 | 60.00 | 66.9 |
| 6.8 | 8.0 | -18.5 | 163.0 | 15.0 | 40.00 | 80.3 |
| 6.9 | 12.1 | -15.5 | 115.0 | 18.0 | 69.00 | 62.5 |
| 9.9 | 9.5 | -18.9 | 144.0 | 20.0 | 96.00 | 60.0 |
| 10.2 | 12.9 | -19.1 | 309.0 | 50.0 | 56.00 | 84.7 |
| 13.9 | 20.4 | -17.5 | 173.0 | 26.0 | 109.00 | 61.3 |
| 14.4 | 24.9 | -13.7 | 279.0 | 61.0 | 59.00 | 82.5 |
| 17.5 | 43.4 | 0.5 | 182.0 | 93.0 | 64.00 | 74.0 |
| 18.2 | 48.6 | 8.6 | 60.0 | 69.0 | 60.00 | 50.0 |
| 20.3 | 47.5 | 4.8 | 29.0 | 124.0 | 12.00 | 70.7 |
| 20.9 | 46.9 | 3.8 | 5.0 | 41.0 | 10.00 | 33.3 |
| PERCENTAGE MATCHED 75.98% AVERAGE ERROR -16.96 dB | | | | | | |

## APPENDIX D. COMPARIABLE STATISTICS

The tables and figures listed in this Appendix were compiled from a subset of AMBCOM data. Earlier computer-based model validations [Ref. 14 and 13] modeled six of the 13 Project NONCENTRIC frequencies, e.g., 6.8, 6.9, 9.9, 13.9, 17.5 and 20.3 MHz. In addition, only site O data were examined. The data presented in this Appendix are for those frequencies and site O only. The figures are directly compareable to the figures produced in the earlier studies.

**Table 25. WINTER SITE O STATISTICS (NORMALIZED TO ZERO MEAN ERROR).**

| % Sporadic E | 90% | 50% | 0% |
|---|---|---|---|
| Standard Dev. (dB) | 15.89 | 17.87 | 19.86 |
| Median Error (dB) | -0.1 | 0.9 | 5.8 |
| # of Samples | 1012 | 928 | 750 |
| % Matched | 89.80 | 82.34 | 66.55 |

**Table 26. SUMMER SITE O STATISTICS (NORMALIZED TO ZERO MEAN ERROR).**

| % Sporadic E | 90% | 50% | 0% |
|---|---|---|---|
| Standard Dev. (dB) | 14.16 | 15.38 | 17.52 |
| Median Error (dB) | 0.2 | -0.6 | 1.1 |
| # of Samples | 922 | 812 | 766 |
| % Matched | 95.05 | 83.71 | 78.97 |

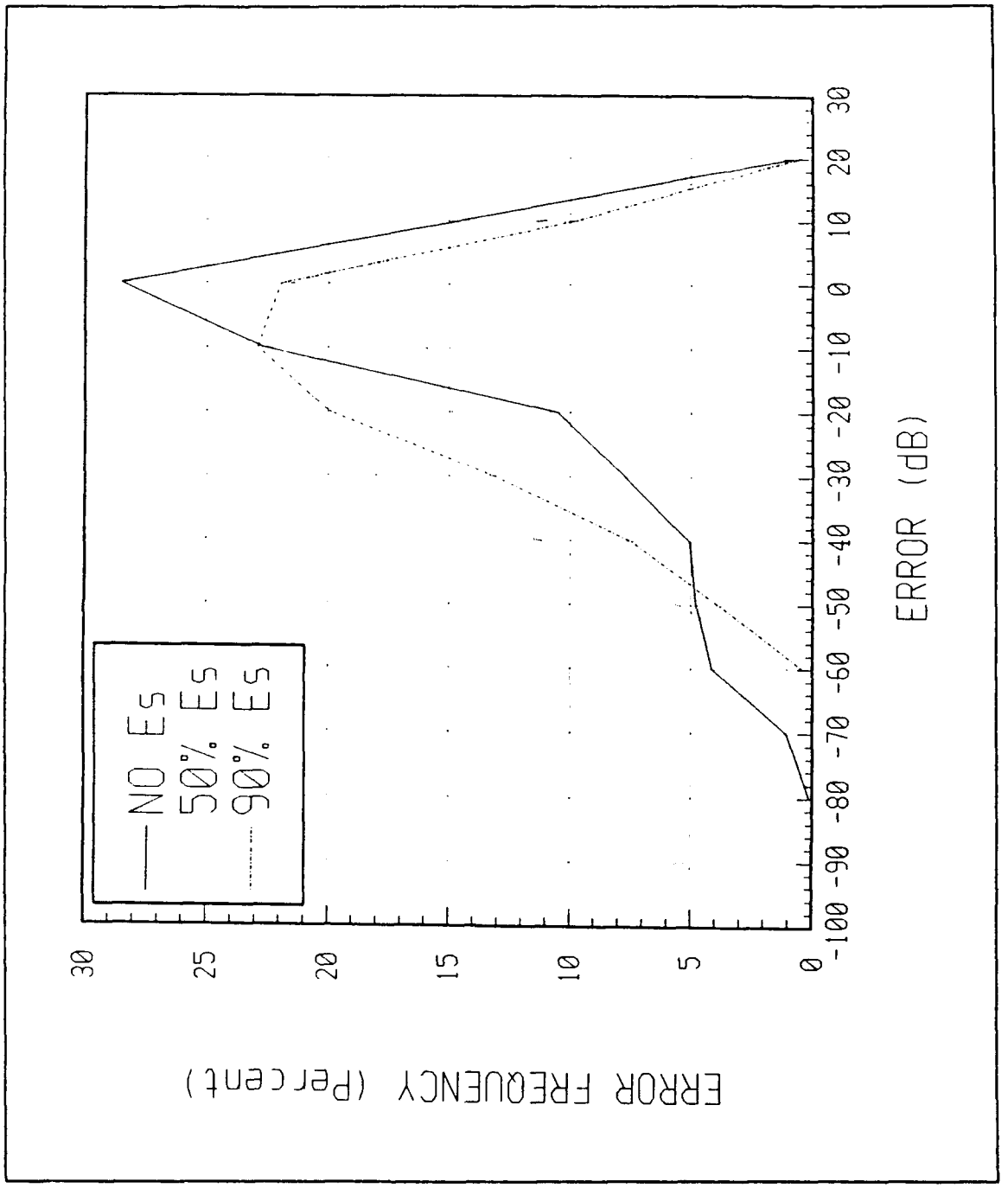


**Figure 33. The 1989 winter campaign average error for all three sporadic E models. (10 dB bins)**

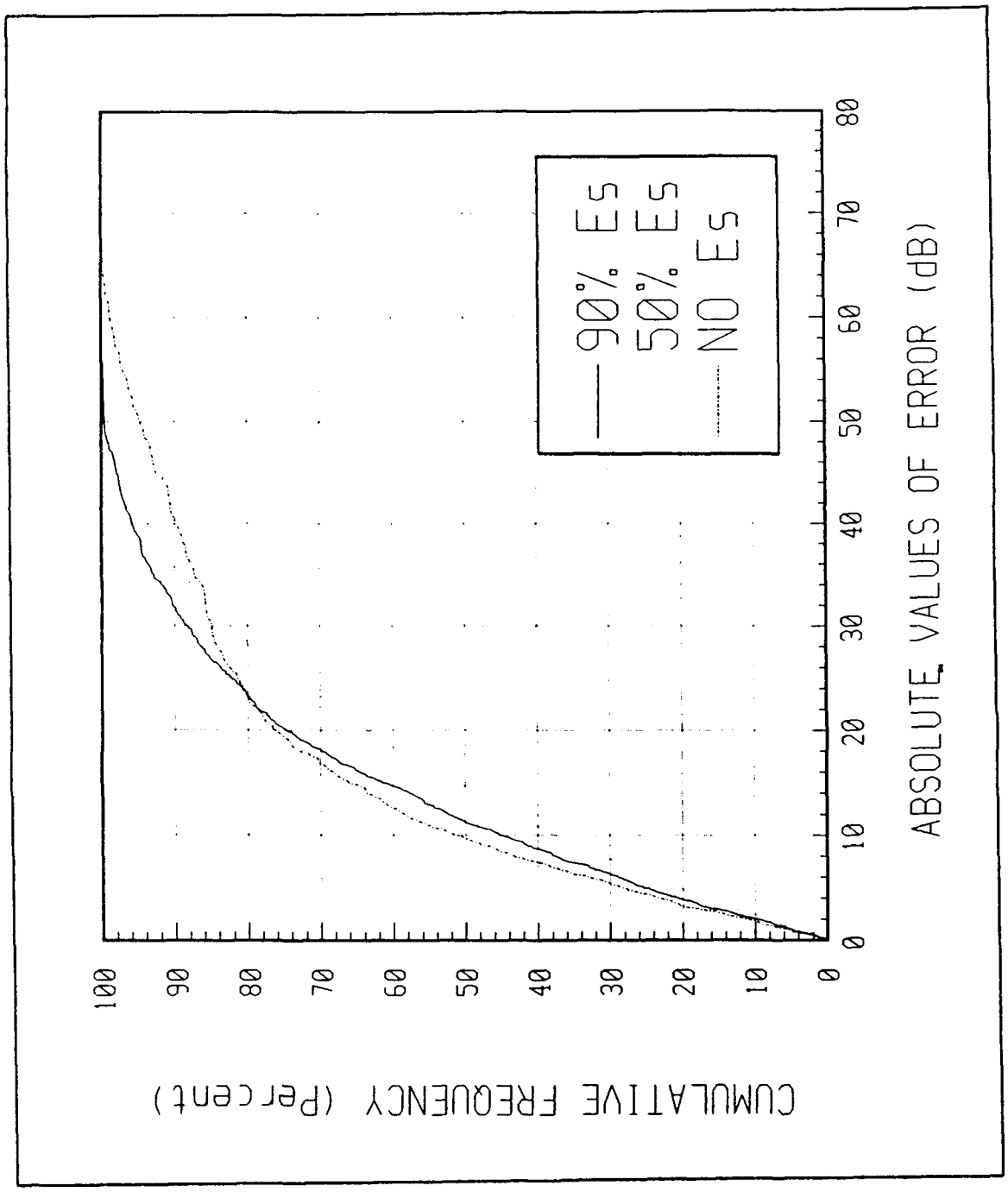


**Figure 34.** **The 1989 winter campaign cumulative error of absolute value of the average error.**

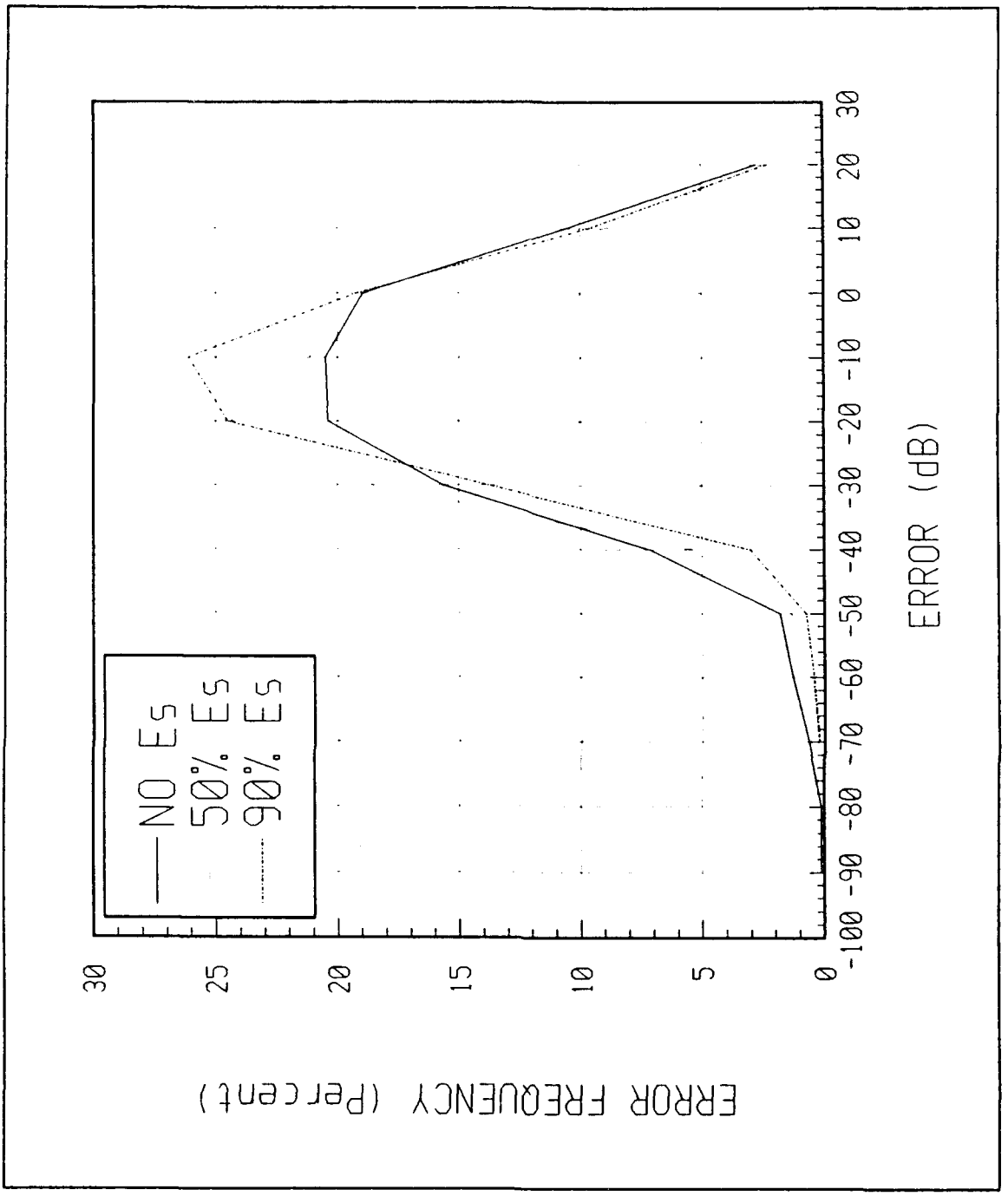


**Figure 35. The 1988 summer campaign average error for all three sporadic E models. (10 dB bins)**

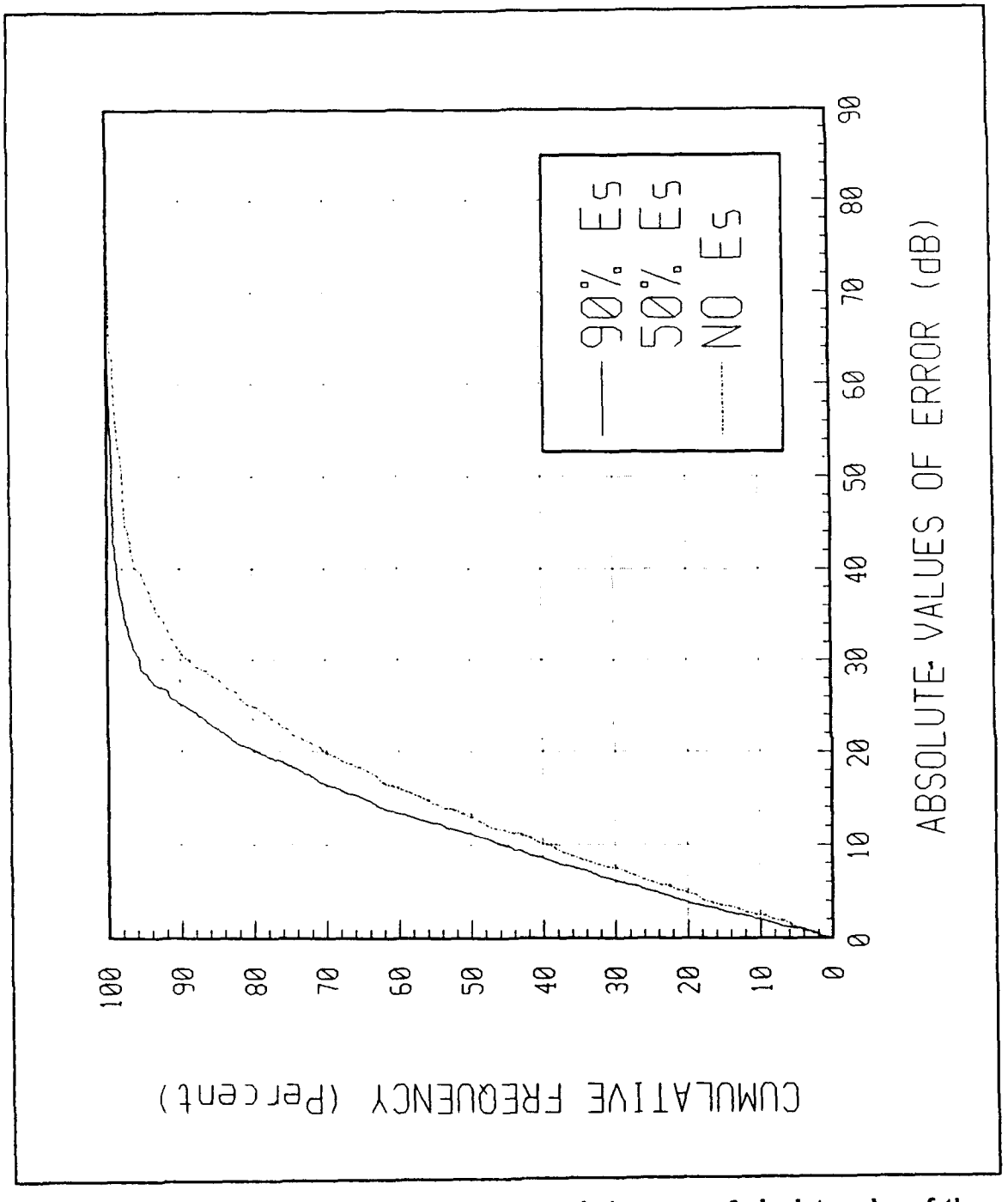


**Figure 36. The 1989 summer campaign cumulative error of absolute value of the average error.**

## LIST OF REFERENCES


1. J.K. Hargreaves, "The high latitude ionosphere: dynamical aspects and models", paper presented at the NATO AGARD Lecture Series, Media Effects on Electronic Systems in the High Latitude Region, LS-162, September 1988.

2. Interview with Tudor Jones, Professor, University of Leicester, July 1990.

3. W. D. Parkinson, *Introduction to Geomagnetism*, Scottish Academic Press Ltd., 1983.

4. Kenneth Davies, *Ionospheric Radio*,Peter Peregrinus Ltd., London, United Kingdom, 1989.

5. Helen E. Coffey, "Geomagnetic and Solar Data", *Journal of Geophysical Research*, Vol. 94, No A6, p. 7020, June 1989.

6. J.K. Hargreaves, "The high-latitude ionosphere: geophysical basis", paper presented at the NATO AGARD Lecture Series, Media Effects on Electronic Systems in the High Latitude Region, LS-162, September 1988.

7. R. D. Hunsucker and H. F. Bates, "Survey of polar and auroral effects on HF propagation", *Radio Science*, Vol. 4, No. 4, pp. 347-365, April 1969.

8. R. R. Vondrak and K. L. Miller, "A high-latitude phenomenological model of auroral precipitation and ionospheric effects", *Radio Science*, Vol. 20, No. 3, pp. 431-438, May-June 1985.

9. R. R. Vondrak and others, "Chatanika model of the high-latitude ionosphere for application to HF propagation prediction", RADC-TR-78-7, Menlo Park, CA, January 1978.

10. J. K. Hargreaves, "Auroral absorption of HF radio waves in the ionosphere: a review of results from the first decade of riometry", *Proceedings of the IEEE*, Vol. 57, No.8, August 1969.

11. D.P. Roesler, *Analysis of Data from A Transauroral HF Experiment*, Report WP88-2010, Rockwell International, March 1988.

12. Nikhil Dave', "Comparison with oblique sounder data of high- latitude HF predictions from RADAR C and AMBCOM computer programs", paper presented at the Ionospheric Effects Symposium, Springfield, VA, May 1987.

13. Marcos D. Tsolekas, "A comparison of high-latitude ionospheric propagation predictions from IONCAP-PC 2.5 with measured data," Master's thesis, Naval Postgraduate School, Monterey, CA, December 1990.

14. Stefanos S. Gikas, "A comparison of high-latitude ionospheric propagation predictions from Advanced PROPHET 4.0 with measured data," Master's thesis, Naval Postgraduate School, Monterey, CA, December 1990.

15. V. Elaine Hatfield and Georgellen Smith, *AMBCOM USER'S GUIDE FOR ENGINEERS*, SRI International, 1987.

16. V. Elaine Hatfield and others, *AMBCOM USER'S GUIDE FOR PROGRAMMERS: Part One -- Description*, SRI International, 1987.

17. V. Elaine Hatfield and others, *AMBCOM USER'S GUIDE FOR PROGRAMMERS: Part Two -- Listings*, SRI International, 1987.

18. John Griffiths, *Radio Wave Propagation and Antennas*, Prentiss-Hall International, Englewood Cliffs, NJ, 1987.

19. Helen E. Coffey, "Geomagnetic and Solar Data", *Journal of Geophysical Research*, Vol.94, No. A7, p. 9161, July 1989.

20. Helen E.Coffey, "Geomagnetic and Solar Data", *Journal of Geophysical Research*, Vol.93, No. A12, p. 14732, December 1988.

21. Helen E. Coffey, "Geomagnetic and Solar Data", *Journal of Geophysical Research*, Vol.94, No. A1, p. 511, 1 January 1989.

22. T. R. Hartz and N. M. Brice,"The general pattern of auroral particle precipitation," *Planetary and Space Science*, Vol. 15.1, p. 301-327, 1967.

23. *Noncentric:Automatic Signal Recognition*, Ionospheric Physics Group, Leicester University, December 1989.

24. Telephone conversation between V. E. Hatfield, SRI, International and the author, 25 February 1991.